# INVESTIGATIONS OF METEORIC PHENOMENA

A thesis presented for the

Degree of

Doctor of Philosophy in Physics

in the University of Canterbury

Christchurch, New Zealand,

by

C. S. L. Keay

1964

# SUMMARY

The radar detection of meteor trails is discussed with reference to the equipment used, the methods developed and employed, and the results gained, particularly those concerning the astronomical aspects of meteoric phenomena.

Part A traces the development of a new method of detecting the radiants of the very numerous small-sized meteors. Their radiants tend to be close to the ecliptic plane but some high declination activity is present. The recognised meteor showers often lose their identity among the overwhelming number of faint meteors.

Part B deals with a survey of meteor rates. This has led to a better knowledge of the distribution of meteors and has revealed that some very large groupings of meteors exist. These "associations", as they have been called, can embrace several meteor showers and appear to be of very recent occurrence on the astronomical time-scale, i.e. they are only some tens of millions of years old.

CONTENTS

PART B THE MEASUREMENT OF METEOR RATES

## PREFACE

Many sections of this volume have already been published, or are about to be published. They have appeared first as Contract Reports, which is the format in which some of them appear here, and later as papers in various journals.

The incorporation of these publications into this volume in such a manner has simplified the difficult problem of reproducing diagrams for which the original tracings are no longer available. This procedure has led to a small amount of recapitulation from chapter to chapter.

The numbering sequence for Figures and Photographs starts afresh for each chapter. To avoid confusion the chapter number and figure number (where applicable) appears at the lower right of each page.

## ACKNOWLEDGEMENTS

The work described in this volume is the result of a team effort. It is a pleasure to express my indebtedness to Dr. C. D. Ellyett, the team leader, for not only making this research possible but also for his constant encouragement and his helpful advice. I would also like to record my gratitude to Messrs. E. C. McLauchlan and P. W. McNabb for keeping the radar equipment in operation in the face of many difficulties.

My thanks are due also to Mr. K. W. Roth for his work in the analysis and plotting of Figures 1(a), (b) and (c), and Figures 2(a) and (b) in Chapter 3.

# INVESTIGATIONS OF METEORIC PHENOMENA

## 1. GENERAL INTRODUCTION:

Prior to 1957, when these studies commenced, considerable progress had been made in radio meteor research, principally in the Northern Hemisphere. Much of the basic physical theory of the interaction of meteors with the earth's atmosphere had been worked out and related to radio observational techniques (see, for example, Kaiser, 1953), radio-meteors were being used as a tool for measurements on the upper atmosphere (e.g. Elford and Robertson, 1953), and the utility of meteor-scattered signals in a new discontinuous type of radio communication had been proved (e.g. Forsyth et al., 1957).

In the field of meteor astronomy early radio observations had shown that fewer than one percent of meteors brighter than magnitude +8 came from outside the solar system, thus refuting earlier theories that meteors are of interstellar origin. These observations had also revealed the presence of several meteor showers active during the daylight hours and therefore inaccessible to visual or photographic observing techniques.

By 1957, fairly accurate radiants had been found for practically all of the major showers in both hemispheres, and it was becoming apparent that such showers contribute very few meteors compared with those classed as sporadic, i.e. unconnected with a recognised shower and of seemingly random occurrence. However, careful analysis of observational data revealed that sporadic meteors exhibit a marked preference for direct motion in or near the plane of the ecliptic (Lovell, 1954), a result which was soon confirmed by Southern Hemisphere observations (see Chapter 2).

Measurements of the annual variation of meteor activity were mainly confined to the Northern Hemisphere, with the result that terrestrial factors could not be evaluated and eliminated to yield the true space density of meteors along the earth's orbit.

Finally, Bowen's hypothesis (1953, 1956) that rainfall is influenced by the influx of meteoric material, together with the launching of the first artificial earth satellites into the environment of space, underscored the fact that many of the answers to the problems of meteor astronomy might be of considerable significance beyond the immediate confines of the subject.

Such was the situation in 1957. Some of the important problem areas at that time were:

1. The possibility of atmospheric and ionospheric effects on meteor rate.

2. The influence of purely terrestrial factors on the apparent variation in meteor activity throughout the year.
3. The unknown extent of meteor shower activity radiating from high southerly declinations.
4. Criteria for identifying very diffuse meteor streams, particularly if they are sparsely populated.
5. The identification of streams of faint meteors if they exist.
6. The possibility that faint sporadic meteors may have a different orbital distribution from the brighter ones.
7. The question of the origin of meteoroids*.

The purpose of the work described herein has been to elucidate as many of these problems as possible, particularly those requiring Southern Hemisphere observational data. The work falls naturally into two areas of investigation, namely:

---

*The term "meteoroid" refers to the physical object in space, while "meteor" refers to the phenomenon when a meteoroid encounters the earth's atmosphere. However, a strict separation of these terms is difficult and the historical usage of the word "meteor" when referring to the actual object in space may sometimes be unavoidable.

(a) the measurement of meteor radiants using highly directional antenna systems, and

(b) the measurement of meteor rates using omni-directional antennas and maintaining equipment sensitivity as constant as possible over extended periods of time.

The above order of presentation will be followed in this volume, but the two parts will not be entirely unrelated since rate data can be made to give information on radiant distributions.

## 2. HISTORICAL BACKGROUND:

The Rolleston Radio Field Station of the University of Canterbury was set up by Dr. C. D. Ellyett in 1950, shortly after his return from Jodrell Bank. Surplus defence gun-laying (GL) radar units provided the basic transmitting and receiving equipment, and a rotatable aerial array consisting of 12 horizontal half-wave dipoles was constructed. The aerial beam was directed to azimuths of 22.5 degrees north of west and 22.5 degrees south of west on alternate days, in order that the Clegg technique (Clegg, 1948 a and b; Aspinall, Clegg and Hawkins, 1951)

could be employed to delineate meteor radiants. The operation of this equipment was steadily improved and in 1953 a survey was made of meteor activity in the Southern Hemisphere (Ellyett and Roth, 1955). A major conclusion was that the greater part of the meteor activity down to magnitude +4.5 is confined to the plane of the ecliptic.

During the 1953 survey the overall sensitivity of the radar system was adjusted to maintain the radar echo rate somewhat similar to the normal visual meteor rate of 5-10 per hour when no major shower activity is present. After 1953 no attempt was made to compare radar and visual meteor rates and the system sensitivity was improved considerably, yielding echo rates much higher than the equivalent visual rates. The echo rates obtained in the early months of 1956, which was considered to be a period of minimum meteor activity, averaged about 100 per hour. This indicated that meteors as faint as the seventh magnitude were recorded.

Analysis of these records revealed discrete radiant activity near the helion and anti-helion positions in the sky and suggested that showers of faint meteors may exist (Ellyett and Keay, 1956). However, the amount of data reduction required for delineating showers from records containing as many as 2,000 meteors each day was prohibitive whenever the classic Clegg methods were used. This led to the development of a new and faster method of inter-

preting the data contained in meteor echo records when the echo-rate exceeds about 30 per hour (Keay, 1957). The new method requires the drawing of "partial rate curves" rather than the range-time plots of individual meteor echoes. A partial rate is simply the time rate of meteor echo occurrence between specified range limits. When this method was first employed, the range band chosen was that which straddled the range at which the greatest number of meteor echoes occurred. This obviated any question of allowing for an asymmetrical distribution of meteors within the range band.

Meanwhile the whole radar system had been steadily improved. A new receiver was built having a noise figure of 2.0 at the operating frequency of 69 Mc. (Ellyett and Fraser, 1955) which meant that the reception of faint meteor echoes was limited by the galactic noise level rather than the internal noise of the receiver. Furthermore, a study of the overall system characteristics (ibid) revealed the need to increase the transmitted pulse width quite considerably in order for the finite spot size on the cathode ray tube display (which is photographed on slowly moving film) to be smaller than the echo pulse. Otherwise the signal-to-noise ratio is degraded and small echoes are lost. Accordingly the transmitter was adjusted to deliver a pulse of approximately 25 microseconds duration.

The transmitter had, by this time, been replaced by an improved version known as the GL Mark II. Also, during 1955-56, two new multiple-yagi arrays were constructed (Bennett, 1958), each having a power gain over isotropic of close to 1000, about eight times that of the rotatable array. These were directed to azimuths of 67.5 and 112.5 degrees east of north and overcame the need to alter the azimuth setting of the rotatable array for alternate days. (The characteristics of the various aerials employed at the field station are tabulated in Appendix I).

Finally, with the possibility of several radars operating simultaneously and the need for phasing them one with another and with the mains supply, a crystal controlled master control unit was built (Keay, 1956). This unit supplied transmitter trigger pulses, range markers, receiver suppression pulses, gating waveforms, and other synchronous signals for the proper functioning of the station equipment.

# PART A

## THE MEASUREMENT OF METEOR RADIANTS

### 3. EXTENSIONS TO THE PARTIAL RATE METHOD OF DELINEATING METEOR RADIANTS

Throughout the second half of 1956 the improved dual-aerial radar system was in full operation, producing records amenable to analysis by the partial rate method. The Delta Aquarid radiants derived from records obtained during the first week of August were published in the paper describing the method (Keay, 1957).

Subsequently the remainder of the records were analysed and finally published in 1961 (Ellyett et al.). A typical partial rate plot revealing the presence of shower activity during the night of July 29 - 30 is shown in Figure 1(a) (which is taken from the 1961 paper). The range limits chosen were 350 and 450 km in order that the range band would be centred on 400 km, which was close to the range at which the maximum number of echoes was received. The rate of occurrence of meteors within these range limits was measured every ten minutes and the values obtained were then smoothed in sliding groups of three, weighted in the ratio 1:2:1 to give a smoothed rate curve.

This amount of smoothing is justifiable on the grounds that any detectable radiant of meteor activity cannot pass through the collecting area of the aerial system in less than half an hour.

The showers appearing in Figure 1(a) are the Delta Aquarids (K), the Pisces Australids (L) and possibly a Cetid shower (M). The method of deriving the radiant co-ordinates of these showers is described in Chapter 6.

Partial rate plots exhibiting possible shower activity are shown in Figure 1(b). The peaks labelled P and Q were present on adjacent days and P yielded a Puppis radiant. The peak to the left of P in both plots was definite enough to enable radiant co-ordinates to be found for it, but it was not present on adjacent days so was not considered reliable. The same is true for the other pairs of peaks in Figure 1(b). This raises the question of which peaks to relate to one another. Could, for example, the peak Q in the lower curve be produced by the meteor activity which gave rise to the peak P in the upper curve? This ambiguity was to a certain extent resolved by considering the persistence of the pairs of peaks on adjacent days. Later a triple aerial technique was evolved (see below) to resolve such difficulties.

However, the two major humps in both partial rate curves clearly bear an unambiguous relationship to one another and indicate concentrations of meteor activity

centred on the co-ordinates defined by the times at which the smoothed maximum rate occurs (see Chapter 6).

The partial rate plots shown in Figure 1(c) exhibit fluctuations in rate which are almost as great as those in Figures 1(a) and (b), but no clear-cut relationship is evident between the two plots and it becomes a problem to assess the validity of the peaks that are present. This is particularly so for the peak at 11 hours L.T. in the upper plot and that near 8 hours L.T. in the lower plot. For this reason it was decided to count and plot the meteor echoes occurring in the two 100 km range bands adjacent to the principal one centred on 400 km range. This led to the sets of triple plots shown in Figures 2(a) and (b). The peaks which are due to continuous meteor shower activity are quite obvious. Of the remaining peaks, the larger ones may be due to short-lived minor streams of meteoroids being intercepted by the earth, or they may be produced solely by random factors. However, a peak such as that at 11 hours L.T. in the upper curve of Figure 1(c) exhibits such a high degree of positive conservation* that

---

*If a time-series of observations yields values that are perfectly random its conservation is said to be zero. If low values tend to occur after high values, and vice versa, the conservation is negative, and if high values tend to be grouped together followed by a group of low values, and so on, the conservation is positive. (See, for example, p.582 of "Geomagnetism" by Chapman and Bartels, 1951.)

it is unlikely to be the product of random fluctuations alone. This aspect of the occurrence of meteors has been the subject of a separate investigation which is not yet concluded. It is sufficient to say that some workers (e.g. Bowden and Davies, 1957) regard sporadic meteors as being completely random in occurrence, while others (particularly Gallagher and Eshleman, 1960) consider that faint meteors have 'sporadic shower' properties. No satisfactory explanation has yet been found for the rather pronounced but isolated peaks which often occur in the partial rate curves such as those in Figure 1(c), although Weiss (1959) has argued that the great majority of peaks in the partial rate plots are due to random fluctuations in the meteor rate.

Some of the ambiguities inherent in the use of partial rates obtained from dual aerials can be removed by incorporating a third aerial equally spaced in azimuth with the original two. A genuine centre of meteoric activity then produces a sequence of peaks in the three aerials in turn, thereby revealing its presence among other peaks of lesser significance. This improved technique, sometimes referred to as the augmented partial rate method of delineating meteor radiants, is fully described in Chapter 6.

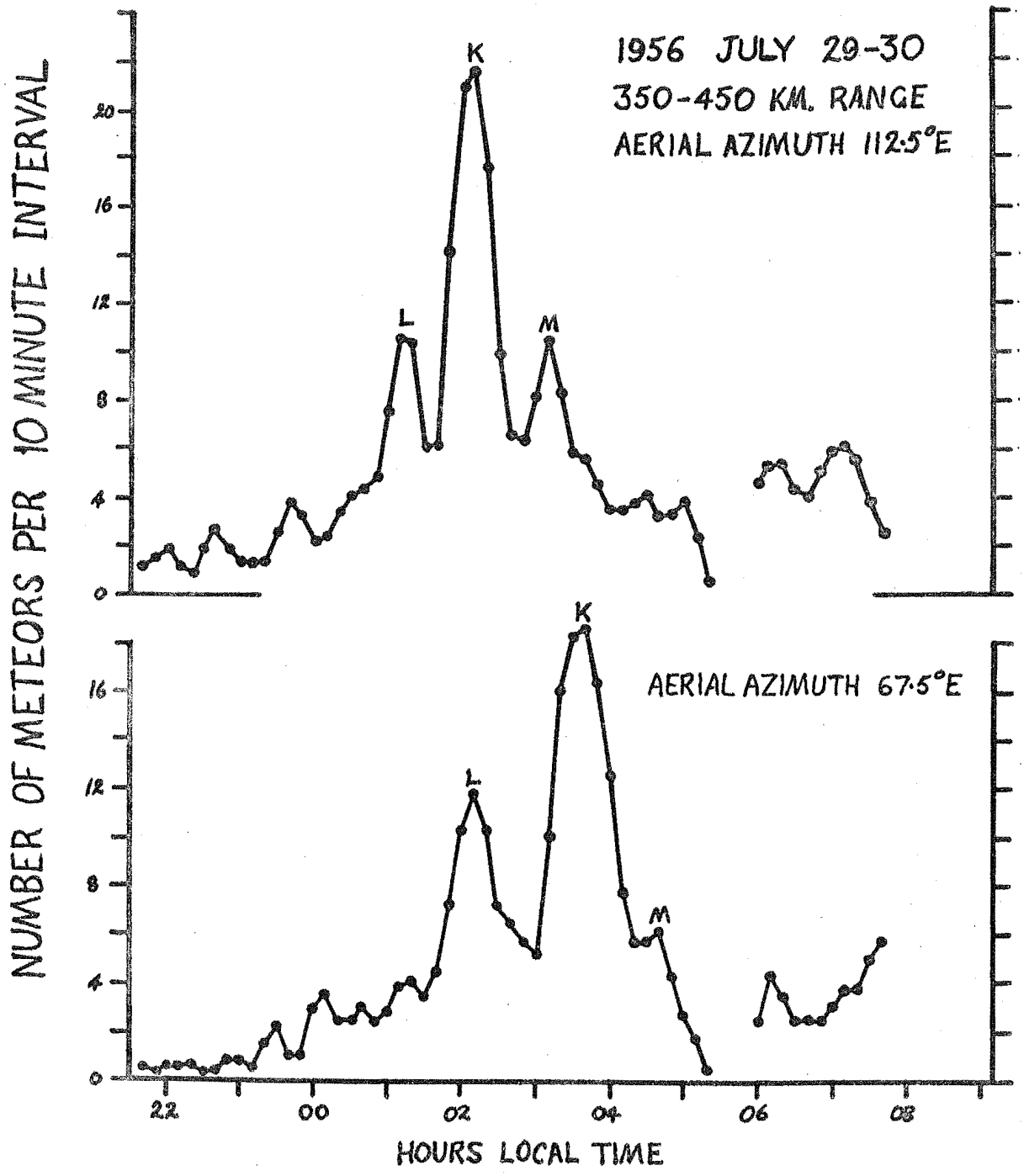
1956 JULY 29-30
350-450 KM. RANGE
AERIAL AZIMUTH 112·5°E
AERIAL AZIMUTH 67·5°E
K
L
M
NUMBER OF METEORS PER 10 MINUTE INTERVAL
HOURS LOCAL TIME
22
00
02
04
06
08
0
4
8
12
16
20

Fig. 1.(a)

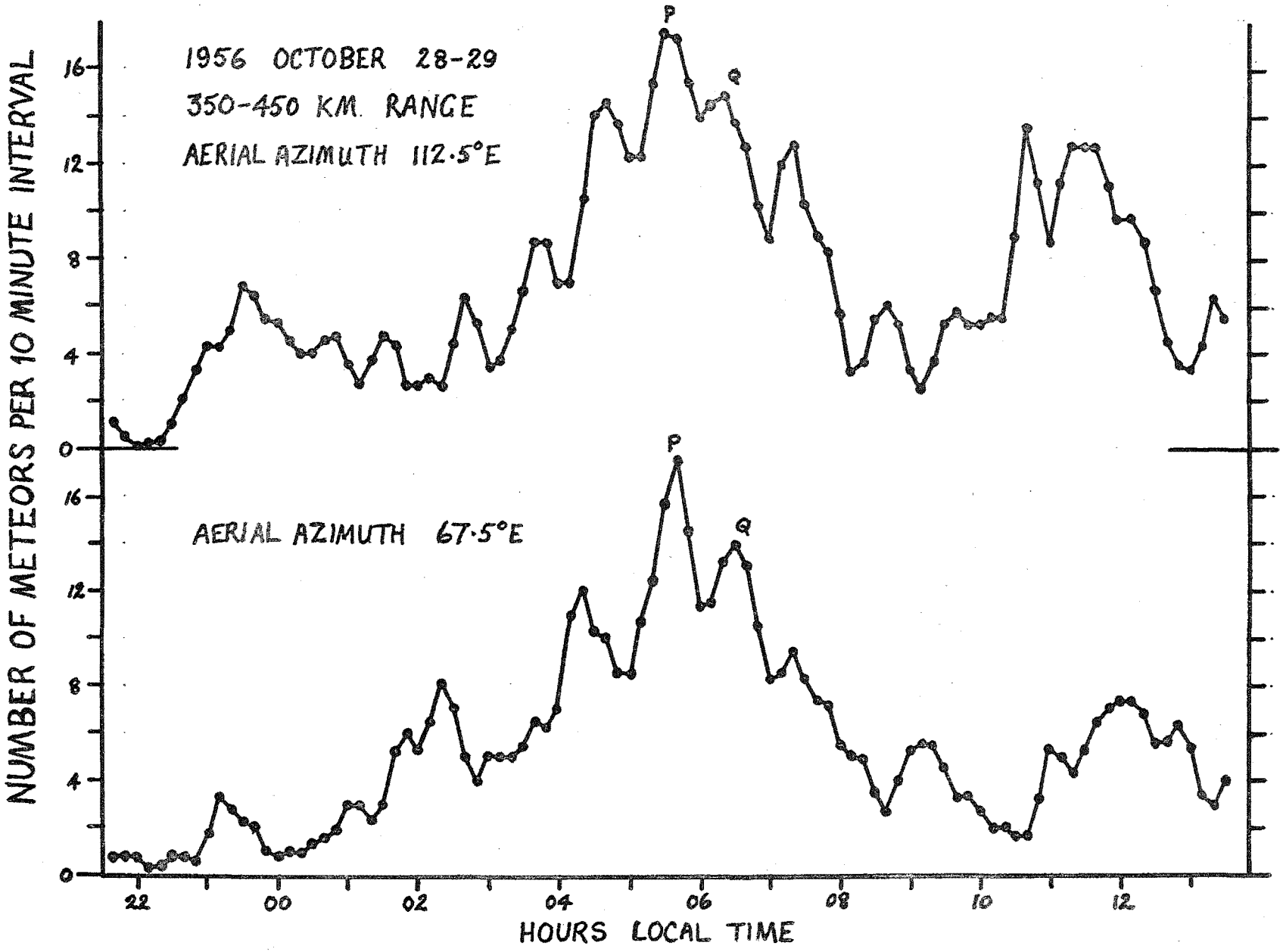
1956 OCTOBER 28-29
350-450 KM. RANGE
AERIAL AZIMUTH 112·5°E
AERIAL AZIMUTH 67·5°E
P
Q
NUMBER OF METEORS PER 10 MINUTE INTERVAL
0
4
8
12
16
22
00
02
04
06
08
10
12
HOURS LOCAL TIME

Fig. 1.(b)

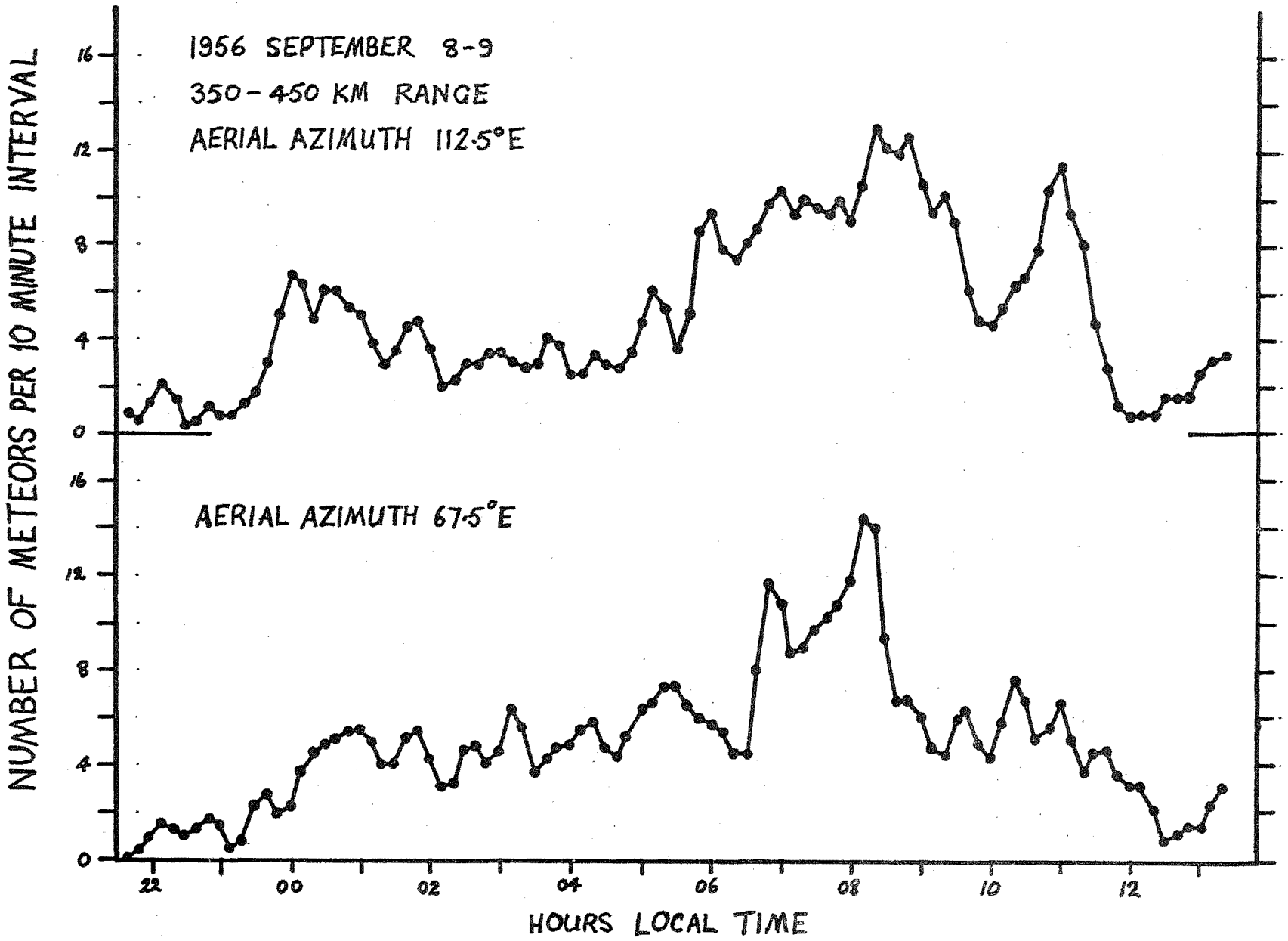
1956 SEPTEMBER 8-9
350 - 450 KM RANGE
AERIAL AZIMUTH 112·5°E
AERIAL AZIMUTH 67·5°E
NUMBER OF METEORS PER 10 MINUTE INTERVAL
0
4
8
12
16
22
00
02
04
06
08
10
12
HOURS LOCAL TIME

Fig. 1.(c)

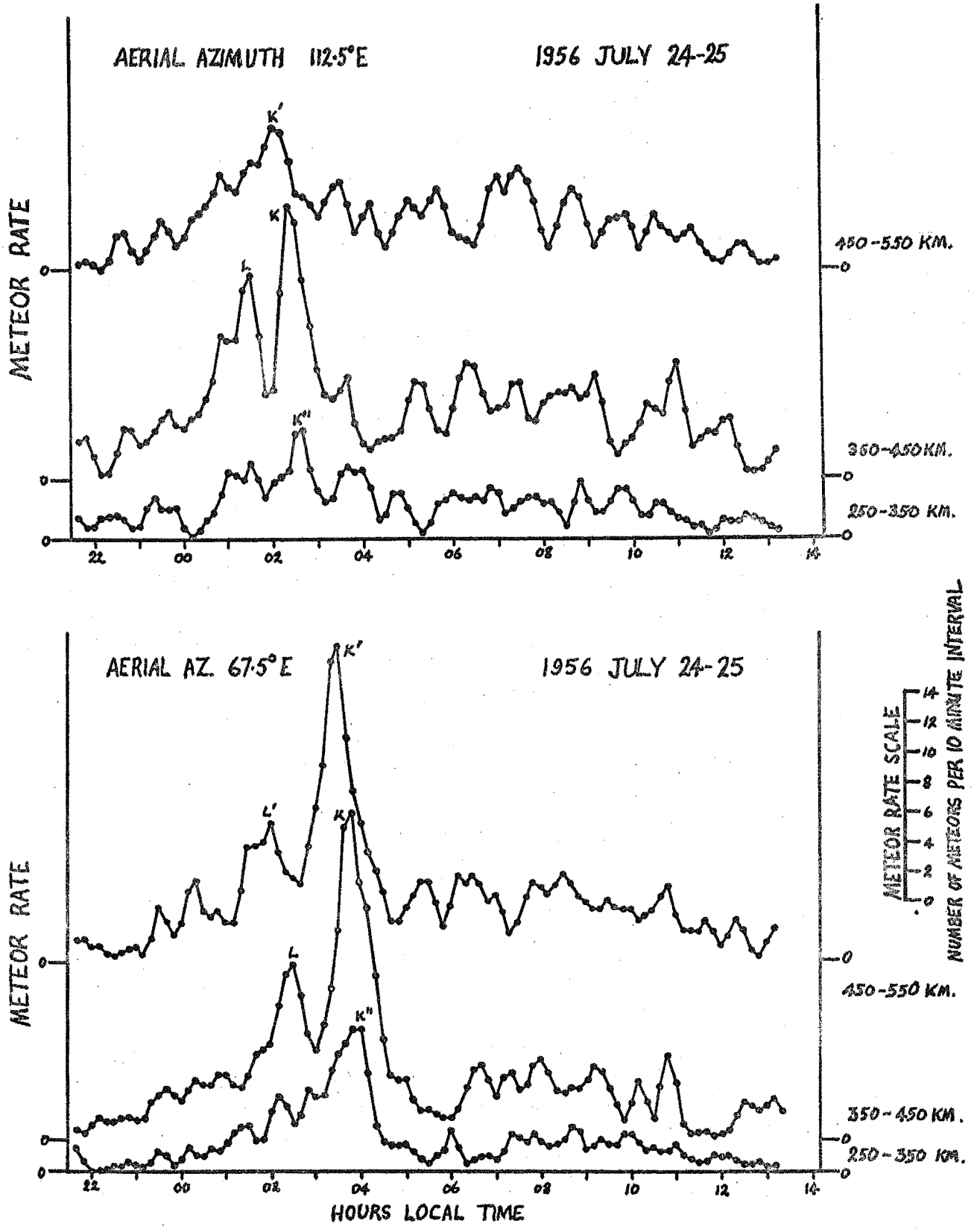
AERIAL AZIMUTH 112·5°E
1956 JULY 24-25
METEOR RATE
K'
K
L
K''
450-550 KM.
350-450 KM.
250-350 KM.
22
00
02
04
06
08
10
12
14
AERIAL AZ. 67·5°E
1956 JULY 24-25
L'
METEOR RATE SCALE
NUMBER OF METEORS PER 10 MINUTE INTERVAL
HOURS LOCAL TIME

Fig. 2 (a)

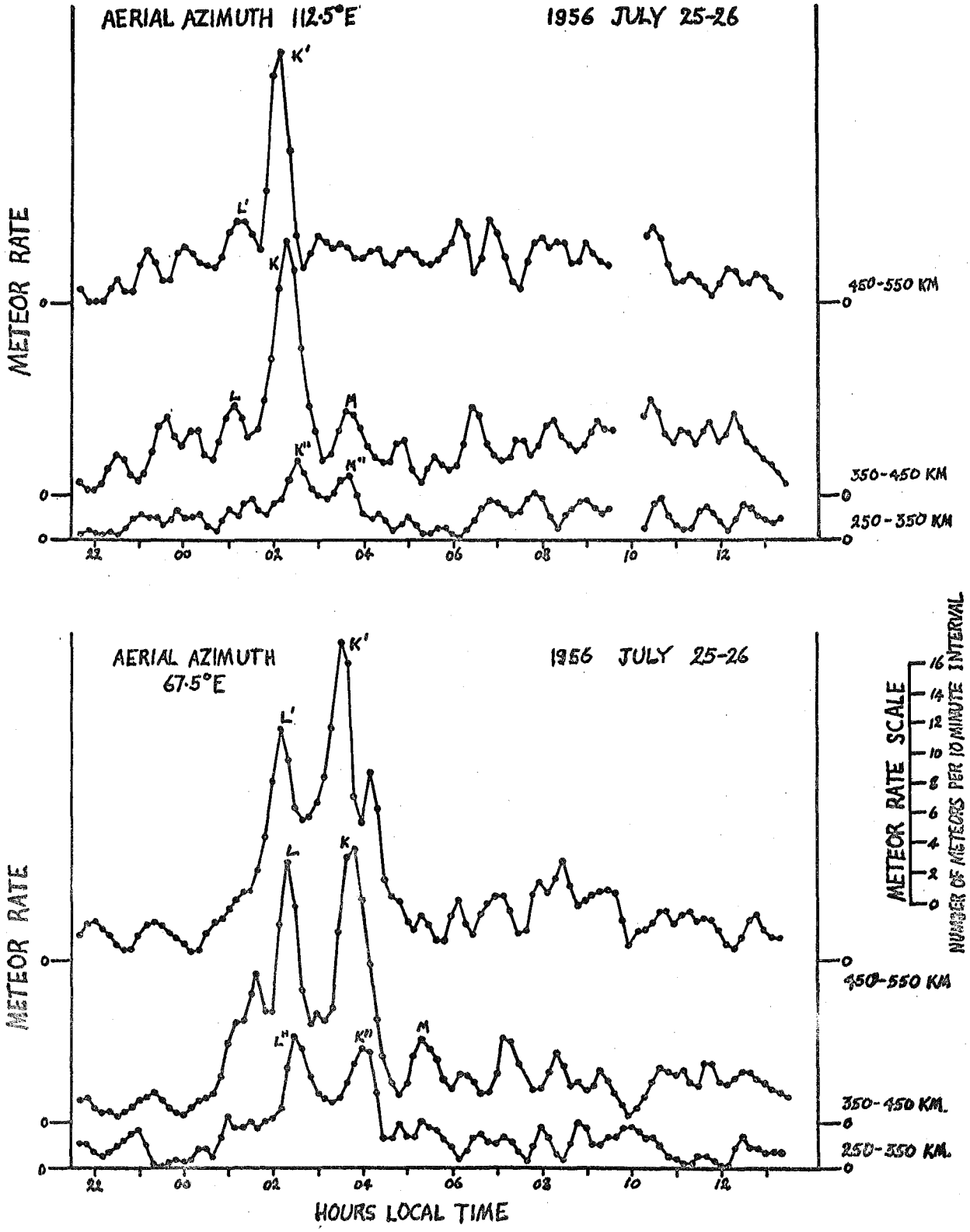
AERIAL AZIMUTH 112·5°E
1956 JULY 25-26
METEOR RATE
K'
L'
K
L
M
K''
N''
450-550 KM
350-450 KM
250-350 KM
22
00
02
04
06
08
10
12
AERIAL AZIMUTH 67·5°E
1956 JULY 25-26
METEOR RATE
L''
K''
METEOR RATE SCALE
NUMBER OF METEORS PER 10 MINUTE INTERVAL
350-450 KM.
250-350 KM.
HOURS LOCAL TIME

Fig. 2 (b)

## 4. THE LATITUDE DEPENDENCE OF RADAR METEOR SHOWER OBSERVATIONS*

One of the principal weaknesses of the partial rate plots is the tendency during analysis to pair peaks occurring at nearly the same time. A glance at Figure 4 of Chapter 6 reveals that the resulting values of radiant declination will tend to cluster around the value corresponding to the latitude of the observing station. Furthermore, peaks due to activity passing directly overhead may be considerably enhanced by the characteristics of the radar system, i.e. on the aerial configuration employed.

This problem was first recognised by Dr. C. D. Ellyett who plotted a histogram showing the total number of pairs of peaks in the 1956 partial rate curves as a function of the declination derived for them. This histogram is shown in Figure 1. A very similar result has been obtained more recently by Hawkins (1963) who simply remarks that the sensitivity of the equipment used in the Harvard Radio Meteor Program decreases as the radiant altitude decreases.

---

*This chapter has been adapted from a paper with the same title written by this author and Dr. C. D. Ellyett. It appeared in the Journal of Geophysical Research, Vol. 66, page 2337, 1961.

Such a latitude bias must inevitably lead to an erroneous impression of the relative strengths of observed meteor showers. In other words, the hourly rates for radio observations quoted in the literature (for example, Whipple and Hawkins, 1959) are without meaning, unless it is understood that they apply only to a particular observing station.

To be meaningful, rate measurements should be converted to incident meteor flux measurements (Kaiser, 1960) but the conversion involves experimental difficulties and laborious calculations. It has been attempted, for example, by Weiss (1957), who obtains values for eight meteor showers.

Kaiser (1960) has published a semigraphical method enabling the incident flux of shower meteors to be deduced from the observed rate. This method is considerably simpler than any previous one, but even so the amount of computation required may not be justified unless it is imperative that an absolute flux measurement be obtained.

However, for the purpose of establishing the relative importance of showers detected from any given observing station, and eliminating the tendency to emphasize those showers which transit close to the zenith, a simple plot of observed rate against declination can be most helpful, as will now be shown.

## 4.1 Theory

Expressions for the total radio echo rate of shower meteors detected by apparatus employing narrow-beam aerials have been derived by Kaiser (1955). For a narrow aerial beam he obtains the following close approximation for the total echo rate, N:

$$N \cong A\Theta(\alpha_o / \cos\chi)\, F(\phi) \qquad (1)$$

where A is a function of the mass distribution parameter s, the aerial beam width, the mean height of the reflection points, and the atmospheric scale height. These will be regarded as constants for the purposes of this discussion.

The flux function $\Theta(\alpha_o / \cos\chi)$ depends also on s and can be rewritten in the form $BN_i \cos^{s-1}\chi$, where B is a function of the minimum detectable line density $\alpha_o$ in the direction of the beam maximum, i.e., it is an equipment parameter, and $N_i$ is the incident meteor flux for the shower concerned. The angle $\chi$ is the zenith angle of the trajectory of a detectable meteor, which to a good approximation is also the zenith angle of the true meteor radiant.

Following Kaiser, the remaining function $F(\phi)$ can be written

$$F(\phi) \cong \cos^{-2}\theta \sin^{-2}\chi \qquad (2)$$

where $\theta$ is the angle between the reflection point and the beam maximum. For narrow beam equipments the variation with

$\theta$ can usually be neglected, and we have finally

$$N \cong C N_i \cos^{s-1}\chi \sin^{-2}\chi \qquad (3)$$

where C is a function independent of $\chi$. Thus the above expression gives the observed echo rate as a function of the radiant zenith angle when the rate is at its maximum.

The recognition of a meteor shower of given flux when using methods essentially dependent on rate measurement is influenced by the radiant declination $\delta$. The sharpness of a peak in the echo rate must depend on the speed with which a radiant moves across the sky, and is, therefore, dependent on the cosine of the radiant declination. Inclusion of the factor $\cos\delta$ in equation 3 then leads to a simple expression showing how well a meteor shower may be recognized by using a given equipment at a given location:

$$W = \frac{\cos^{s-1}\chi \cos\delta}{\sin^2\chi} \qquad (4)$$

where W may be termed the recognition factor.

The variation of recognition factor with declination is strongly dependent on the range, R, at which echoes are received, since the zenith angle $\chi$ of a shower radiant at the time of maximum echo rate is itself a function of R. The variation with s and other parameters is relatively unimportant.

Figure 2 shows W plotted for various values of range

in the case of an equipment located at latitude $-43^{\circ}31'$ utilizing a narrow-beam aerial directed to a local azimuth of $112^{\circ}30'$E. The dotted curve is drawn for echoes received from a range of 400 km by an aerial directed to a local azimuth of $67^{\circ}30'$E.

The resemblance between the sum of the full and dotted 400 km range curves in Figure 2 and the envelope of the histogram in Figure 1 (referring to partial rate curves for range bands centred on 400 km range) is close enough to indicate that the assumptions made in deriving the expression for W are quite reasonable.

It is evident from Figure 2 that any method of meteor shower detection that depends on the presence of long-range echoes will greatly favor radiants culminating near the zenith. To avoid this source of bias as far as possible, methods of meteor-shower delineation should utilize short-range echoes.

## 4.2 Application to Christchurch Results

During 1953 a survey of Southern Hemisphere meteor activity was carried out (Ellyett and Roth, 1955) and the results were analyzed by drawing envelopes enclosing meteors from specific radiants on daily range-time plots of meteor echoes (Aspinall, Clegg, and Hawkins, 1951). The major showers detected by this survey, together with

the significant meteor showers detected in 1956, are shown in Figure 3 in which the maximum hourly rate of each shower is plotted against the shower declination.

Superimposed on the shower plot are two curves representing the shower recognition factors for the two aerials of the system. These have been calculated on the assumption that the range of maximum occurrence of meteors (400 km) leads to fair values for the shower recognition factor in the case of meteors recorded over a wide-range interval as in the range-time plot method. For the partial-rate method, of course, it is perfectly valid since the range interval used was centred on 400 km.

In Figure 3 and subsequent figures the recognition curves have been normalized by making the peak value of W correspond to an hourly echo rate of 100. The showers of highest flux in Figure 3 are those which rise above the two recognition curves by the greatest amount. Examples are the $\delta$-Aquarids and the $\beta$-Taurids.

Similarly, showers whose observed echo rates cause them to lie well below the recognition curve are of lowest flux. The showers shown dotted in Figure 3 yielded echo rates higher than many of the major showers shown, but it is obvious from the figure that they are of much less importance. (These particular showers did not, in fact, meet the requirements of consistency necessary for shower acceptance, and have been excluded from published lists.)

## 4.3 Application to other observing stations

Simple calculations have been made for two other observing stations which have used narrow-beam dual-aerial systems for the delineation of meteor radiants. For these two stations, namely, Jodrell Bank and Adelaide, meteor shower recognition curves are shown in Figures 4 and 5. The curves are based on parameters published by Aspinall, Clegg and Hawkins (1951), and Weiss (1960), respectively. It must again be stressed that the height and sharpness of the peak in each curve depends on the way echoes are selected to yield the transit times necessary for determining radiant co-ordinates. However, the form of the curves will be accurate enough for qualitative discussion.

Superimposed on the shower recognition curves of Figure 4 and 5 are the rates and declinations of the main meteor showers observed at the two stations. (See Hawkins and Almond, 1952a and b; Almond, Bullough and Hawkins, 1952; Bullough, 1954; and Davidson, 1956, for the Jodrell Bank results, and Weiss, 1960, for the Adelaide results.) The showers shown dotted in Figure 5 are those classified by Weiss as possible showers, the others as accepted showers.

These figures are particularly illuminating if the Christchurch and Adelaide results are compared with those from Jodrell Bank. The relative importance of the different meteor showers is easily seen, and the results from both

hemispheres agree well as far as the major low declination showers are concerned.

Showers which transit close to the zenith, such as the Quadrantid shower detected at Jodrell Bank, appear reduced in importance compared with showers such as the $\eta$-Aquarids, whose low observed rate from all three stations belies their true strength. The $\delta$-Aquarids emerge as the strongest known meteor shower.

In each of the three figures it is seen that the recognition curves give a reasonable fit to the plotted shower rates, except in the case of the Adelaide results where the Arietids, $\zeta$-Perseids and $\beta$-Taurids are taken together, and where the Geminids appear to have produced a surprisingly high rate. The known low value of s for the Geminid shower does not entirely account for its observed rate of 60 per hour from Adelaide.

In a recent paper Kresak (1964) has calculated the latitude variation of the actual influx of shower and sporadic meteors. He does not include the effect of the detection characteristics of the observing equipment and therefore his findings for shower meteors cannot be directly compared with this work.

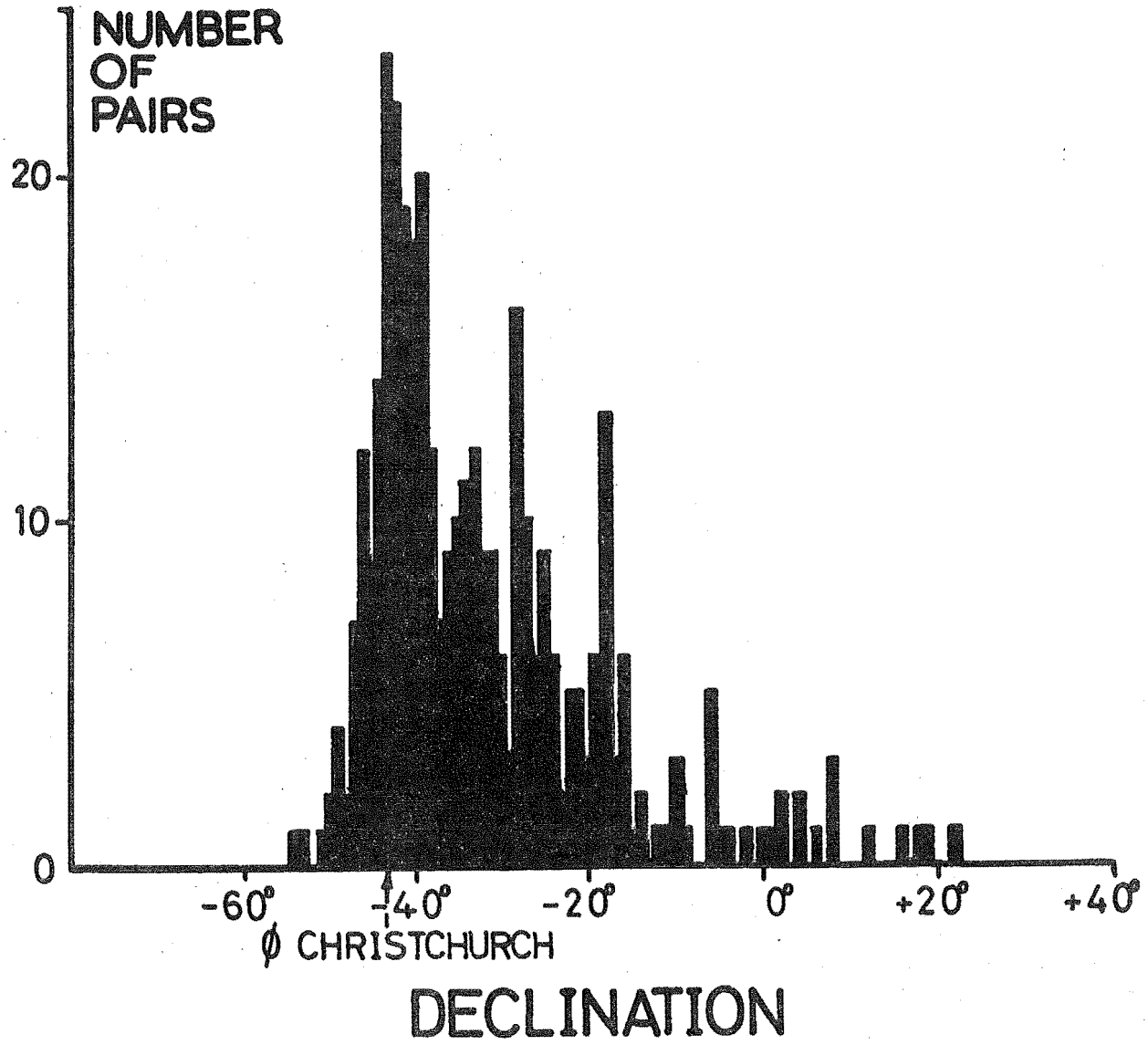


Fig. 1 - Histogram showing number of pairs of peaks in measured rate plotted against the resulting value of declination.

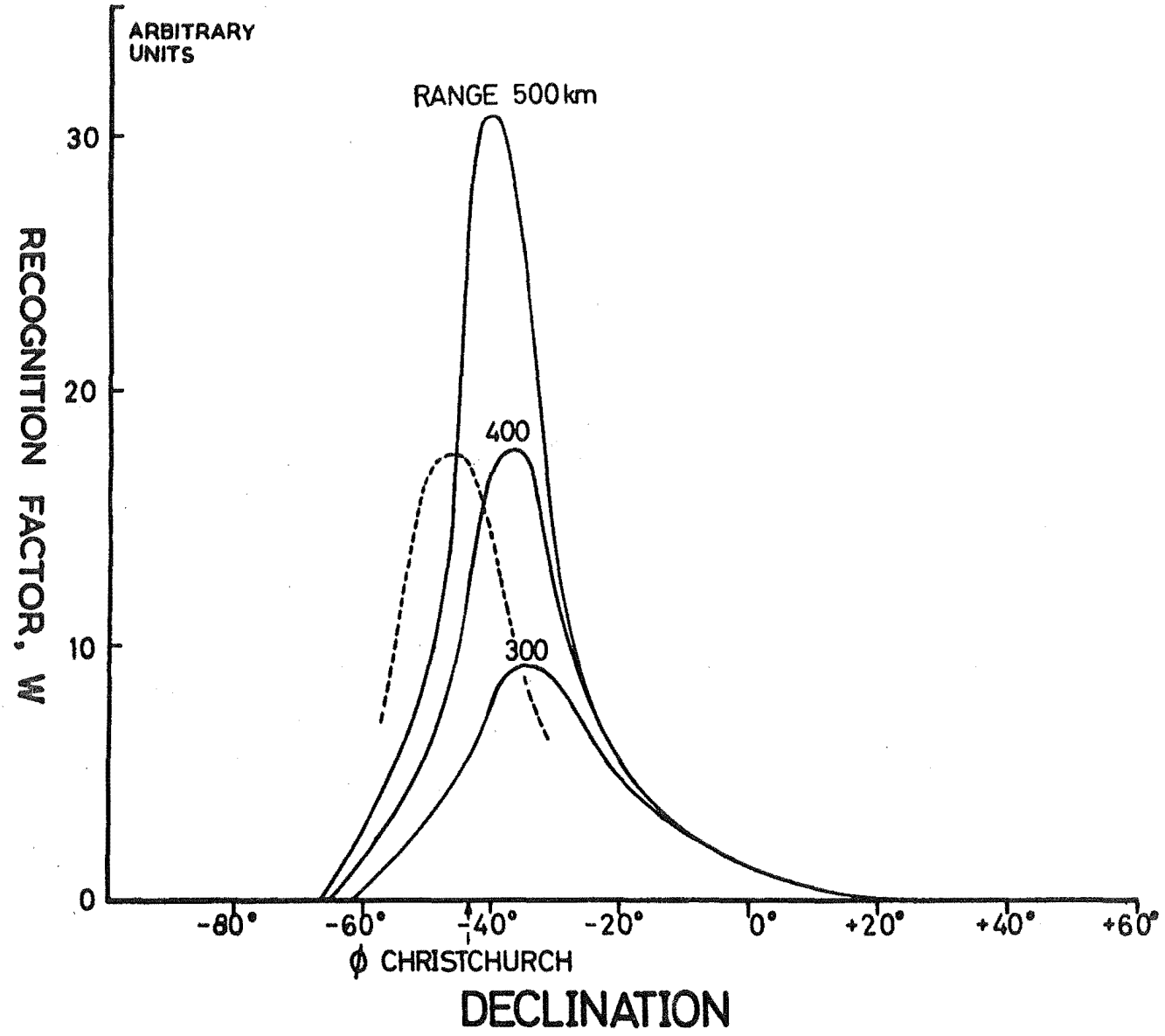


Fig. 2 - Meteor shower recognition factor, W, plotted as a function of shower declination.

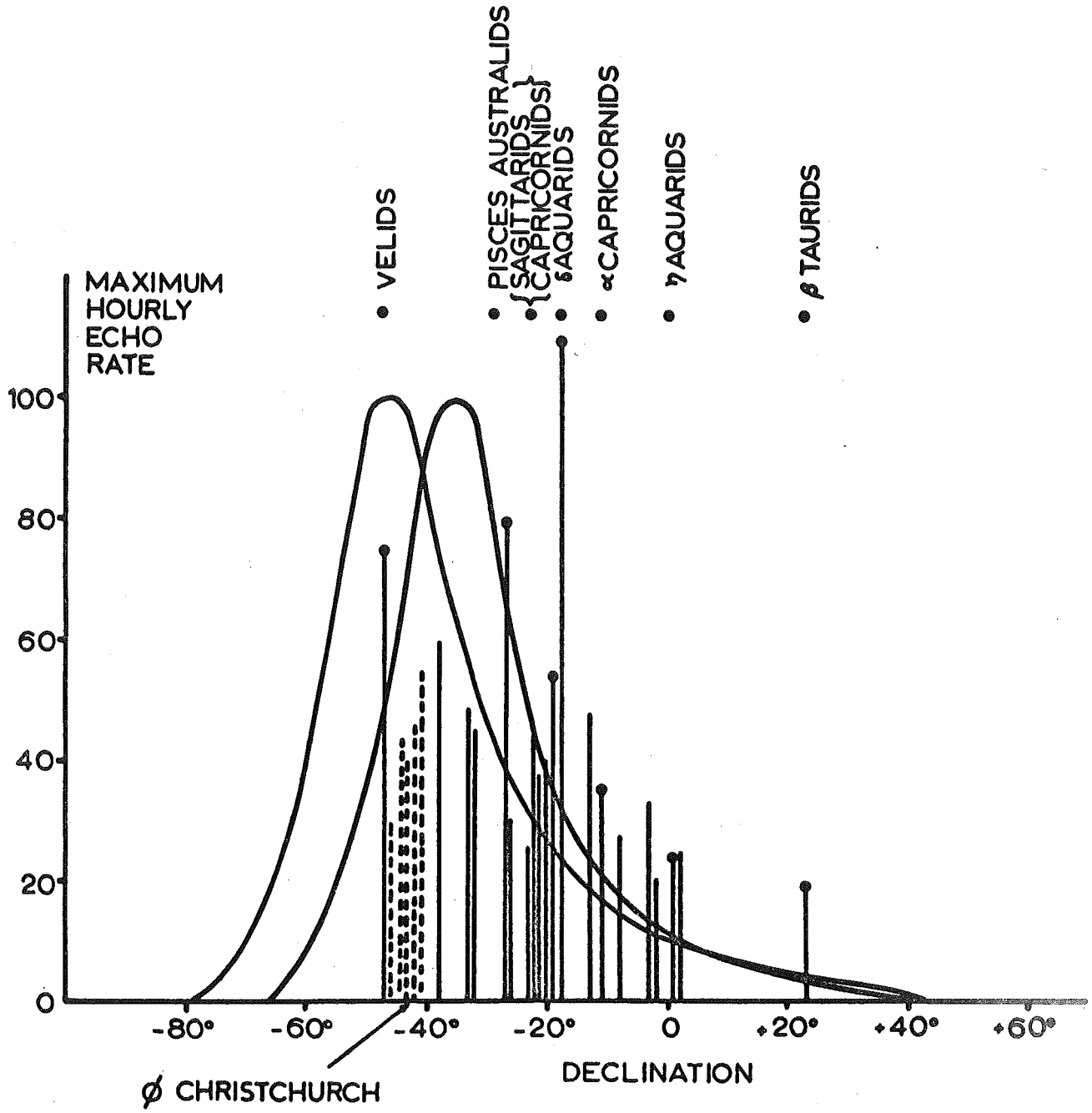


Fig. 3 - Maximum hourly echo rates of meteor showers observed from Christchurch compared with the shower recognition factors for the two aerials employed.

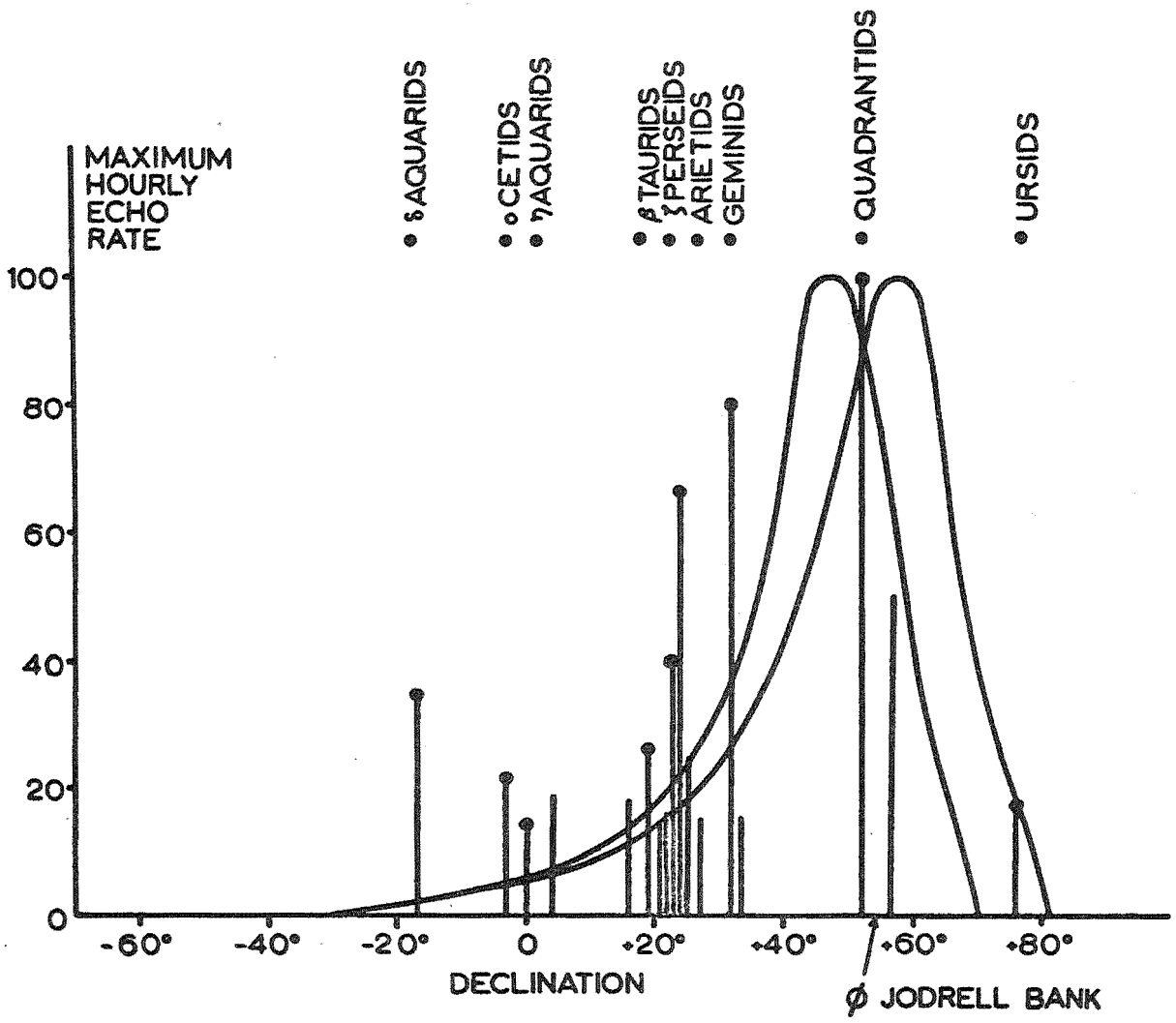


Fig. 4 - Maximum hourly echo rates of meteor showers observed from Jodrell Bank compared with the estimated shower recognition factors for the two aerials employed.

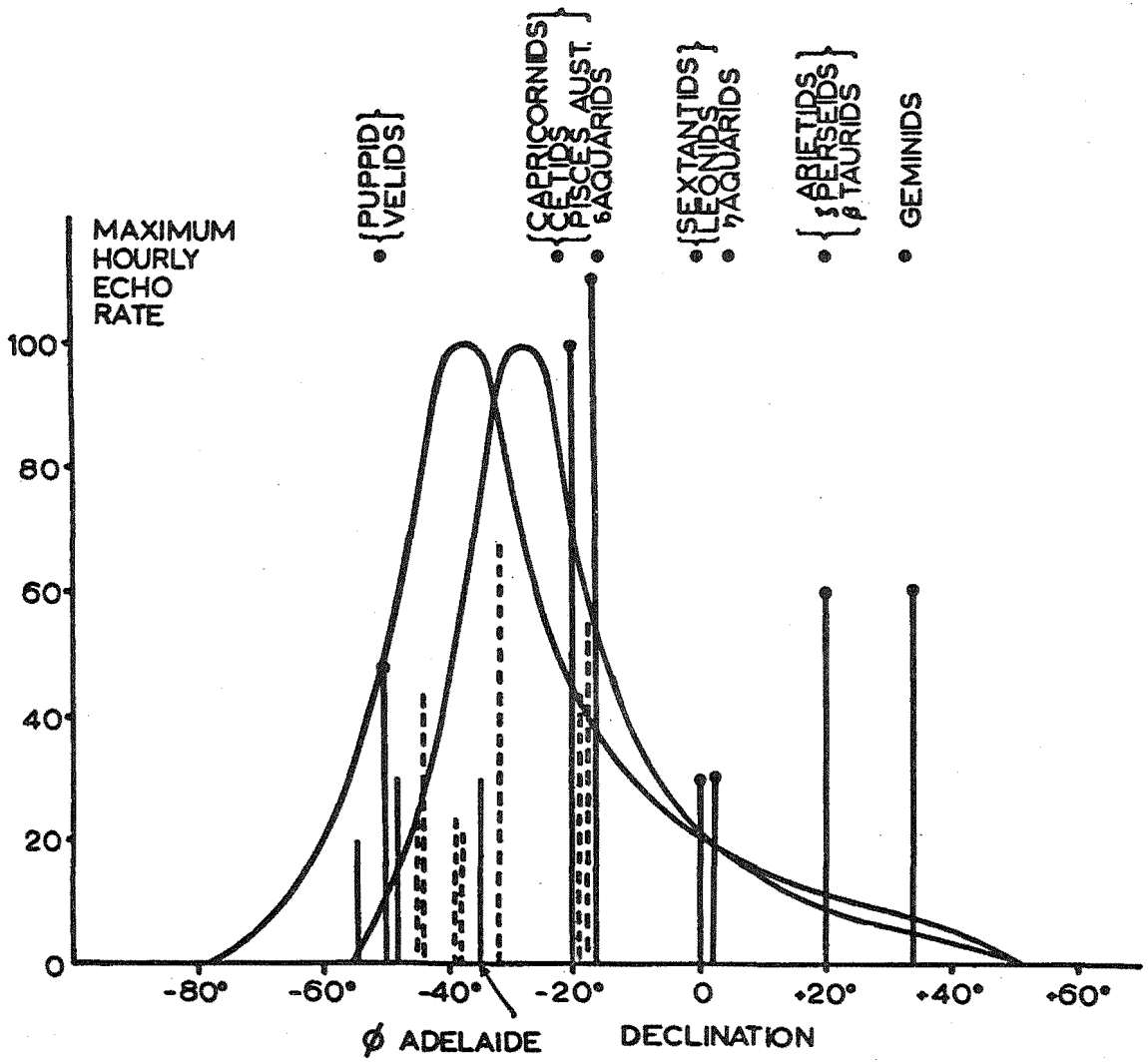


Fig. 5 - Maximum hourly echo rates of meteor showers observed from Adelaide compared with the estimated shower recognition factors for the two aerials employed.

## 5. THE TRIPLE-CHANNEL RADAR SYSTEM*

The introduction of the augmented partial rate system involved the following changes and extensions to existing equipment:

(a) Aerials: Design and construction of a new array.

(b) Transmitters: No alteration.

(c) Receivers: Construction of a third receiver.

(d) Display: Development of new video circuitry.

(e) Control: Minor modifications to the Master Control Unit.

A block diagram of the complete system is shown in Figure 1. The principal changes will now be described separately.

This Chapter is intended to supplement the discussion of the system given in the next chapter.

---

*Parts of this chapter and the one which follows have appeared in a contract report (Ellyett, Keay and McLauchlan, 1963.)

## 5.1 Aerials

The development of the aerials necessary for introducing the augmented partial rate method was eased by the existence of the original rotatable array which could be turned and locked to an azimuth midway between the azimuths of the yagi arrays (see Appendix 1 for details). By using each of these three aerials for transmitting as well as receiving, the aerial requirements would have been met had it not been for long-standing difficulties encountered in connection with the necessary spark-gap transmit-receive switching. Unreliability, noisiness and breakthrough all combined to force the abandonment of spark-gaps as a means to this end. In addition it was considered desirable, if possible, to use one transmitter for the whole system instead of having one for each antenna. Accordingly a single wide-beam transmitting antenna was built capable of floodlighting the region searched by the three narrow-beam antennas, which could then be used for reception only (a plan of the actual coverage of the antennas is shown in Figure 1 of Chapter 6). The shape of the radiation pattern of the transmitting antenna led to it being referred to as a fan-beam antenna. Although the power gain of the fan-beam antenna is low, this loss has been offset by the elimination of spark-gap switching and has led to better overall system performance.

The design requirements of the fan-beam antenna were that it had to provide, as economically as possible, an azimuthal distribution of radiated power which would enable all three narrow beam arrays to receive meteor echoes. By iterative calculations it was found that a vertical stack of dipoles spaced 0.35 of a wavelength in front of a reflecting screen would produce the required azimuthal pattern. The gain factors used in the design are given in TABLE 1, the notation of which applies to the array geometry shown in Figure 2.

The vertical radiation pattern of the fan-beam antenna had to be compatible with those of the three narrow-beam arrays, although it was considered that a slight increase in elevation of the main lobe would be beneficial (see next chapter).

The above design requirements were satisfied by using a vertical stack of three half-wave folded dipoles spaced half a wavelength apart, with the lowest dipole one quarter of a wavelength above a ground screen, as indicated in Figure 2. The gain factors used are given in TABLE 2. Several other designs were considered, but this one has the advantage of a null at 40 degrees elevation which reduces the effect of the principal secondary lobes present in the other arrays near that angle of elevation.

The half-wavelength spacing of the folded dipoles

| $\alpha^{\circ}$ | $F_o(90-\alpha)$ | $G^2_{\frac{1}{2}},\ ^{0.7}(\alpha)$ | Product |
|---|---|---|---|
| 0 | 1.000 | 1.6181 | 1.6181 |
| 5 | 0.995 | 1.6278 | 1.6197 |
| 10 | 0.978 | 1.6564 | 1.6200 |
| 15 | 0.955 | 1.7015 | 1.6249 |
| 20 | 0.914 | 1.7592 | 1.6079 |
| 25 | 0.868 | 1.8243 | 1.5835 |
| 30 | 0.817 | 1.8896 | 1.5438 |
| 35 | 0.758 | 1.9470 | 1.4758 |
| 40 | 0.696 | 1.9870 | 1.3830 |
| 45 | 0.627 | 1.9999 | 1.2539 |
| 50 | 0.557 | 1.9754 | 1.1003 |
| 55 | 0.490 | 1.9050 | 0.9335 |
| 60 | 0.418 | 1.7820 | 0.7449 |
| 65 | 0.346 | 1.6026 | 0.5545 |
| 70 | 0.275 | 1.3668 | 0.3759 |
| 75 | 0.205 | 1.0779 | 0.2210 |
| 80 | 0.141 | 0.7453 | 0.1051 |
| 85 | 0.080 | 0.3810 | 0.0305 |
| 90 | 0.000 | 0.0000 | 0.0000 |

$$G^2_{\frac{1}{2}},\ ^{0.7}(\alpha) = \frac{\text{Sin } 2(0.5\pi - 0.7\pi \text{ Cos } \alpha)}{\text{Sin } (0.5\pi - 0.7\pi \text{ Cos } \alpha)}$$

TABLE 1 Gain factors for calculating the horizontal radiation pattern of the Fan-Beam Antenna.

| $\beta^{\circ}$ | $F^{3,\ 0.5(90-\beta)}$ | $G_{\frac{1}{2}}^{2,\ 0.7(\beta)}$ | $G_{\frac{1}{2}}^{2,\ 1.5(90-\beta)}$ | Product |
|---|---|---|---|---|
| 0 | 3.000 | 1.618 | 0.000 | 0.000 |
| 5 | 2.926 | 1.628 | 0.799 | 3.806 |
| 10 | 2.710 | 1.656 | 1.460 | 6.552 |
| 15 | 2.375 | 1.702 | 1.878 | 7.591 |
| 20 | 1.952 | 1.759 | 1.999 | 6.864 |
| 25 | 1.481 | 1.824 | 1.826 | 4.933 |
| 30 | 1.000 | 1.890 | 1.414 | 2.672 |
| 35 | 0.539 | 1.947 | 0.852 | 0.894 |
| 40 | +0.128 | 1.987 | +0.223 | 0.057 |
| 45 | -0.213 | 2.000 | -0.382 | 0.163 |
| 50 | -0.486 | 1.975 | -0.908 | 0.872 |
| 55 | -0.684 | 1.905 | -1.317 | 1.716 |
| 60 | -0.827 | 1.782 | -1.614 | 2.379 |
| 65 | -0.916 | 1.603 | -1.808 | 2.655 |
| 70 | -0.957 | 1.367 | -1.919 | 2.510 |
| 75 | -0.989 | 1.078 | -1.974 | 2.105 |
| 80 | -0.998 | 0.745 | -1.995 | 1.483 |
| 85 | -1.000 | 0.381 | -2.000 | 0.762 |
| 90 | -1.000 | 0.000 | -2.000 | 0.000 |

TABLE 2 Gain factors for calculating the vertical radiation pattern of the Fan-Beam Antenna.

made feed and matching arrangements very simple. Each of the three elements was fed equally in amplitude and phase. The impedance match to the transmission line was very close to optimum, with only a small adjustment of a quarter wave support stub being necessary to bring the standing wave ratio to less than 1.1.

When it was completed the performance of the fan-beam antenna proved to be very satisfactory. Measurements of its directivity were made using a balloon technique, yielding the results shown in Figures 3 and 4. Figure 5 is a photo of the antenna.

The horizontal radiation pattern has a slight dip at azimuth 90 degrees east which indicates that the radiating elements are a little too far away from the reflecting screen. The difference in pattern is so slight that no correction has been made.

The vertical radiation pattern is also fairly close to the calculated design. The main lobe appears to be one degree lower than anticipated, but this may be due to errors of measurement. The small upper lobe is much broader than the calculated size, due to the limited height of the reflector screen, which was restricted by the need to have clearance between it and a 200 Mc. rotatable array mounted on the same structure (see Figure 5). The resulting backward radiation from the uppermost dipole completely accounts for the broadness of the upper lobe.

## 5.2 Aerial Measurements

The balloon technique for measuring the radiation patterns of the fan-beam and other aerials at the Field Station has been fully described elsewhere (Keay and Gray, 1964 a and b). The method was suggested by this author to R. E. Gray who undertook its development as a supervised project (Gray, 1961), which resulted in the measurement of the vertical radiation patterns of the yagi and rotatable arrays. Some idea of the effectiveness of the balloon technique may be gathered from Figure 6, which shows the vertical radiation pattern of the rotatable array, as measured by Mr. Gray, compared with that calculated for the array.

Briefly, the technique consists in flying a small balloon-borne transmitter in a controlled arc centred on the aerial under test. A calibrated receiver connected to the aerial provides a record of the strength of the received signal which can be related to sightings of the transmitter's position to yield the radiation pattern almost immediately. The physical arrangement is shown in Figure 7.

Following some improvements, which included rebuilding the balloon-borne transmitter, measurements were made on the omni-directional aerials (see Chapter 7) and the fan-beam array as outlined earlier.

The balloon-borne transmitter had to be kept as simple as possible, consistent with good stability. The

circuit shown in Figure 8 uses a single OC170 transistor operated in common emitter mode with a small overtone crystal as frequency determining feedback element. It delivered a power output of 12 milliwatts which is ample for any measurement. The simplicity of the transmitter construction is revealed by the photo (Figure 9). The underneath compartment contains the battery which was of sufficient size to sustain full R.F. power output for at least twelve hours without any detectable departure from constancy. The variation of output power with changes in ambient temperature was not very great and its effect, if present, was largely cancelled by immediately repeating every balloon run in the opposite direction.

## 5.3 Receivers

A third receiver was constructed by E. C. McLauchlan to a design which had been developed as a result of many years of experience. A block diagram of a complete receiver is shown in Figure 10 and a photo of one in Figure 11.

The initial design was by G. J. Fraser (1954). Following modifications to the I.F. strip by the author (Keay, 1956), it was shown by R. G. T. Bennett that a second I.F. strip, of wider bandwidth than the first and off-tuned to a neighbouring frequency, could, by virtue

of its faster response time, provide a signal which could be used to gate the main I.F. strip off whenever broad-band impulse-type interference was present. The design of the second I.F. strip was fairly straightforward: it has a bandwidth of 300 kc, five times that of the main I.F. strip, and is tuned 400 kc higher. The second, or sub-I.F., strip was constructed by E. C. McLauchlan, who built all three of the receivers now in service. Mr. McLauchlan also redesigned the R.F. input stage to a cascode circuit and developed a new video amplifier which compressed the video signal to match the narrow dynamic range of the intensity modulated spot on the cathode ray tube screen and automatically adjusted itself to changing noise levels (McLauchlan, 1960).

A very useful check on the performance of the narrow beam antennas and their associated receivers was provided by a pen recorder which continuously monitored the detector current in each receiver. All records exhibited a prominent peak which recurred every day at the sidereal time corresponding to the passage of the Sagittarius region of the Local Galaxy through the associated antenna beam. This is apparent in Figure 12 which shows superimposed tracings of the records obtained over a period of one fortnight. The differences in beam-width of the antenna arrays are also clearly revealed.

Figure 12 also provides convincing verification of

the earlier conclusion by Ellyett and Fraser (1955), that further improvements to the noise figure of the receiver cannot improve the input signal to noise ratio, the limit being set by galactic radio noise.

## 5.4 Display Unit

The actual operation of this part of the system is described in detail in the next chapter. When the triple-channel radar system was first under consideration it was realised that a concise presentation of the outputs of the three channels was essential. It was suggested by the author that the most promising solution lay in the use of delay lines in the video section to time-code the three outputs.

An investigation of alternative methods was undertaken by B. J. Fraser (1961) who finally developed and built a system based on the use of delay lines as in the block diagram shown in Figure 13.

Two samples of the resulting film presentation are shown in Figure 14. Each sample represents a three-minute interval, but the clocks (and detector current meters) at the side of the film are not shown. Figure 14(a) was recorded at 1830 hours N.Z.S.T. when the diurnal rate is at its lowest, while Figure 14(b) is of a typical high rate period. The three different dot-spacings are quite

evident; narrow spacing corresponds to meteors detected on the East antenna, (Receiver - 1), the medium spacing to the North of East antenna (Receiver - 2), and the wide spacing to the South of East antenna (Receiver - 3). In both samples it will be noticed that the lower dot of each medium spaced pair is fainter than the upper dot: this temporary fault was due to a slight inaccuracy in the gain setting of the undelayed signal through that channel. Such a simple maladjustment can easily happen and its effect is exaggerated by the narrow dynamic range of the cathode-ray tube screen.

In Figure 14(a) there is a total of nine echoes, corresponding to an echo rate of 180 per hour. In Figure 14(b) there are 67 discernable echoes, corresponding to a rate of 1340 per hour. It may be remarked that even if the lowest rate of 180 per hour continued throughout the day, the resultant total of over 4000 echoes would be far too many to be handled by the original Clegg method of analysis.

Figure 14(b) shows many echoes which have been detected by more than one antenna, usually by the main beam of one and a side lobe of another. Such cases are easily sorted out by heeding the strongest echo. However, there are four of the 67 echoes which are completely ambiguous and must be disregarded.

## 5.5 Master Control Unit

The master control unit was already in existence and very little modification was required to make it supply all of the necessary timing wave forms. Its block diagram is shown in Figure 15. The 150 c/s repetition frequency for the 69 Mc. transmitted pulses (p.r.f.) was derived from the 50 c/s mains supply frequency, with provision for phase shifting to avoid bursts of interference which are sometimes locked to the supply frequency. The 150 c/s p.r.f. controls the output from a 900 Kc/s crystal oscillator by means of a gating circuit and resets the subsequent pulse divider stages which provide range-markers and other essential timing waveforms following each transmitted pulse. Thus the advantages of crystal control are combined with those of mains-locked operation.

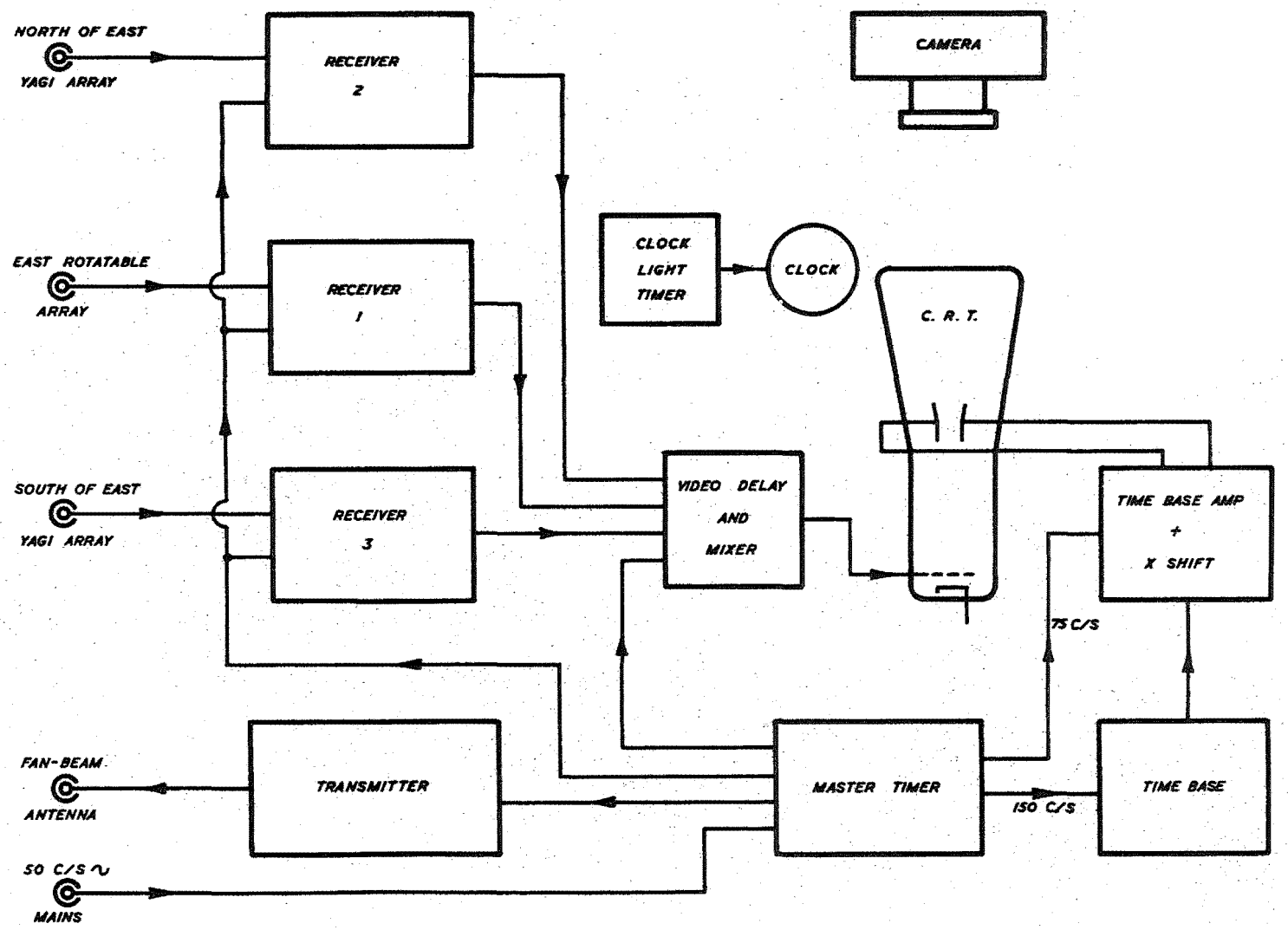


FIGURE 1. BLOCK DIAGRAM OF THE COMPLETE TRIPLE CHANNEL RADAR SYSTEM

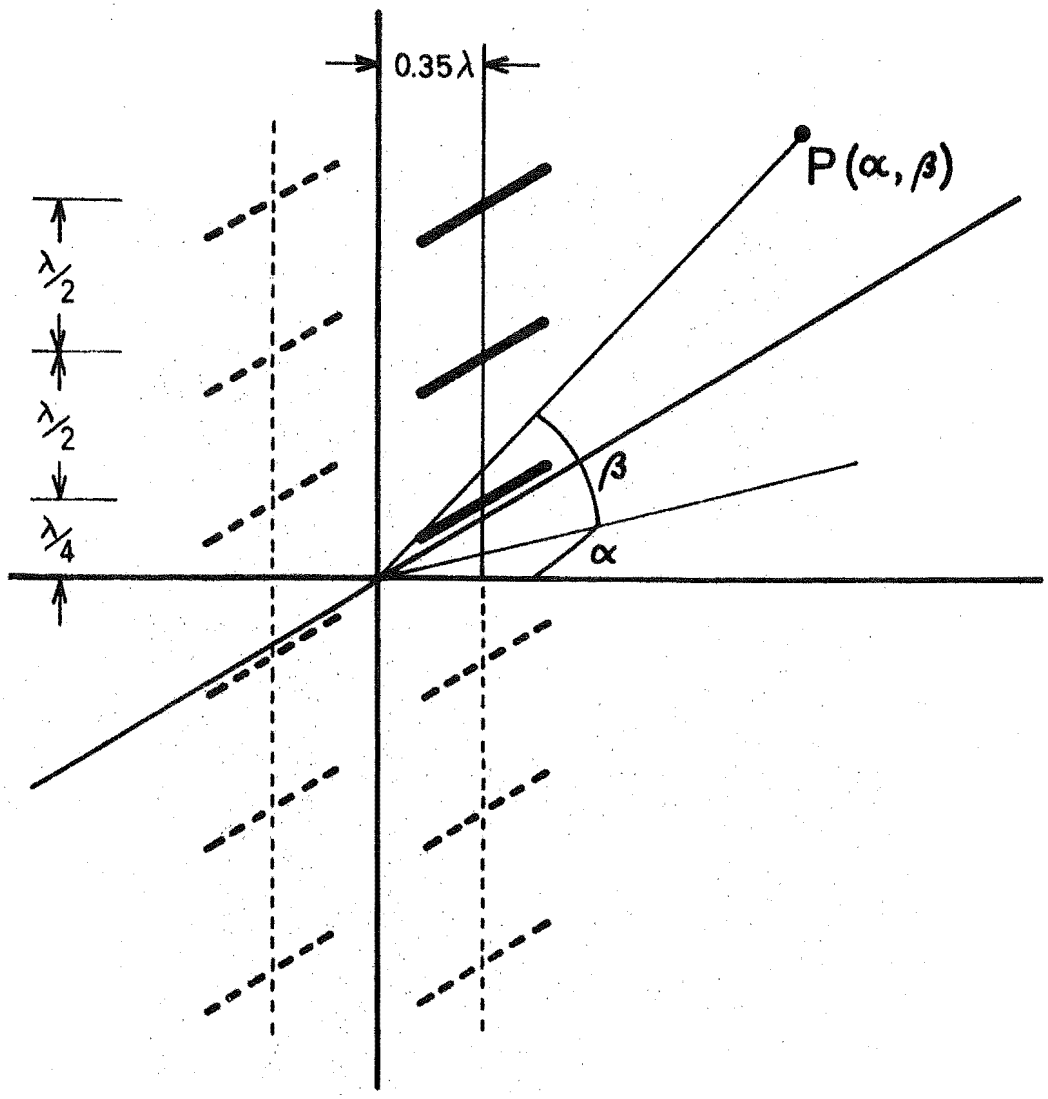


FIGURE 2. GEOMETRY OF THE FAN-BEAM ANTENNA ARRAY, SHOWING IMAGES.

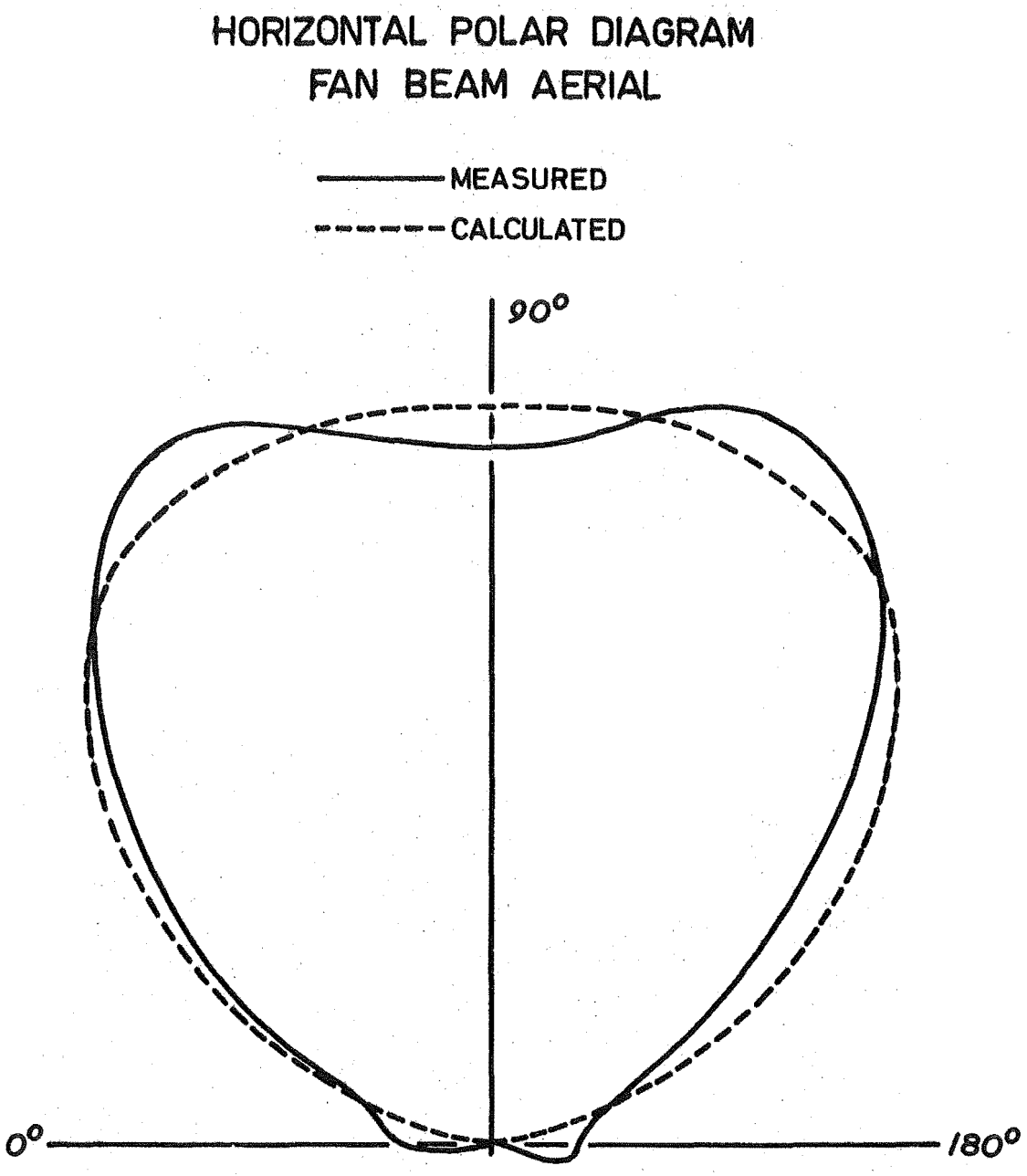


FIGURE 3. Comparison of the measured and calculated horizontal radiation patterns of the Fan-Beam antenna.

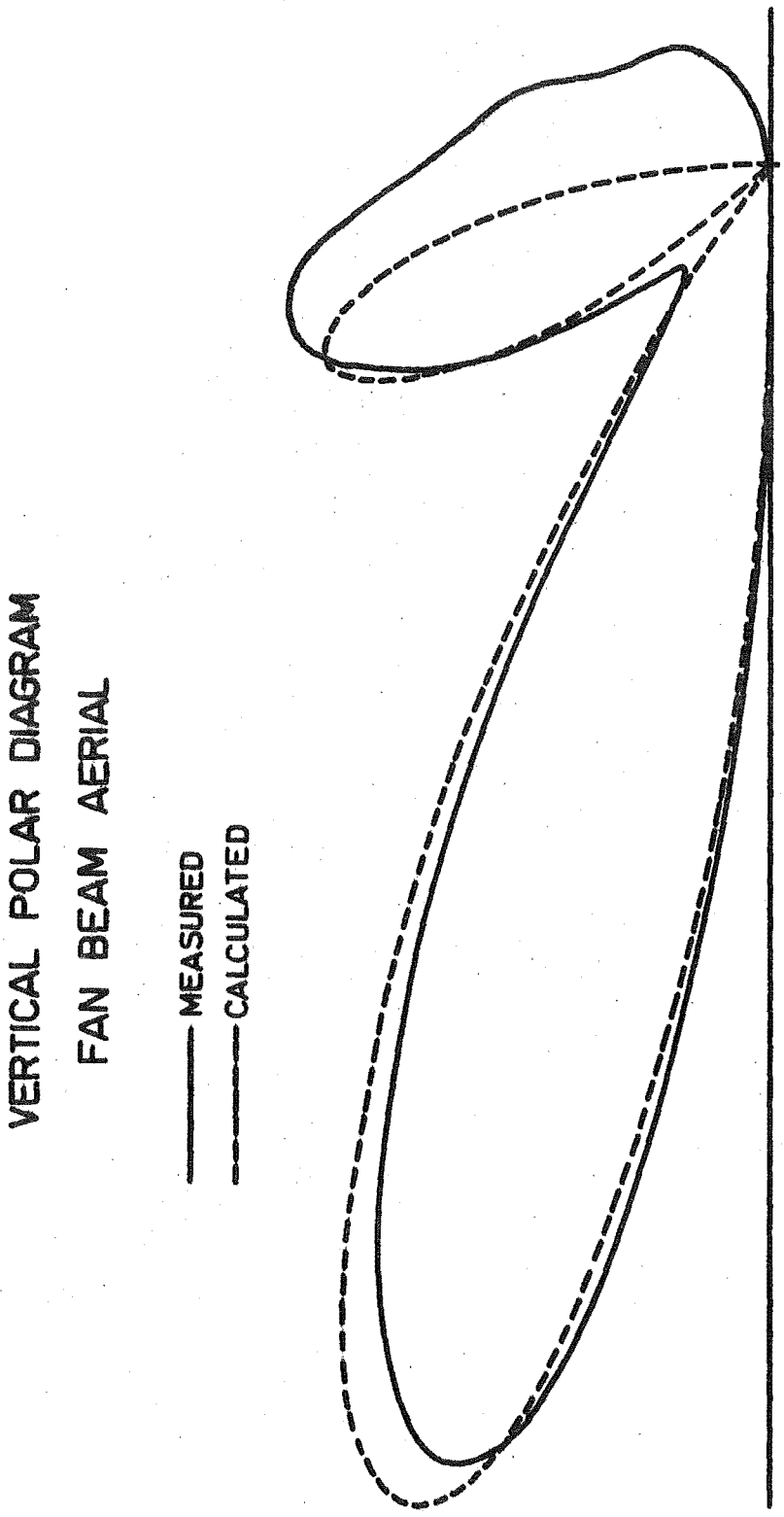


FIGURE 4. Comparison of the measured and calculated vertical radiation patterns of the Fan-Beam antenna.

FIGURE 5

The Fan-beam aerial system

(A rotatable 200 mc. array is partly visible at the top of the tower)

A. CALCULATED

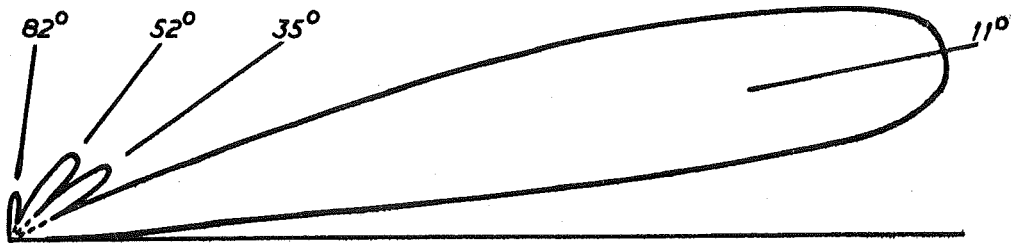


B. MEASURED

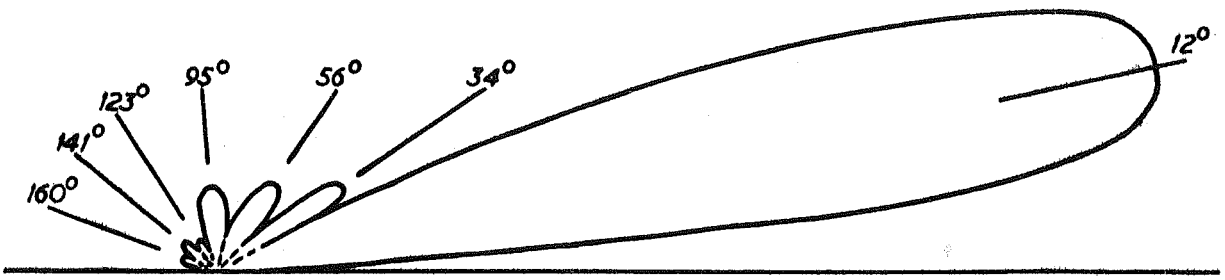


FIGURE 6. Vertical Radiation Pattern of a 4x3 Array at 69Mc/s.

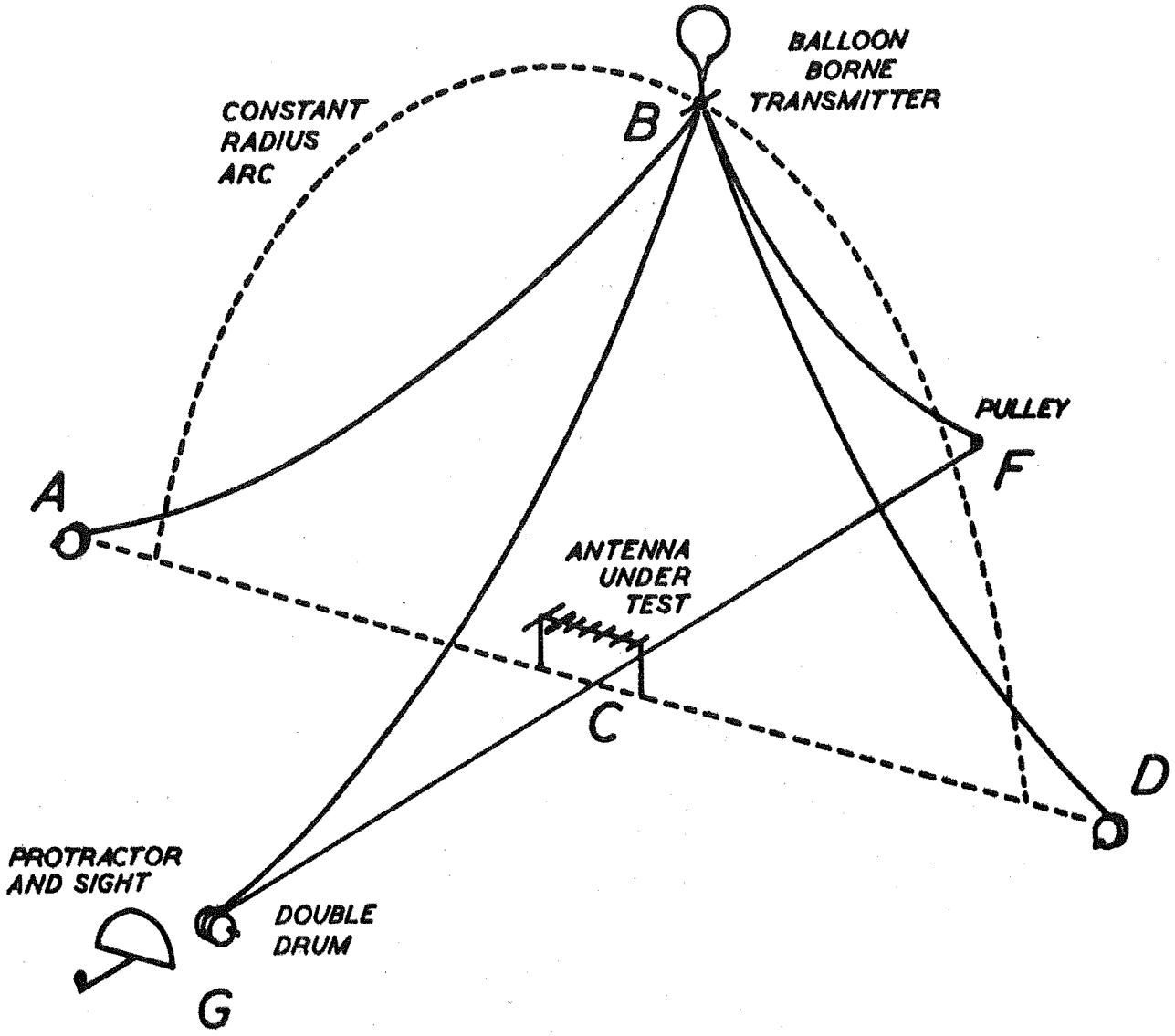


FIGURE 7. PHYSICAL LAYOUT OF THE CABLES AND SIGHTING APPARATUS FOR CONTROLLING THE BALLOON AND MEASURING ITS POSITION.

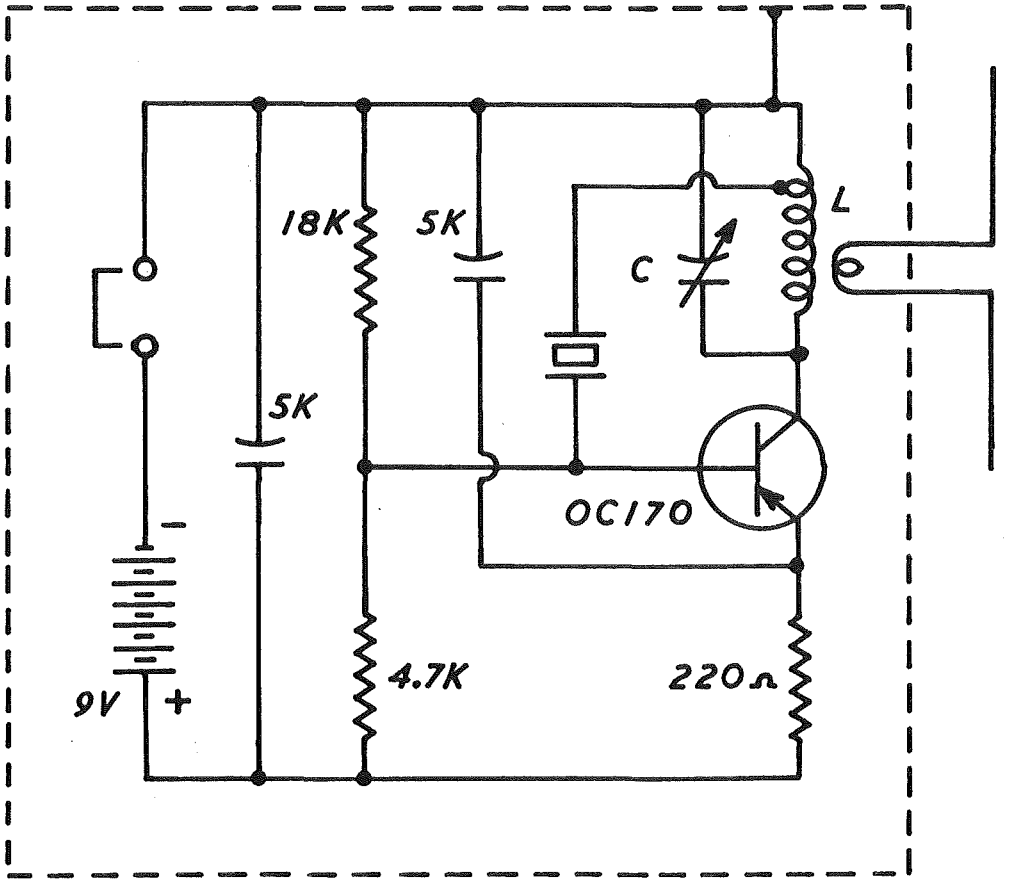


FIG. 8.

69 MC/S BALLOON-BORNE TRANSMITTER

FIGURE 9

The balloon-borne transmitter
with cover plate removed

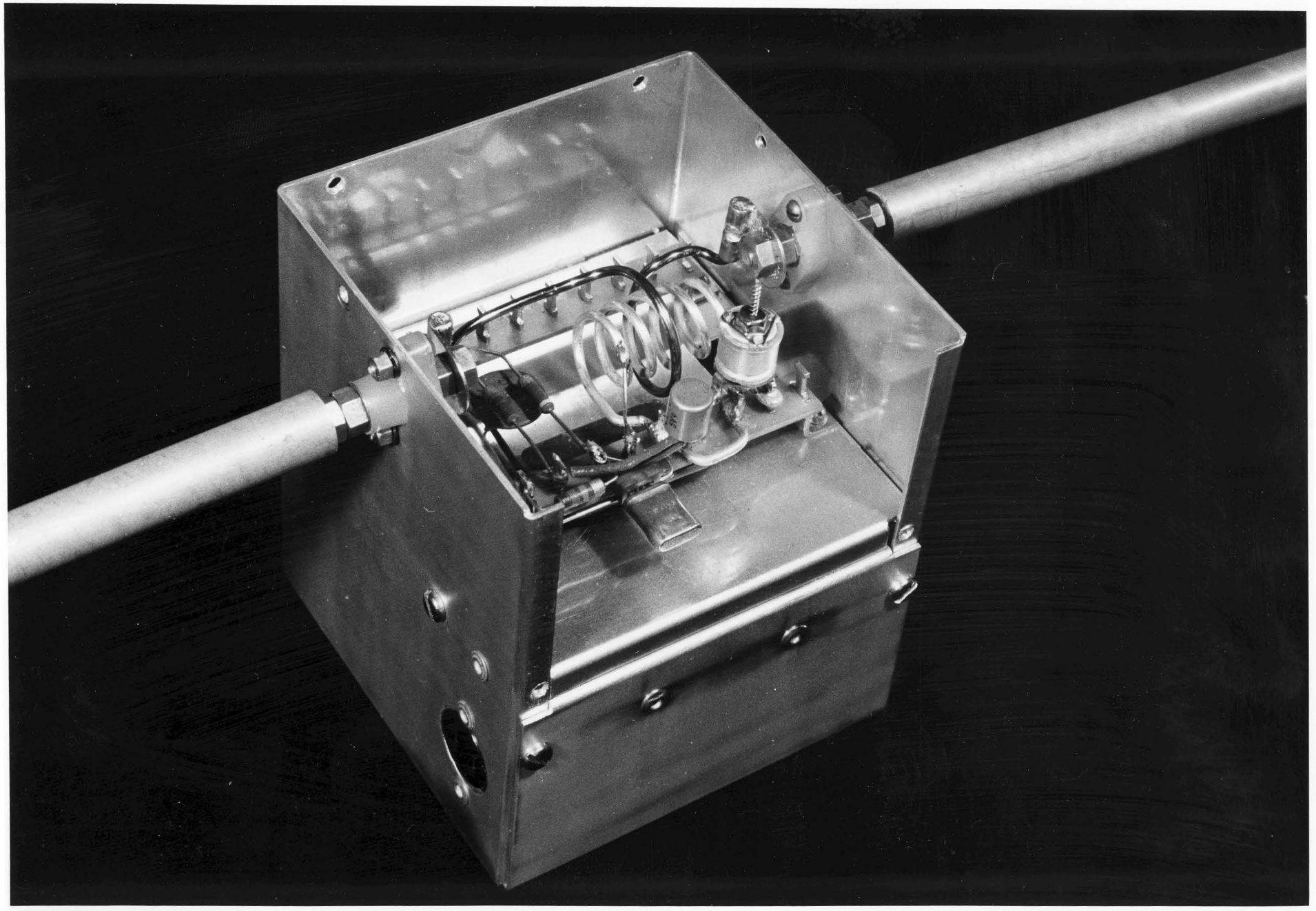

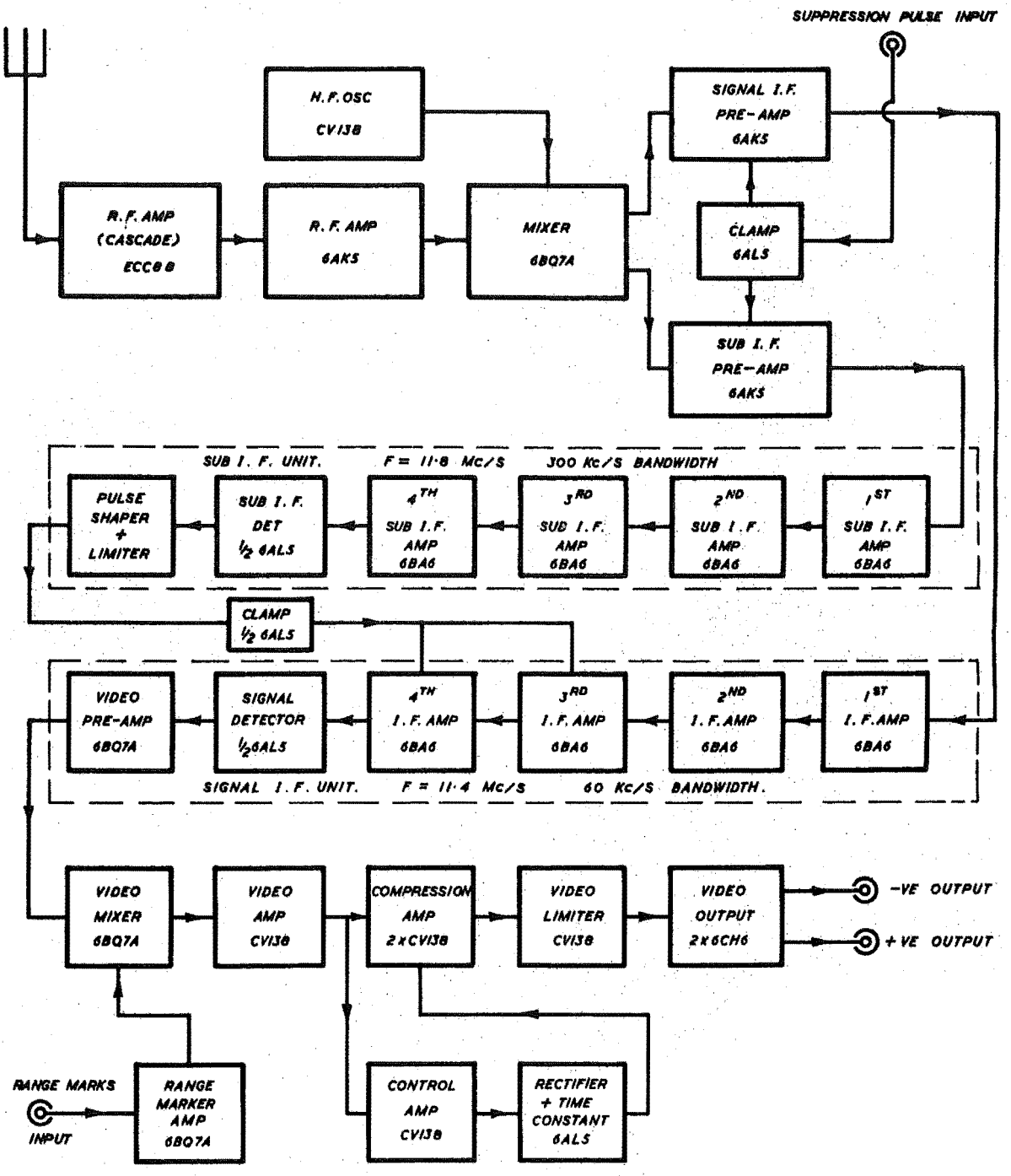


FIGURE 10 RECEIVER BLOCK DIAGRAM

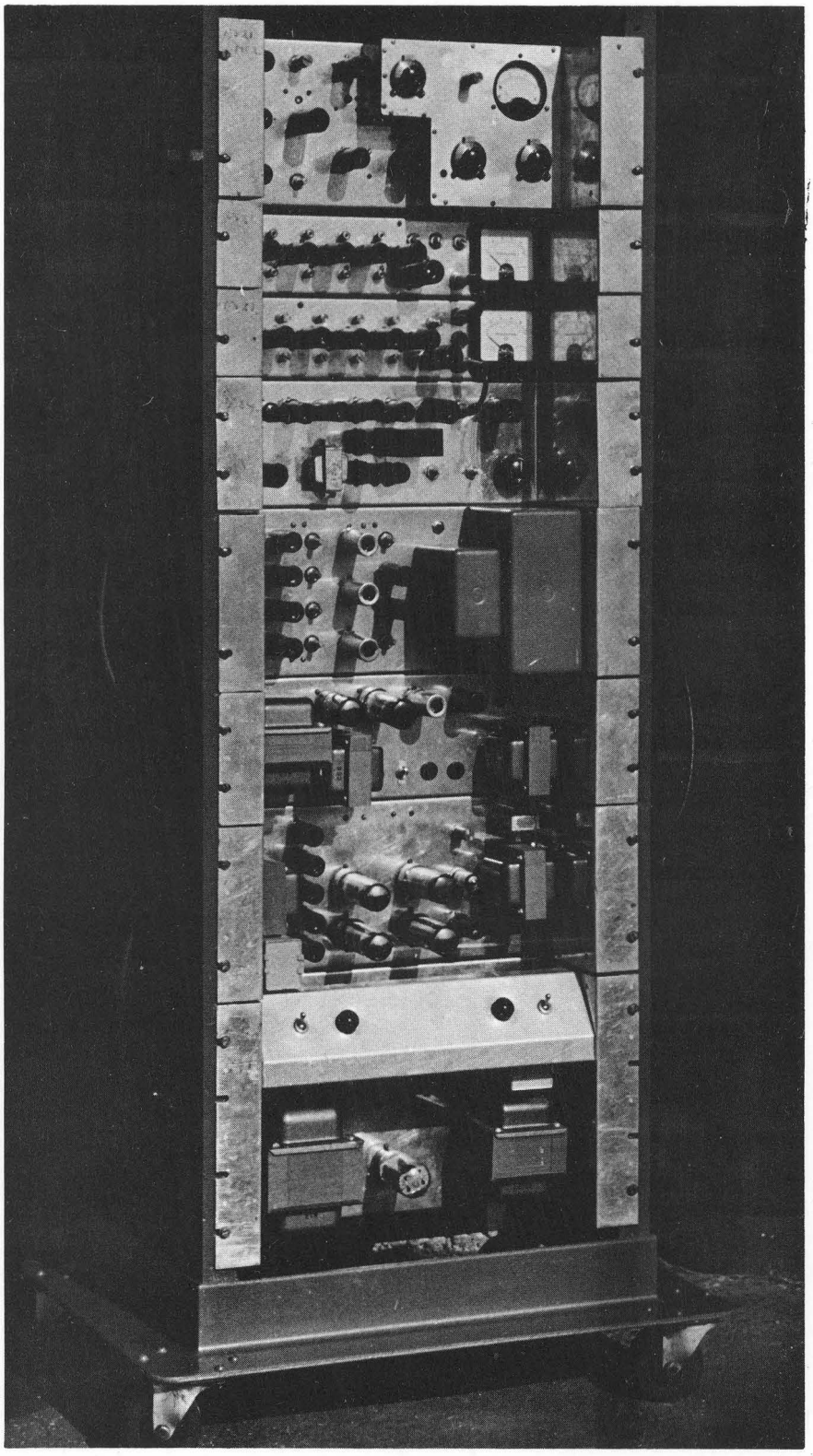


FIGURE 11. ONE OF THE THREE RECEIVERS. THIS RACK ALSO CONTAINS THE VIDEO DELAYS AND MIXING CIRCUITRY.

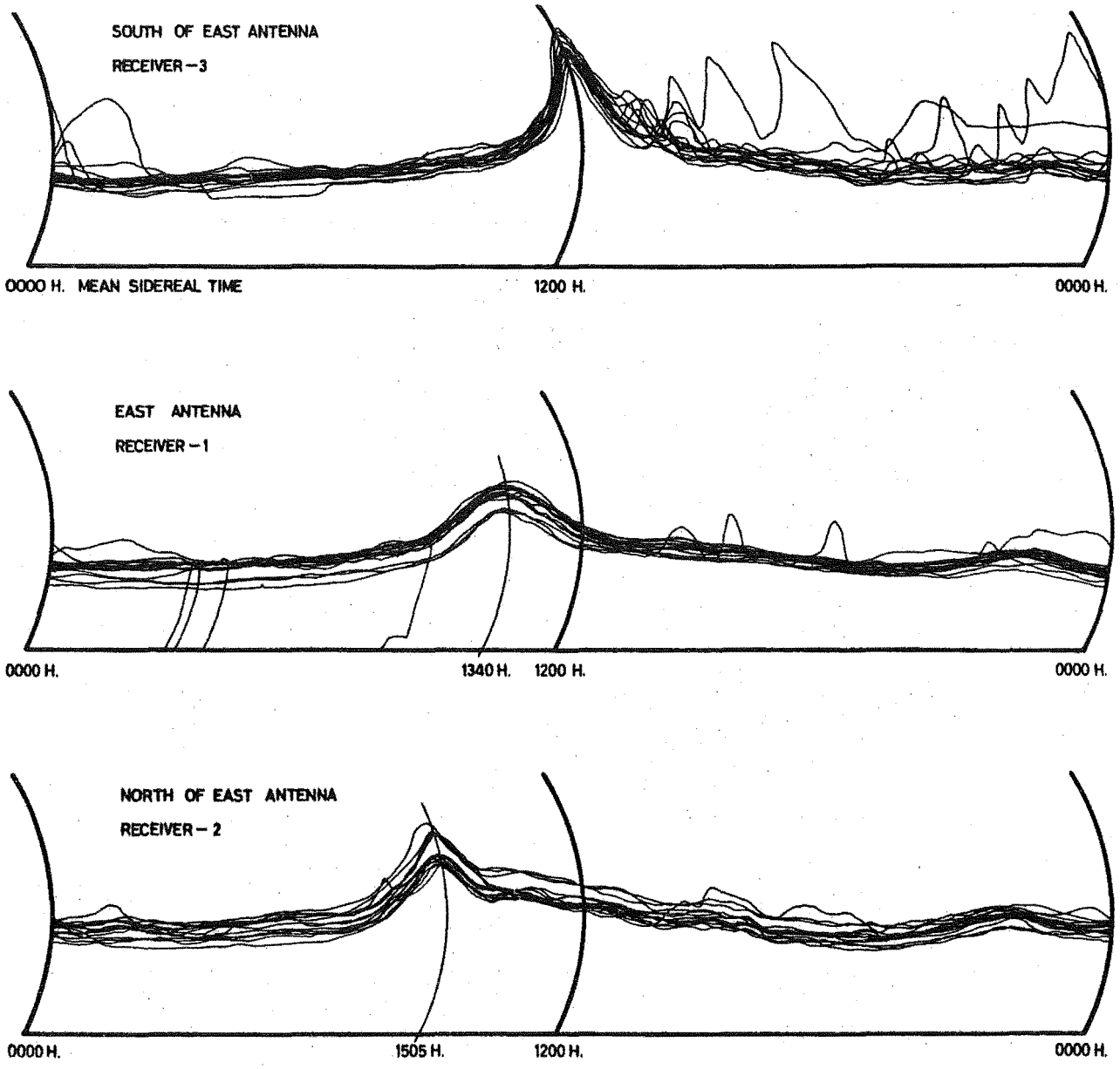


FIGURE 12. Chart tracings of the detector current of each of the three receivers over a period of two weeks (from 23 Nov. to 6 Dec. 1962). In each case the constancy of the receiver sensitivity is revealed by the constant amplitude (relative to the average level) of the noise peak produced by the Sagittarius region of the galaxy as it moves through the respective antenna beam.

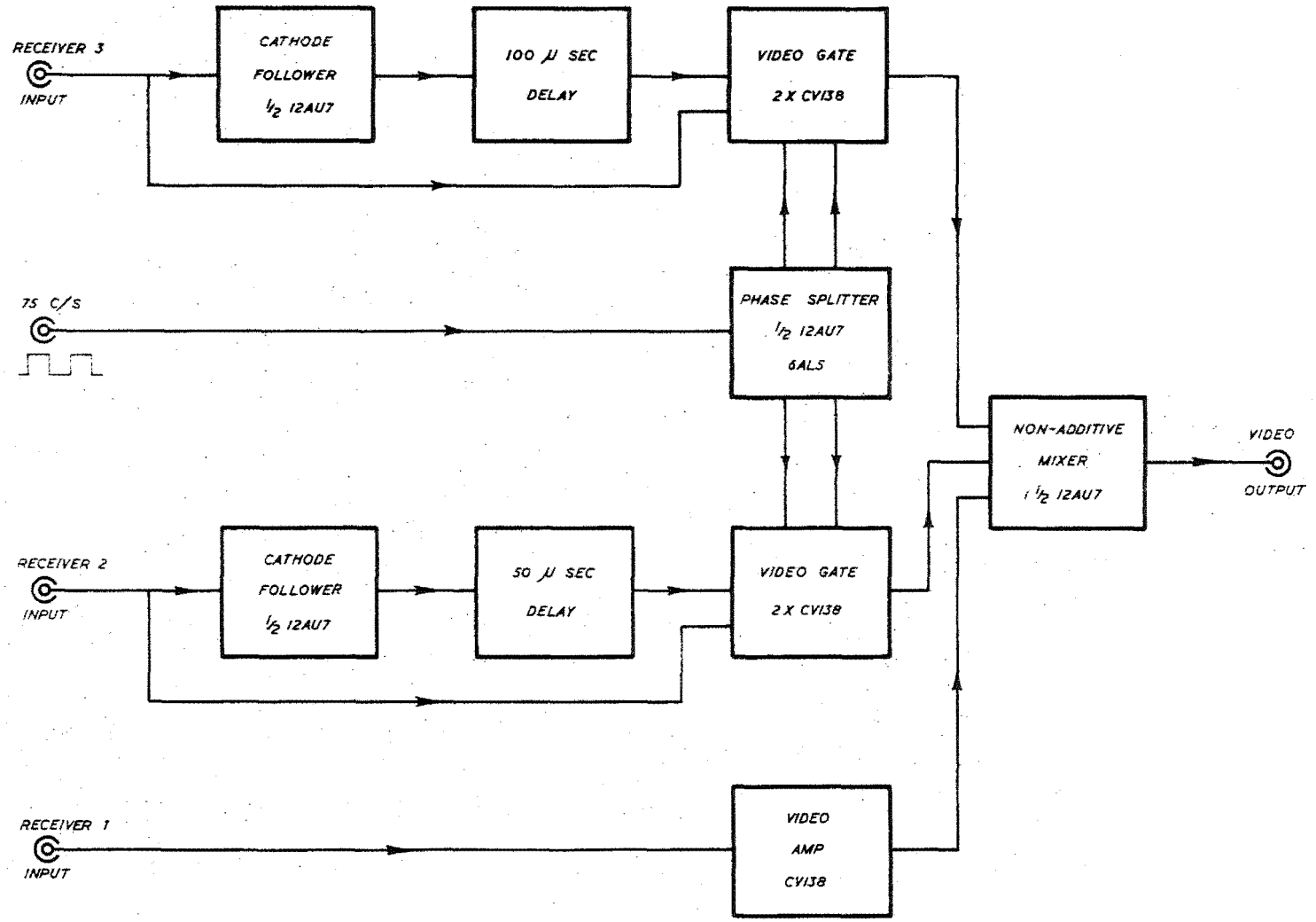


FIGURE 13. BLOCK DIAGRAM OF VIDEO SIGNAL DELAY AND MIXING CIRCUITS.

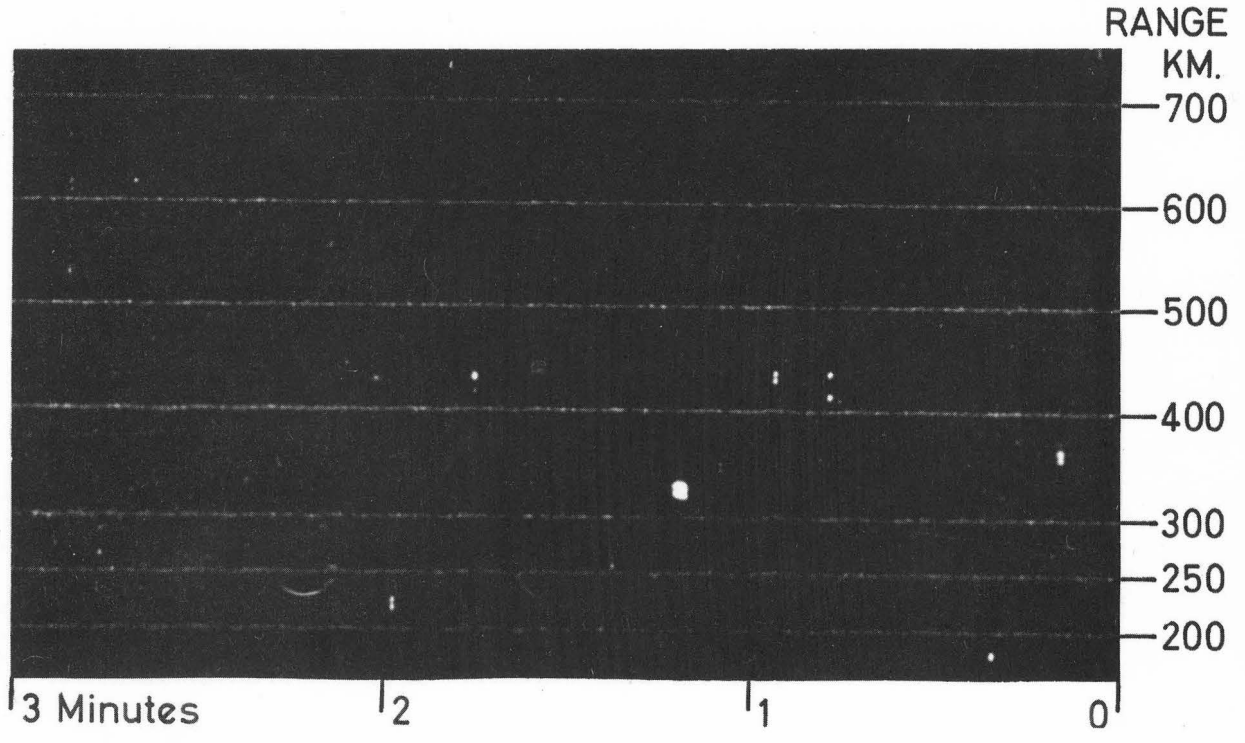


A. 1830 H. N.Z.S.T. 1962 DEC. 9.

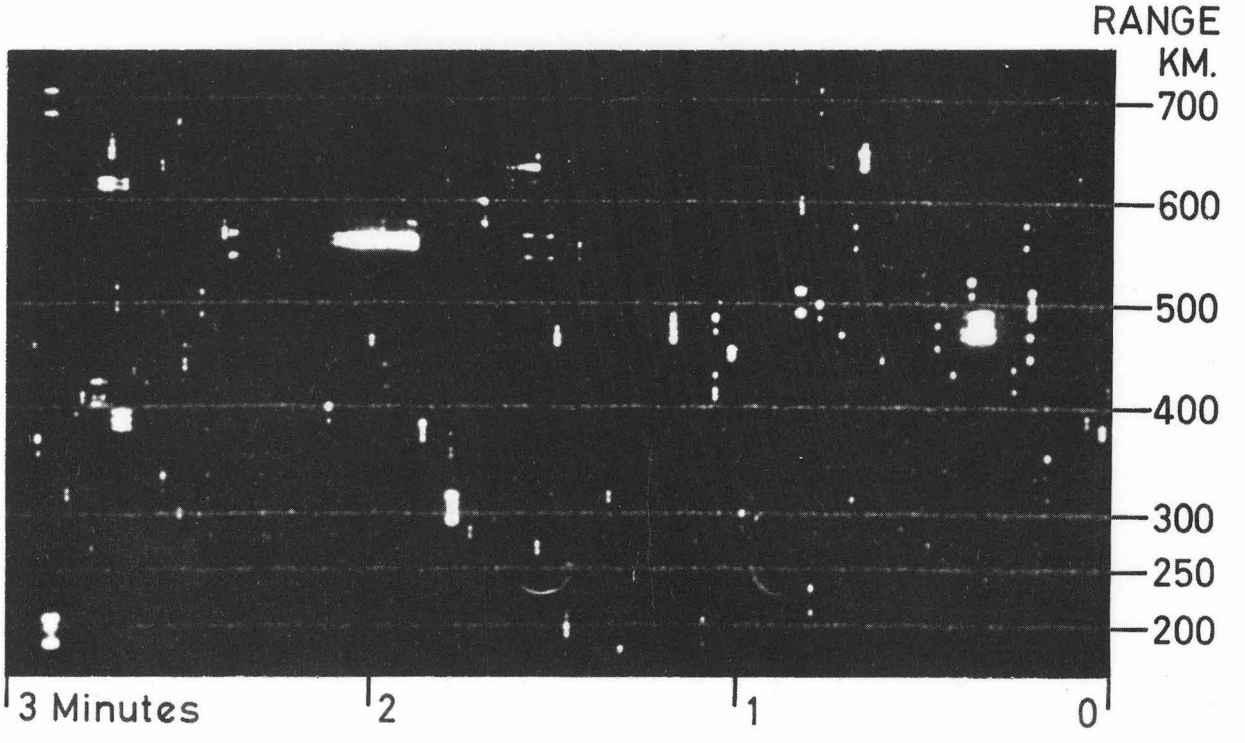


B. 0450 H. N.Z.S.T. 1962 DEC. 5

FIGURE 14. LOW AND HIGH-RATE METEOR ACTIVITY AS SHOWN ON THE FILM RECORDS.

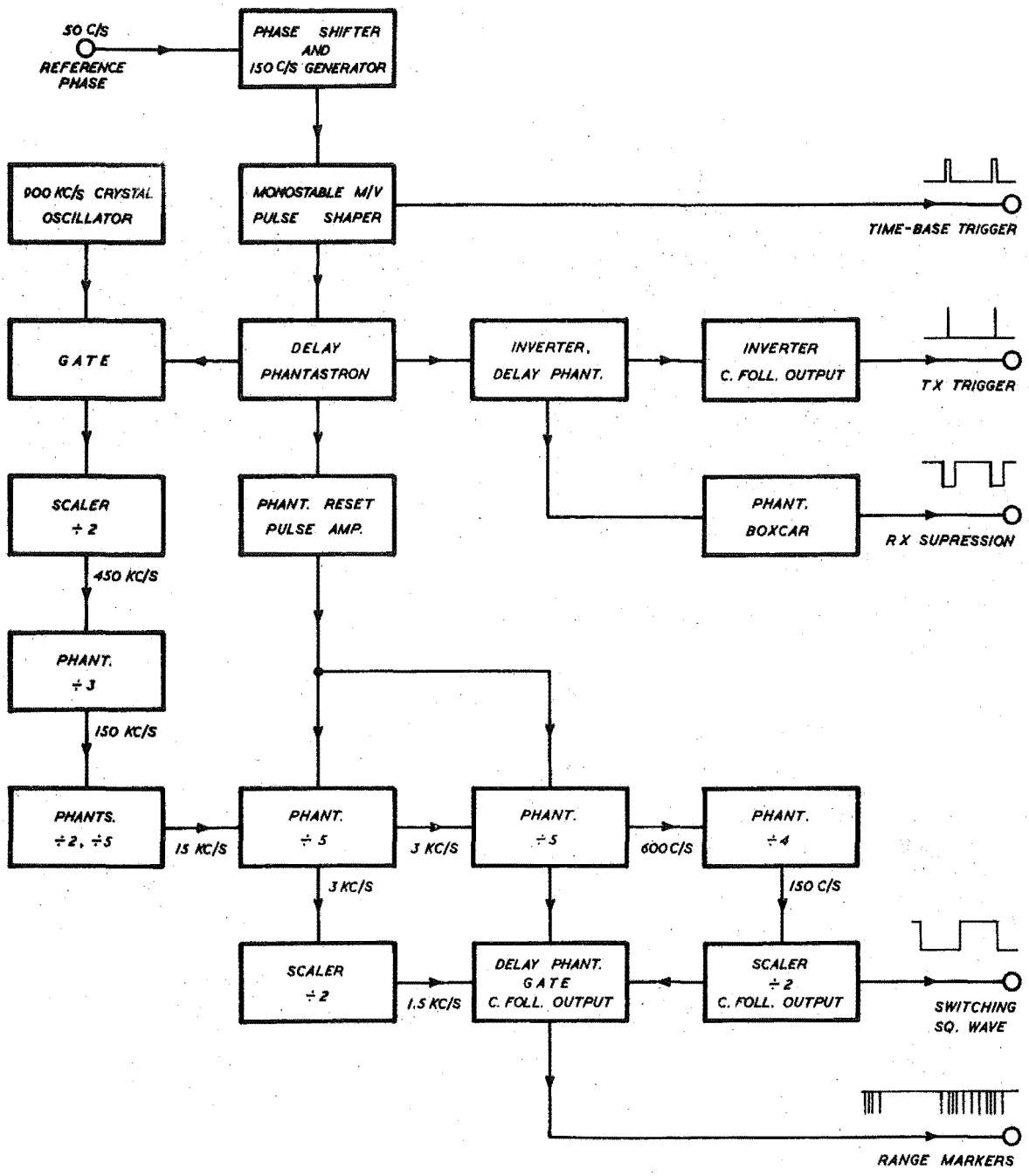


FIGURE 15 BLOCK DIAGRAM OF THE MASTER CONTROL UNIT WHICH SUPPLIES NECESSARY TIMING WAVEFORMS.

# 6. RESULTS FROM THE TRIPLE-CHANNEL SYSTEM

(This chapter has been submitted for publication under the title "Radar Investigations of Tenth-Magnitude meteors".)

In this chapter the operation of the triple-channel radar system is described. At the high rates of meteor detection obtained it is found that some of the recognized showers are completely masked by the dense background of faint meteors, while other shower streams appear to degenerate into scattered sporadic centres of activity.

## 6.1 Introduction

The classic method of delineating meteor shower radiants from radar observations is that due to Clegg (1948a, 1948b), which utilises the directive properties of an antenna array in conjunction with the specular reflection of radio waves by a meteor trail. Meteors emanating from a given radiant are generally detected only when the radiant point on the celestial sphere passes through the plane normal to the axis of the antenna beam. When the recorded echoes are plotted as a function of time and range the characteristic range-time envelopes of the Clegg method are obtained. From their shape and time of occurrence the co-ordinates (right ascension, $\alpha$, and declination, $\delta$) of the radiant may be deduced. If two antenna arrays are used (Aspinall, Clegg and Hawkins, 1951) the accuracy of the radiant co-ordinates obtained is greatly improved.

When more than 1000 echoes per day have to be plotted, the Clegg method becomes too laborious and time-consuming. A modified approach due to Keay (1957) enables the radiant co-ordinates to be determined by plotting the echo rate from two narrow-beam antennas as a function of time. Only those echoes which lie in a range interval straddling the range of maximum echo occurrence need be used. This "partial rate method", as

it is called, speeds the data processing and allows higher echo rates to be dealt with.

Both methods lead to ambiguities whenever two or more radiants are simultaneously active. These may be resolved, at the price of increased system complexity, by incorporating a third antenna, the beam of which should be spaced equally in azimuth with the other two. Each radiant then produces a time-displaced sequence of peaks in the partial rate curves and it becomes very much easier to relate the individual peaks to one another, or show their non-relationship, as the case may be. If three range intervals are recorded from each of the three antennas, nine partial rate curves are obtained, thus giving a ninefold check on the validity of a radiant.

The importance of this augmented partial rate method lies in its ability to delineate the radiants of minor showers which produce too few large meteors to make the ordinary Clegg method feasible. Or, putting the matter another way, this method is capable of detecting the presence of shower structure in the sporadic meteor background level.

## 6.2 The Triple-Beam System

A plan of the antenna coverage is shown in Figure 1. Three narrow-beam antennas are used for reception and a

wide angle, low elevation transmitting antenna (fan-beam) directs the R.F. energy to the region searched by the three receiving antennas. All were designed for the operating frequency of 69 Mc. The two outer receiving antennas are multiple yagi arrays giving a beam 4.4 degrees wide in azimuth (Ellyett, Keay, Roth and Bennett, 1961) while the center antenna is a rotatable planar array of half wave dipoles giving a beam 22 degrees wide in azimuth (Ellyett and Roth, 1955). For the purposes of this experiment the rotatable array was directed to a fixed azimuth of 90 degrees east of north. The fan-beam transmitting antenna consists of a vertical stack of folded dipoles spaced 0.35 of a wavelength in front of a reflecting screen. The elevation of the fan-beam produced by this antenna was intentionally made a little higher than that of the beams produced by the other antennas, in order to shorten the range at which the maximum number of echoes is received. This has the desirable effect of reducing the bias towards detecting radiants passing close to the local zenith (Keay and Ellyett, 1961). The resulting composite elevation response of the fan-beam antenna together with each of the two yagi arrays has a peak at 11 degrees elevation, while that with the fan-beam antenna and the planar array peaks at 13.5 degrees elevation.

The transmitter produced 25-microsecond pulses

with a peak power of almost 100 kilowatts at a pulse repetition frequency of 150 pulses per second derived from the frequency of the mains supply.

The detection system consists of three identical receivers (one to each receiving antenna) and a video mixing unit which mixes and codes the echoes for display on the screen of a cathode ray tube. Continuous photographic recording is employed at a film rate of 30 cm per hour. The identification of meteor echoes is based on the principle of doubling each genuine echo to distinguish it from random spikes due to noise and various forms of impulse interference. A small square-wave voltage added to the time-base at half the sweep frequency causes recurrent signals (such as genuine meteoric echoes which last for the duration of several sweeps) to be doubled while random signals stay random. This is illustrated in Figure 2 where the echo from Receiver 1 is doubled with a spacing t proportional to the amplitude of the applied square wave. The echoes from Receivers 2 and 3 are spaced more widely by switching the output signals from these receivers through 50 and 100 microsecond delay lines, respectively, on each alternate sweep in such phase as to add to the displacement caused by the square wave. The effect of this is shown in Figure 2. On the alternate sweeps, when displaced signals are displayed, the range markers

are suppressed in order that the undisplaced dot of every echo can be used for range determination.

There are numerous occasions when echoes from a given meteor are received by more than one antenna, due to overlapping radiation patterns. Usually, however, one antenna produces a stronger signal than the others and identification is still possible - as may be seen from the example depicted in Figure 2.

From the system parameters it can be shown that the limiting zenithal magnitude of meteors detected via the fan-beam/yagi array antenna combination is $10.9 \pm 0.4$. These smallest meteors are detected at an elevation of 14 degrees, corresponding to a range of 360 km. This agrees with the measured value of 365 km at which the maximum occurs in the range distribution of observed meteor echoes.

The limiting zenithal magnitude of meteors detected via the fan-beam/planar array antenna combination is $10.0 \pm 0.3$. These are detected at an elevation of 17 degrees, corresponding to a range of 305 km. This too is in fair agreement with the 280 km range at which the maximum number of echoes is received via this particular antenna combination.

## 6.3 Theory and Calculations

The basic theory underlying the partial-rate method needs no modification when three instead of two narrow-beam antenna are employed. The counting of meteors in more than one range-band has also been described in a paper (Ellyett, Keay, Roth and Bennett, 1961) in which it is referred to as a multiple rate-count method, and an example of its usefulness was given. It is the combination of these methods which is referred to as the augmented partial-rate method.

Briefly, short time-interval counts of meteor echoes, whose ranges lie in a band centred on the range of maximum occurrence, give a partial-rate curve when plotted against time. The times when peaks occur in the partial rate curves from two or more antennas yield the radiant co-ordinates of the meteor activity which gave rise to the peaks. The same is true when meteors in range-bands adjacent to the central range-band are used, although an allowance must be made for the asymmetrical distribution of meteors within the range-band when high accuracy is required.

The way radiant co-ordinates are derived from the observed times of occurrence of peaks in meteor rate may be seen from Figure 3. This Figure represents a horizontal projection of the intersection with the celestial hemisphere of the planes in which meteor trails must lie

in order to be detectable at the range concerned. It is the same as saying that meteors from a given radiant are only detectable as the radiant passes through the appropriate "collecting" plane. For the easterly directed antenna the collecting planes for echoes detected near ranges of 300, 400 and 500 Km intersect the celestial hemisphere in the lines N1S, N2S and N3S respectively. In reality the lines are narrow strips due to the finite size of the range interval in which echoes are counted (each "range-band" extended 50 Km on either side of the nominal range, i.e. the range intervals were 100 Km wide) and to the spread in azimuth of the antenna beam.

As a somewhat ideal example, the radiant 'A'will first produce echoes in the 500 Km range-band of the South of East antenna (at point 'a' in Figure 3), then in its 400 Km range-band at a time which happens to coincide with the meridian passage of the radiant in this particular case (point 'b'). Echoes will next appear in the 500 Km range-band of the East antenna (point 'c') and almost at the same time in the 300 Km range-band of the South of East antenna (point 'd'). And so on. The important point is that the order of appearance of echoes in the range-bands of the three antennas will be quite different for radiant 'B', and is a function of the radiant declination. However, up

to quite high values of declination, the order of appearance of echoes in the various range-bands associated with a given antenna is always the same. Also for radiants passing further north than a few degrees of the zenith, the peak echo rate in a given range-band from the East antenna is always mid-way in time between the peak rates in the same range-band from the other two antennae. These characteristics assist the recognition of discrete meteor shower activity whenever it occurs, but if the measured rates are low (less than about 15 per 12 minute interval in each 100 Km range-band) it must be borne in mind that random fluctuations in echo rate may cause small peaks to vanish entirely from some of the rate curves.

For each range-band of the three antennas the time difference between peak echo rate and the time of meridian passage (local transit) of any culminating radiant have been calculated as a function of radiant declination by using the theory already published (Keay, 1957). A suitable computer program was developed in order to enable this considerable task to be performed on an IBM-1620 computer*. The nine tables produced by the computer are shown plotted in Figure 4, which is, in effect, a cartesian projection of Figure 3, using declination and hour angle as co-ordinates.

---

*A sample of the output from the computer is presented in Table 3, overleaf.

TABLE OF AERIAL COLLECTING PLANE TRANSIT TIMES

COMPUTED FOR LATITUDE -43.62 DEGREES

AERIAL AZIMUTH (EAST) = 112.5 DEGREES

ECHO HEIGHT = 95.0 KILOMETERS

SLANT RANGE OF MEAN ECHO = 500.0 KILOMETERS

ELEVATION OF MEAN ECHO = 8.75 DEGREES

MAXIMUM DECLINATION = 67.74 DEGREES

DECLINATION VALUE AT HORIZON = 41.97 DEGREES

| DECL. | HOUR ANGLE | DECL. | HOUR ANGLE | DECL. | HOUR ANGLE |
|---|---|---|---|---|---|
| | | 19 | -0 H 5.0 M | -31 | -1 H 34.4 M |
| | | 18 | -0 H 6.9 M | -32 | -1 H 36.7 M |
| 67 | 4 H 21.0 M | 17 | -0 H 8.7 M | -33 | -1 H 39.1 M |
| 66 | 3 H 49.7 M | 16 | -0 H 10.5 M | -34 | -1 H 41.6 M |
| 65 | 3 H 27.9 M | 15 | -0 H 12.3 M | -35 | -1 H 44.1 M |
| 64 | 3 H 10.7 M | 14 | -0 H 14.0 M | -36 | -1 H 46.7 M |
| 63 | 2 H 56.2 M | 13 | -0 H 15.8 M | -37 | -1 H 49.3 M |
| 62 | 2 H 43.8 M | 12 | -0 H 17.5 M | -38 | -1 H 52.0 M |
| 61 | 2 H 32.8 M | 11 | -0 H 19.2 M | -39 | -1 H 54.9 M |
| 60 | 2 H 23.0 M | 10 | -0 H 20.9 M | -40 | -1 H 57.8 M |
| 59 | 2 H 14.2 M | 9 | -0 H 22.6 M | -41 | -2 H .8 M |
| 58 | 2 H 6.1 M | 8 | -0 H 24.3 M | -42 | -2 H 4.0 M |
| 57 | 1 H 58.7 M | 7 | -0 H 25.9 M | -43 | -2 H 7.2 M |
| 56 | 1 H 51.9 M | 6 | -0 H 27.6 M | -44 | -2 H 10.6 M |
| 55 | 1 H 45.5 M | 5 | -0 H 29.2 M | -45 | -2 H 14.1 M |
| 54 | 1 H 39.6 M | 4 | -0 H 30.9 M | -46 | -2 H 17.8 M |
| 53 | 1 H 34.0 M | 3 | -0 H 32.5 M | -47 | -2 H 21.6 M |
| 52 | 1 H 28.8 M | 2 | -0 H 34.2 M | -48 | -2 H 25.6 M |
| 51 | 1 H 23.9 M | 1 | -0 H 35.8 M | -49 | -2 H 29.8 M |
| 50 | 1 H 19.2 M | 0 | -0 H 37.5 M | -50 | -2 H 34.2 M |
| 49 | 1 H 14.8 M | -1 | -0 H 39.1 M | -51 | -2 H 38.9 M |
| 48 | 1 H 10.6 M | -2 | -0 H 40.7 M | -52 | -2 H 43.8 M |
| 47 | 1 H 6.6 M | -3 | -0 H 42.4 M | -53 | -2 H 49.0 M |
| 46 | 1 H 2.8 M | -4 | -0 H 44.0 M | -54 | -2 H 54.6 M |
| 45 | 0 H 59.1 M | -5 | -0 H 45.7 M | -55 | -3 H .5 M |
| 44 | 0 H 55.6 M | -6 | -0 H 47.3 M | -56 | -3 H 6.9 M |
| 43 | 0 H 52.2 M | -7 | -0 H 49.0 M | -57 | -3 H 13.7 M |
| 42 | 0 H 48.9 M | -8 | -0 H 50.6 M | -58 | -3 H 21.1 M |
| 41 | 0 H 45.8 M | -9 | -0 H 52.3 M | -59 | -3 H 29.2 M |
| 40 | 0 H 42.8 M | -10 | -0 H 54.0 M | -60 | -3 H 38.0 M |
| 39 | 0 H 39.9 M | -11 | -0 H 55.7 M | -61 | -3 H 47.8 M |
| 38 | 0 H 37.0 M | -12 | -0 H 57.4 M | -62 | -3 H 58.8 M |
| 37 | 0 H 34.3 M | -13 | -0 H 59.1 M | -63 | -4 H 11.2 M |
| 36 | 0 H 31.6 M | -14 | -1 H .9 M | -64 | -4 H 25.7 M |
| 35 | 0 H 29.1 M | -15 | -1 H 2.6 M | -65 | -4 H 42.9 M |
| 34 | 0 H 26.5 M | -16 | -1 H 4.4 M | -66 | -5 H 4.7 M |
| 33 | 0 H 24.1 M | -17 | -1 H 6.2 M | -67 | -5 H 36.0 M |
| 32 | 0 H 21.7 M | -18 | -1 H 8.0 M | | |
| 31 | 0 H 19.4 M | -19 | -1 H 9.9 M | | |
| 30 | 0 H 17.1 M | -20 | -1 H 11.7 M | | |
| 29 | 0 H 14.9 M | -21 | -1 H 13.6 M | DECL. | HOUR ANGLE |
| 28 | 0 H 12.7 M | -22 | -1 H 15.5 M | | |
| 27 | 0 H 10.6 M | -23 | -1 H 17.5 M | | |
| 26 | 0 H 8.5 M | -24 | -1 H 19.5 M | | |
| 25 | 0 H 6.5 M | -25 | -1 H 21.5 M | | |
| 24 | 0 H 4.4 M | -26 | -1 H 23.5 M | | |
| 23 | 0 H 2.5 M | -27 | -1 H 25.6 M | | |
| 22 | 0 H .5 M | -28 | -1 H 27.7 M | | |
| 21 | -0 H 1.3 M | -29 | -1 H 29.9 M | | |
| 20 | -0 H 3.2 M | -30 | -1 H 32.1 M | | |
| DECL. | HOUR ANGLE | DECL. | HOUR ANGLE | | |

TABLE 3

## 6.4 Preliminary Results

The system as a whole was in operation for several months during 1962 and early 1963. In February 1963 the experiment was discontinued in order to commence a meteor survey (using omni-directional antennas) which could not run simultaneously. However, the results from the preliminary period of operation indicate the desirability of further work when the meteor survey is completed.

During the experiment much valuable experience was gained, particularly on the problems of displaying the outputs of three receivers on a single cathode ray tube. Varying noise levels, particularly when man-made interference was present on any one of the receivers, were difficult to compensate for. The preservation of equal signal-to-noise ratios in each of the three outputs was essential in view of the narrow dynamic range of the cathode ray tube spot intensity and the requirement that a single brilliance setting had to be correct for recording all three signals. This, at present, is the weakest link in the whole system.

One of the first occasions when the complete triple-antenna system was operating successfully was during July, 1962. The partial rate curves obtained on July 25 are shown in Figure 5. In each of the nine curves the δ-Aquarid shower has produced a very prominent peak,

allowing quite a good value to be obtained for its radiant position, as follows:

Right ascension $337.8^{\circ} \pm 0.5^{\circ}$

Declination $-13.7^{\circ} \pm 2.9^{\circ}$

The peak in the partial rate curve for the 250 - 350 Km range interval from the North of East antenna was incomplete because of a gap in the record due to a severe burst of man-made interference. Otherwise the peaks were quite clear and there is no doubt as to their identification. None of the other peaks in these partial rate curves are as prominent, except, perhaps, for the activity from the East antenna near 0800 hours. However, there is very little supporting activity from either of the other two antennas and no radiant can be determined for it. This situation has proved to be surprisingly common in this work, lending support to other evidence (Kaiser, 1961) that meteor showers lose their identity and merge into the sporadic background when large numbers of very faint meteors are being detected. The Pisces Australid, Southern $\iota$-Aquarid, Capricornid and Cetid showers have disappeared in this way from the curves in Figure 5, even though they are known to be active at that date. At least two of them (Pisces Australids and Cetids) were present in similar records obtained at lower sensitivity, and hence lower rate, on the same date in 1956.

The above situation is well illustrated by the

records obtained in early December, 1962, a time of the year when several well known southern showers are active (Ellyett, Keay, Roth and Bennett, 1961). The principal two are the Velids and the Puppids, which, together with the Librids and the Orionids, are marked on the partial rate curves obtained during December 4 (Figure 6) and December 5 (Figure 7). Of the 72 times when a peak should have been present fewer than five coincidences were obtained. Even when allowance is made for inaccuracies in the quoted radiant positions there are no clear sequences of peaks (such as that for the δ-Aquarids in Figure 5) which reveal shower activity. Furthermore, when the corresponding partial rate curves for each of the two days are intercompared there is very little continuity between them, despite the fact that each of the showers mentioned above lasts for several days. It is also noticeable that some of the sharper and more prominent peaks one day are replaced by dips in the curve on the next day.

Only the gross characteristics of the partial rate curves relate to one another or persist from day to day. They are the gradual rise in rate from midnight to approximately 0600 hours, the hollow centred near 0900 hours and the broad hump at around 1200-1300 hours followed by the decline in rate towards the evening. Such a finding is consistent with the pattern which emerged from

a year-long survey of meteor activity in 1960-61: the broad helion and anti-helion peaks or groupings then also overshadowed almost all shower activity (Ellyett and Keay, 1963). This is clearly shown by combining the daily partial rate curves over a period of one week, as has been done in Figure 8. Although each successive daily curve was shifted four minutes to minimise the spreading of peaks due to the shift in solar longitude, there is little sign of peaks due to discrete meteor showers. (The points for each curve were smoothed in sliding groups of three in order to reduce statistical fluctuations and show genuine peaks of activity more clearly.)

In all of the curves shown in Figure 8 the two diurnal peaks are evident and there is a third peak in at least two of the records obtained from the antenna directed due east. While the two principal peaks are not as sharp as those in Figure 5, indicating less concentrated activity, the mean radiant positions have been calculated by the method outlined earlier.

The co-ordinates obtained for the mean radiant of the early morning activity are

Right ascension $138.4^{\circ} \pm 3.4^{\circ}$

$(\lambda_{\odot} = 255^{\circ})$

Declination $-44.2^{\circ} \pm 8.7^{\circ}$

which definitely associates it with the well-known Velid shower, as illustrated in Figure 9(a). This radiant is well removed from the vicinity of the ecliptic. It is

situated at an ecliptic latitude of $-56^{\circ}$ which suggests that there may exist, for this part of the year at least, a southern counterpart to the high inclination meteoric activity observed from the northern hemisphere (Hawkins, 1963).

The midday peak of activity yields the co-ordinates

Right ascension $238.8^{\circ} \pm 3.5^{\circ}$ ($\lambda_{\odot} = 255^{\circ}$)

Declination $-26.4^{\circ} \pm 12.4^{\circ}$

for its mean radiant. This activity therefore originates from the vicinity of the ecliptic, as revealed by Figure 9(b), and is very close to the Librid radiants found in earlier work (Ellyett, Keay, Roth, Bennett, 1961).

At the high rates of meteor detection obtained with the present apparatus (total rates exceeding 1000 per hour were quite usual during December 1962) it was found that the small peaks in the daily partial rate curves rarely coincided from day to day, yet the broad peaks remained present. In view of this fact it would appear that each of the two mean radiant position obtained represents a centre of rapidly and constantly shifting activity. This type of behaviour has previously been observed in the case of the Velid shower by Weiss (1960), who reports that its radiant is very ill-defined. In a series of observations from 1953 to 1960 (at lower echo rates than the present work) recently collated by Ellyett and Roth (1964), several centres of activity were found. Two of the strongest centres are plotted in Figure 9(a). The con-

servation exhibited by most of the small peaks in the daily partial rate curves (which are unsmoothed) is, however, quite high, which tends to suggest that the activity occurs in sporadic bursts of a few hours duration from numerous radiants scattered around the mean position.

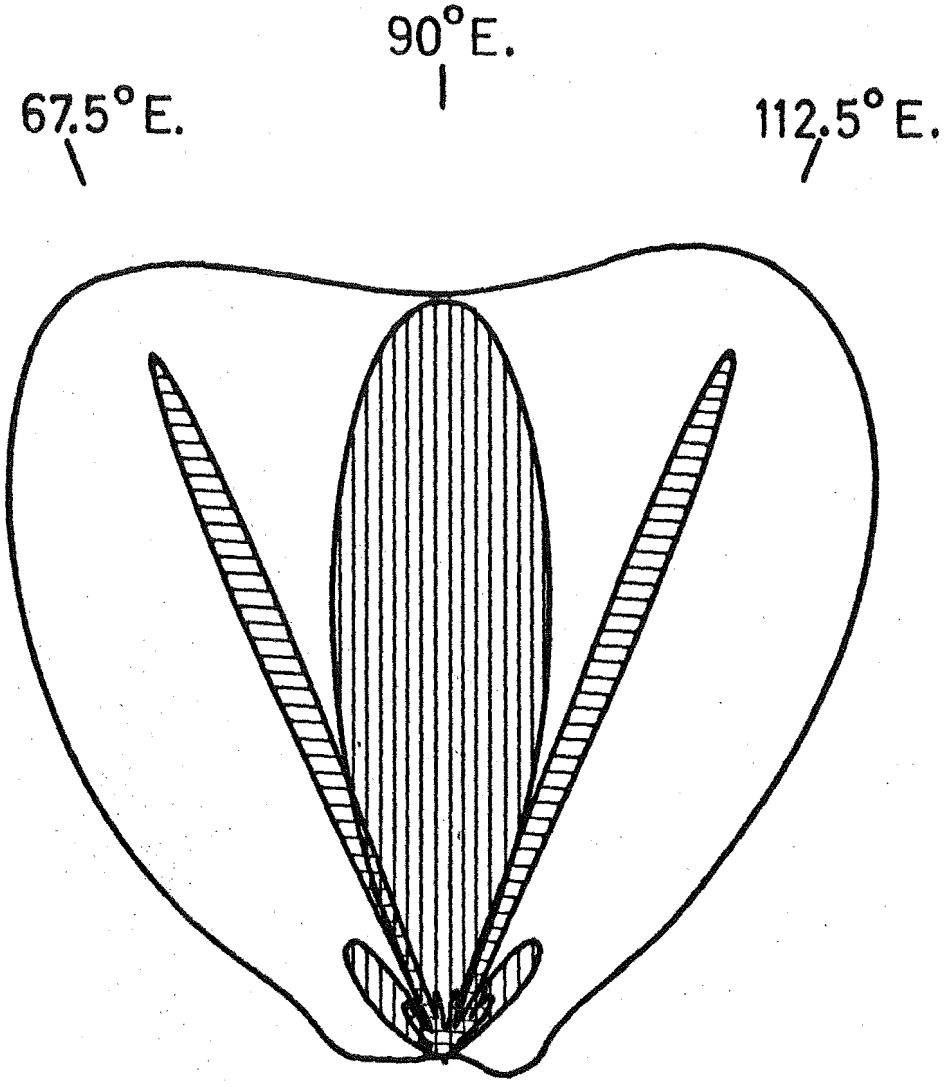


FIGURE 1. Plan view of antenna coverage. The outer curve represents the horizontal radiation pattern of the Fan-Beam transmitting antenna, while the horizontal patterns of the three narrow-beam antennas used for reception are shown shaded.

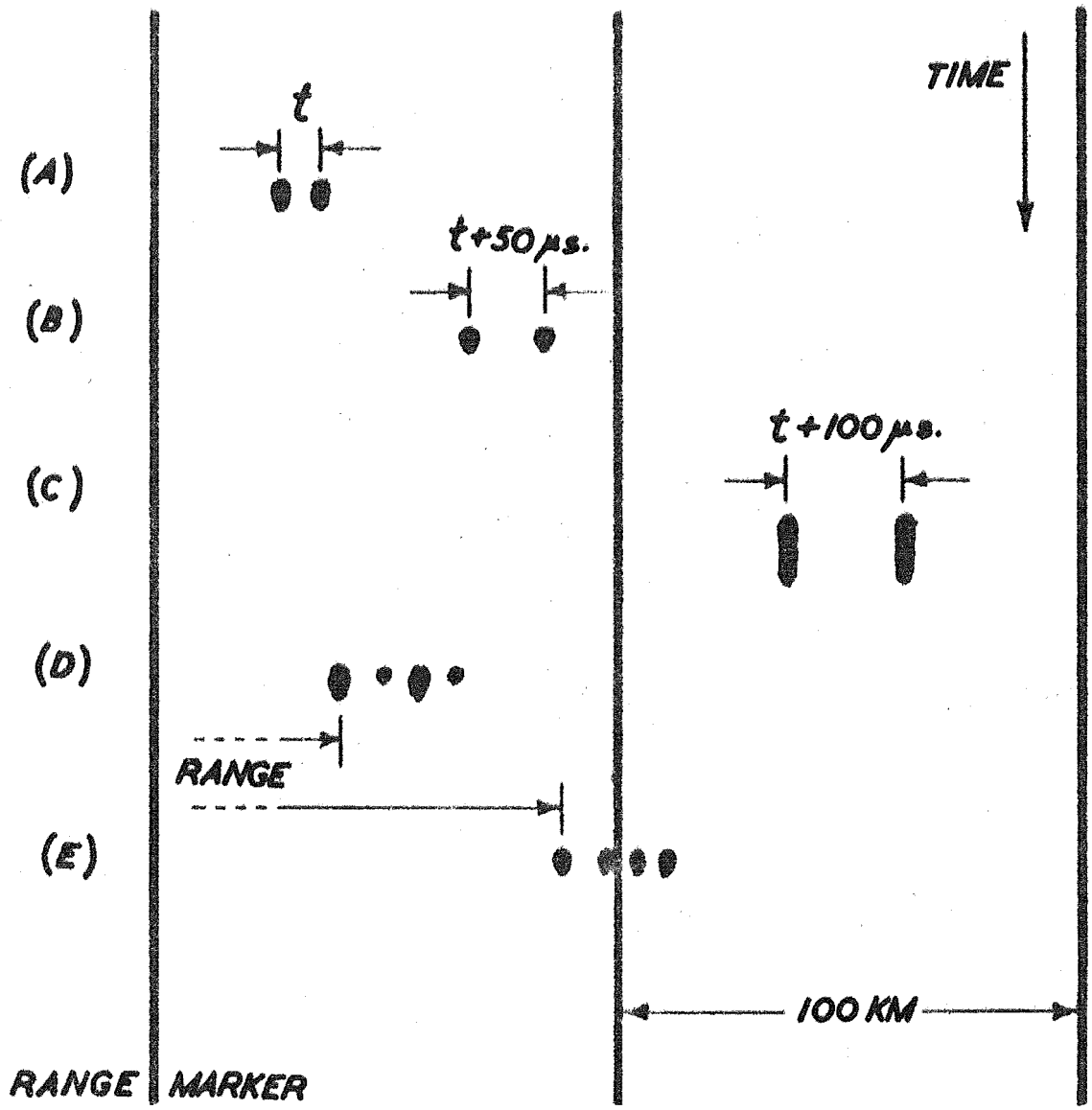


FIGURE 2. Triple-channel display of echoes. These schematic examples represent (A) an echo via Receiver 1, (B) an echo via Receiver 2, (C) a moderately long-duration echo via Receiver 3, (D) a strong echo received by Receiver 2 with weak returns via Receivers 1 and 3, (E) a relatively rare type of echo for which the signal amplitude appears the same from all three receivers.

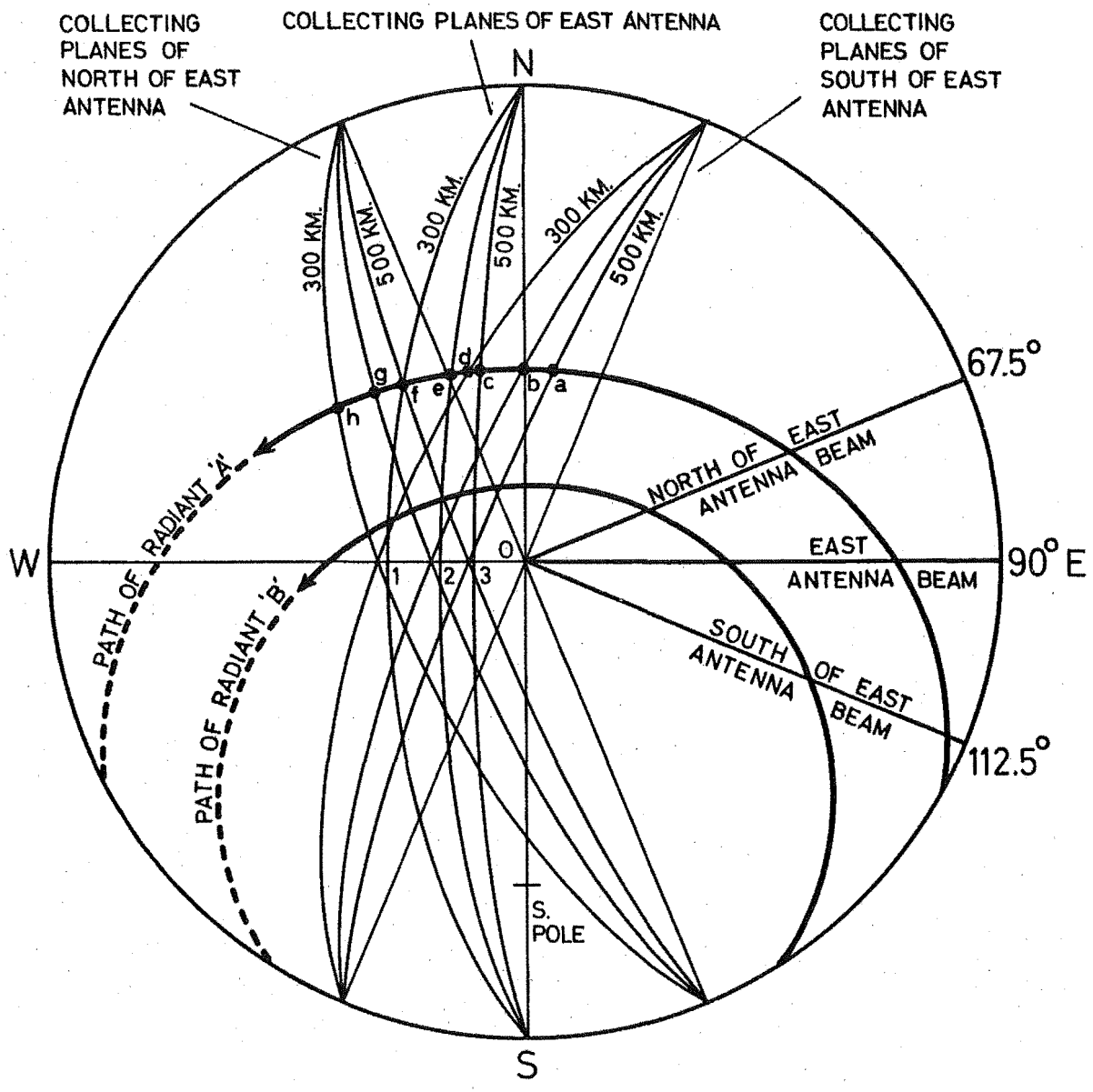


FIGURE 3. Horizontal projection of celestial hemisphere, showing the collecting planes for each of the three narrow beam antennas.

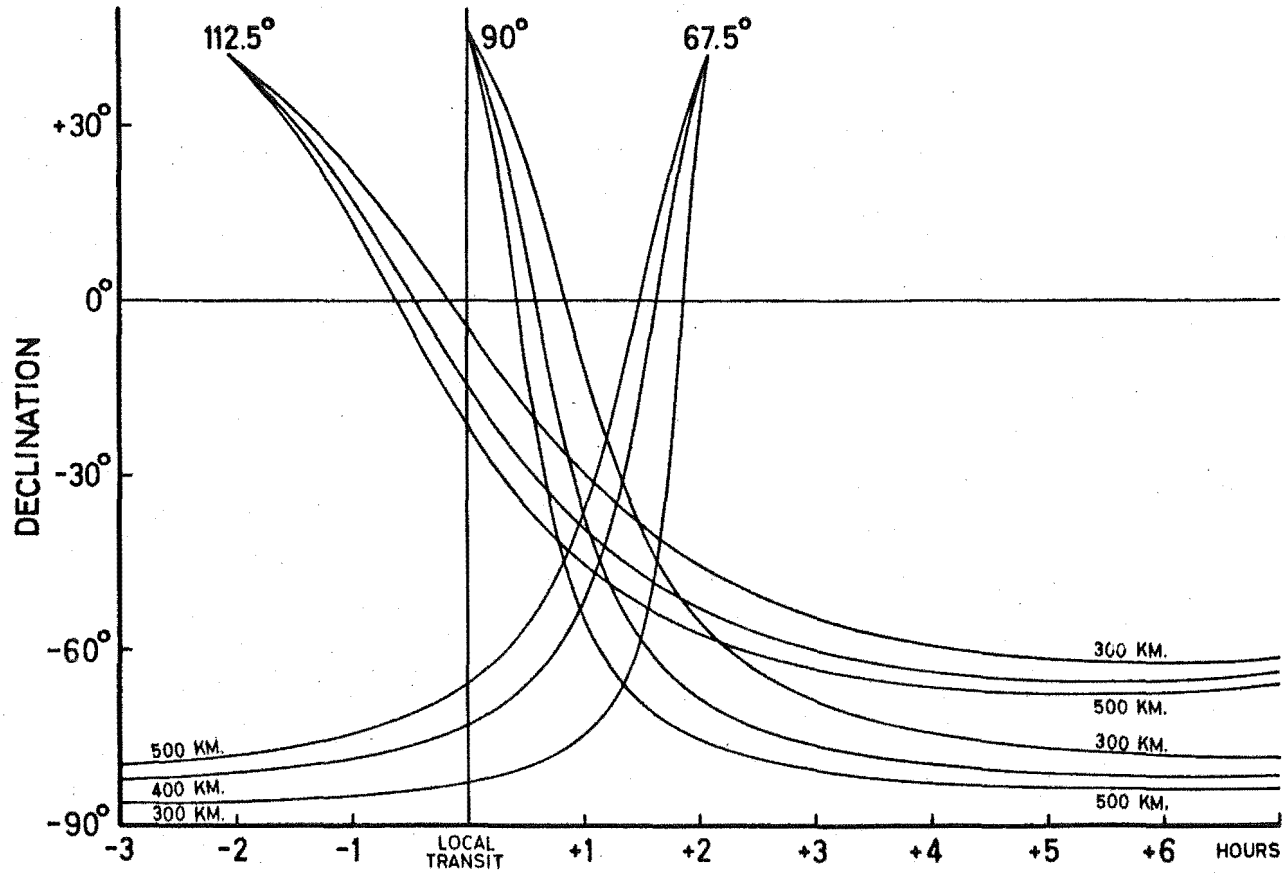


FIGURE 4. Times of reception of meteor echoes at various ranges in each of the three antennas, plotted as a function of radiant declination.

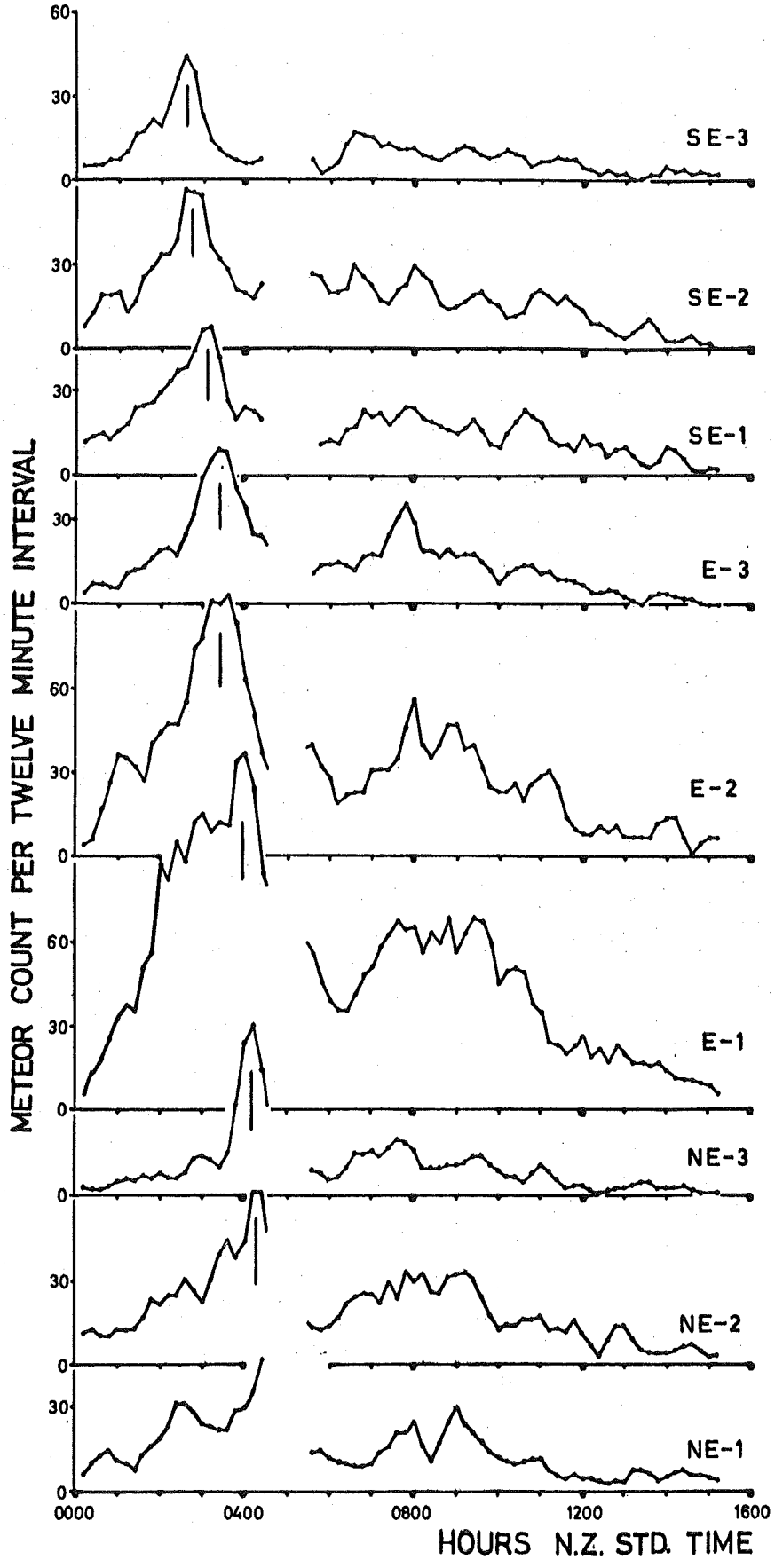


FIGURE 5. Partial rate curves for 1962, July 25. The Delta Aquarid shower is marked.

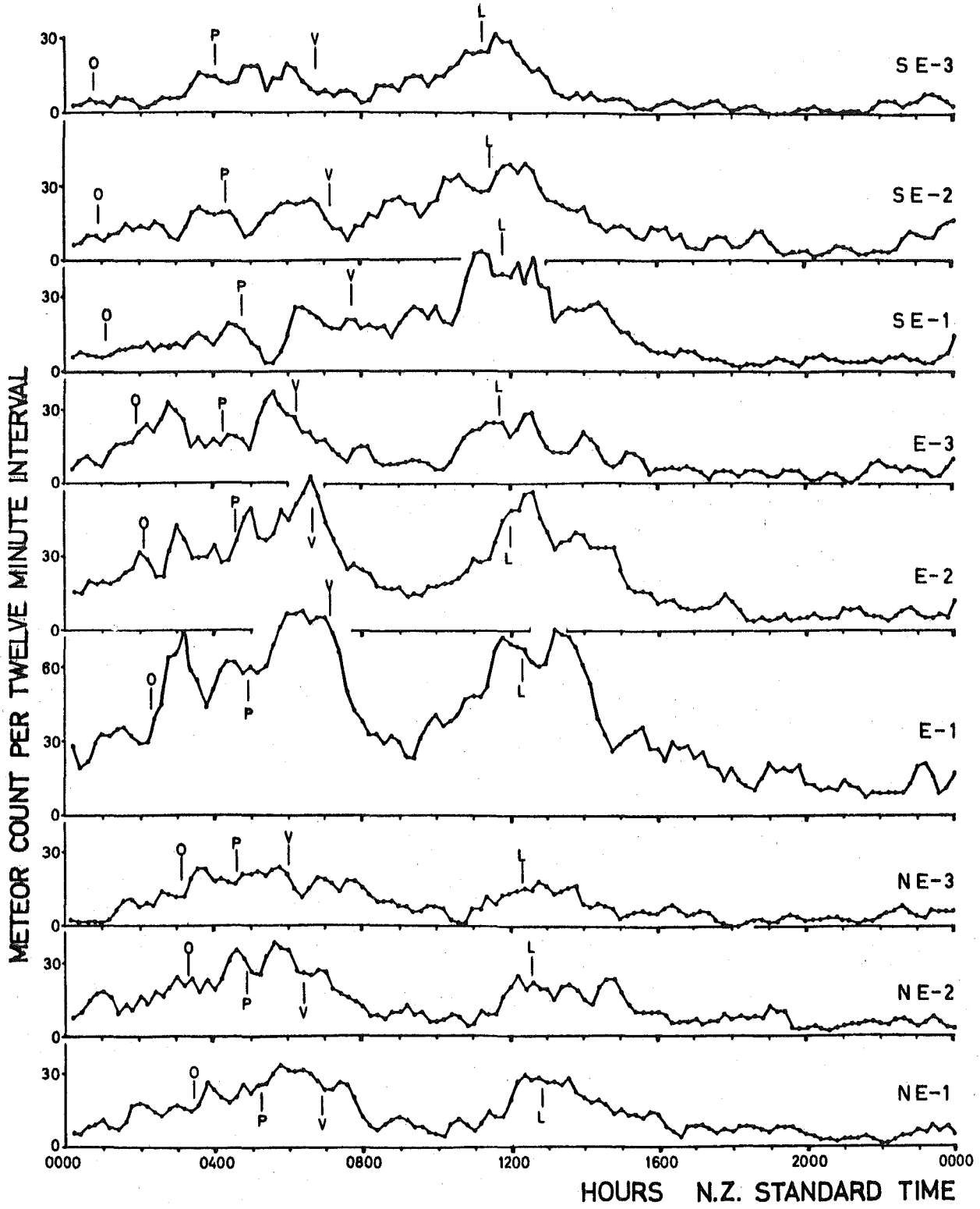


FIGURE 6. Partial rate curves for 1962, December 4.
"O" is where the Orionid shower was expected to appear
"P" " " " Puppid " " " " "
"V" " " " Velid " " " " "
"L" " " " Librid " " " " "

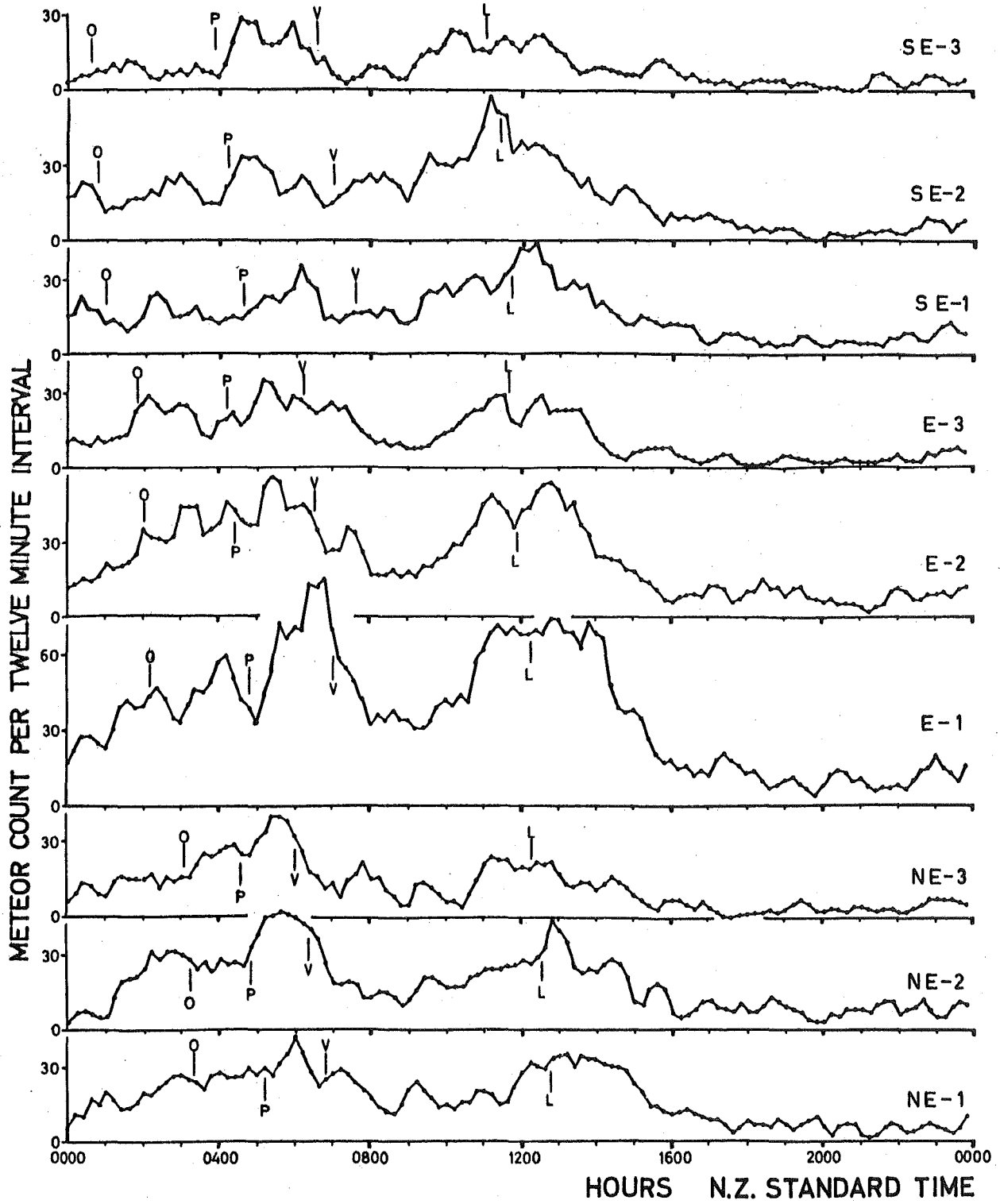


FIGURE 7. Partial rate curves for 1962, December 5.
"O" is where the Orionid shower was expected to appear
"P" " " " Puppid " " " " "
"V" " " " Velid " " " " "
"L" " " " Librid " " " " "

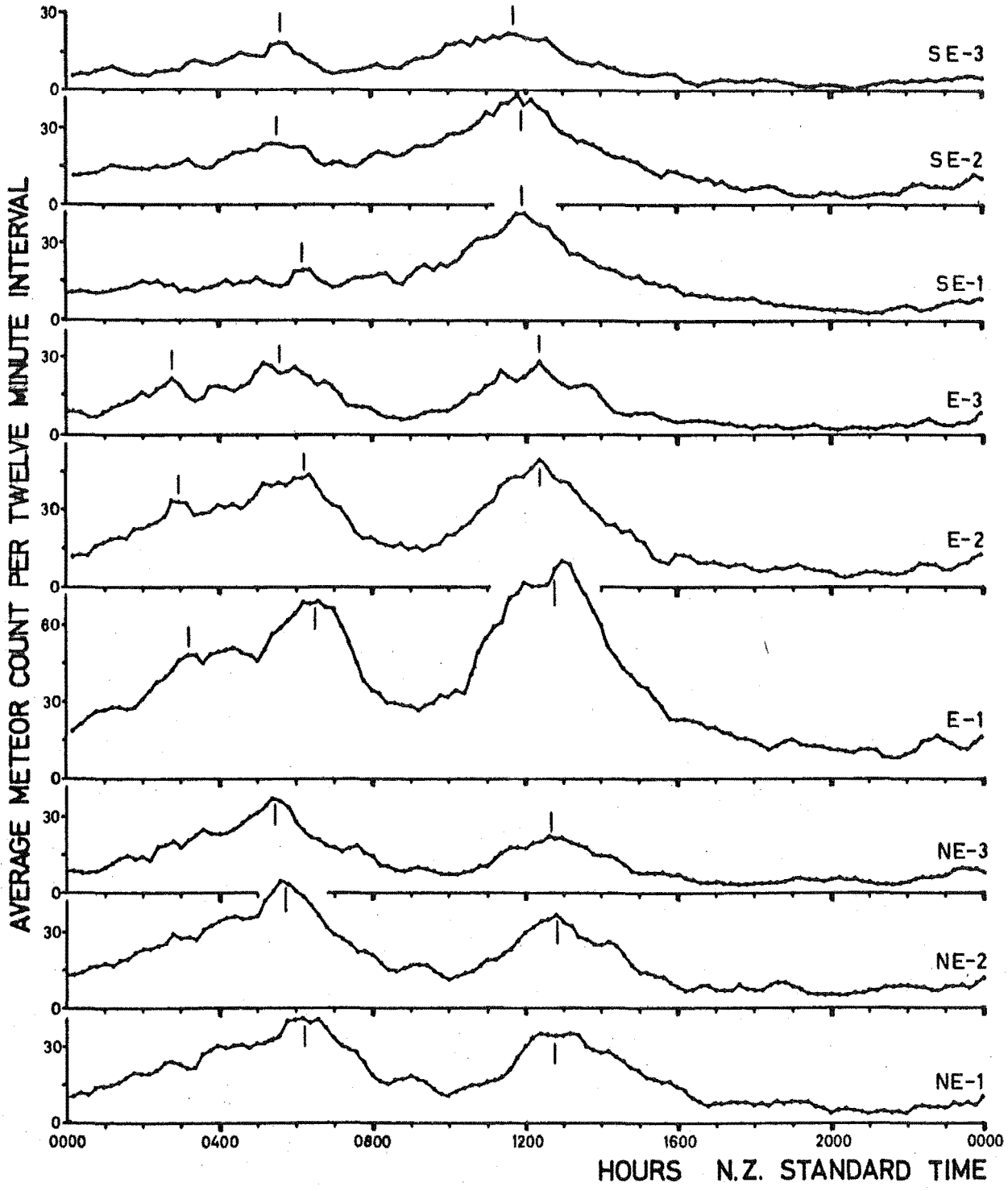


FIGURE 8. Mean partial rate curves for the whole week from December 4 - 10, 1962. The times adopted for the passage of each principal maximum of activity are marked.

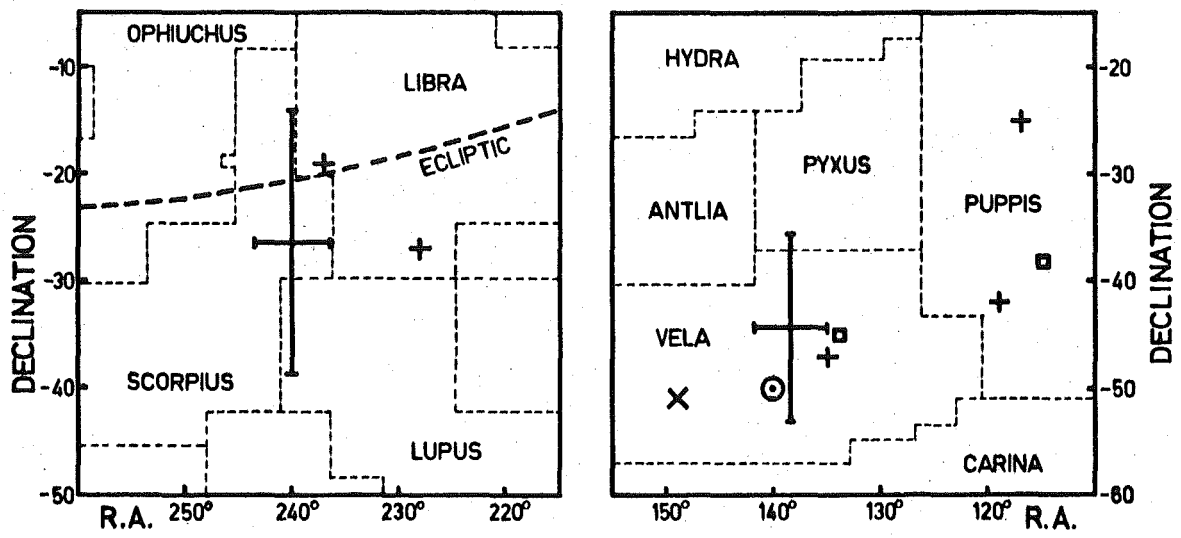


FIGURE 9. (a) A plot of the radiant position derived for the Librid-Scorpid activity together with the positions of Librid activity (crosses) found by Ellyett, Keay, Roth and Bennett (1961); (b) the radiant position derived for the Velid activity is shown together with the other Velid-Puppid radiants found by

- X Hoffmeister (1948),
- ⊙ Weiss (1960),
- \+ Ellyett, Keay, Roth and Bennett (1961),
- ◘ Ellyett and Roth (1964).

# PART B

# THE MEASUREMENT OF METEOR RATES

## 7. A YEAR-LONG SURVEY OF METEOR RATES

In 1958 it was decided to conduct a survey of meteor rates, and work commenced on the necessary equipment. The primary object of the survey was to determine as accurately as possible the annual and diurnal variations in the rate of detection of meteors in the southern hemisphere. Such information was badly needed to provide a comparison with data gathered in the northern hemisphere. For example, the non-shower meteor activity observed in the northern hemisphere reaches a maximum in the late northern summer months of July, August and September (see Chapter 9). It was not known whether this was a terrestrial summer effect or whether it was brought about by the presence of a greater density of meteoric matter along the earth's orbit.

There was, therefore, a distinct need for meteor rate data to be gathered over periods of a year or more. The equipment used for obtaining it had to satisfy several requirements, namely:

(a) Non-selectivity. Ideally the detection threshold for meteors from all radiants above the horizon should be the same. There should be no latitude bias apart from the normal horizon cut-off.

(b) Long-term parameter constancy. Ideally there should be no change in equipment performance over the entire period of observation.

(c) High sensitivity. Neither of the above requirements should be at the expense of sensitivity although low-gain aerials are necessary to attain the greatest possible non-selectivity.

Up to the commencement of the present survey, no meteor rate data satisfying these requirements was available from the southern hemisphere. During 1960, however, the results of some radar meteor observations made in South Australia during 1957-58 were published (Weiss and Smith, 1960). These results were obtained from equipment primarily designed for radiant measurements. They showed a peak of activity during March, 1957, and suggested another peak between December 1957 and April 1958. This pointed to a late summer peak of activity but could not be regarded as conclusive.

In the northern hemisphere a survey using equipment satisfying the above requirements was commenced in 1957 (Neale, 1958), but results have only very recently been tabulated and are not yet readily available (Millman, 1963).

All available information concerning the diurnal variation of meteor activity was also rather inconclusive. Again, this was probably due to the general use of equipment designed for measuring radiants. Such equipment is intentionally selective in operation and the observed diurnal variation in meteor rate is a function of the aerial orientation.

Early Christchurch work, using radiant measuring equipment, revealed that diurnal maxima occur at approximately 2 a.m. and 10 a.m. local time throughout the year (Ellyett and Keay, 1956). The meteor rate averaged only 10 per hour. There was no sign of a maximum at 6 a.m. local time caused by meteors arriving from the apex of the earth's way, which is the direction of influx of meteors being swept up by the orbital motion of the earth. This result was in contrast to that published by Lovell (1954). In his case the equipment was similar to that at Christchurch, the average hourly meteor rate was the same, but the 6 a.m. peak was as prominent as those at 2 a.m. and 10 a.m.

As well as the need to resolve this puzzling inconsistency there was a desire to extend the detection threshold as far as possible to include very small meteors, which, by virtue of their greater numbers, would eliminate any random effects present in the low rate results.

The Christchurch rate-measuring radar equipment was designed with the above points in mind. It will now be described.

## 7.1 Aerial System

The requirement of non-selectivity dictated the use of an omni-directional aerial system. In azimuth this was achieved by the use of two horizontal dipoles set and fed at 90 degrees to one another. This turnstile arrangement, as it is called, followed an earlier design by G.J. Fraser (1954). The original version was set 0.325 wavelengths above the ground in order to give a vertical radiation pattern which kept the returned echo power constant over as great a range of elevation as possible (ibid). However, Fraser's original version had the disadvantage that the feeder system was too close to the ground and susceptible to damage by grazing animals. This has been overcome by standing the dipoles on four lengths of 1" brass tubing, each 0.75 wavelengths long, as shown in Figure 1. This enabled the reflector plane to be in the form of a wire mesh screen at a height of over six feet above the actual ground level. Support for the four lengths of brass tubing was provided by insulators mounted in the plane of the reflector screen. The 480 ohm open wire feeder was brought in under the reflector screen.

The vertical radiation pattern of the aerial was slightly modified by the finite size of the ground plane, as may be seen from Figure 2 which reveals a small lobe at 20 degrees elevation. Figure 2 is a plot of power gain as a function of elevation and was obtained by the balloon technique described in Chapter 5. The maximum power gain (compared with an isotropic radiator) was found to be 4.35 at an elevation of 60 degrees, which is very close to the calculated maximum value of 4.37 at 55 degrees elevation.

The minor lobe in the radiation pattern at 20 degrees elevation produces a small hump at 250 km in the range distribution of meteor echoes (Figure 3). As a rather fortunate result of this, the equipment response function is practically flat for a 40 degree spread of radiant elevations (see Figure 4, Chapter 9).

At the commencement of the survey a single aerial was in use but this proved inadequate due to trouble with the common aerial transmit-receive switching. The CV1507 spark-gaps used as switching devices had a very limited life and caused considerable trouble with the receiver. By December, 1959, a duplicate aerial, fed directly from the transmitter, was in operation, and the original aerial was used for reception only, thus eliminating the spark gaps.

## 7.2 Transmitter

A modified G.L. Mark II radar transmitter was used. An identical unit was kept on standby. Whenever a fault developed, an automatic transmitter controller designed by R.G.T. Bennett (1953) made three attempts to restore full power. If the fault did not clear, the transmitter was switched off. Very little work was required to bring the standby transmitter into operation and as a result the time lost due to transmitter failure was kept to a minimum.

## 7.3 Receiver and Display, etc.

The receiver has been adequately described in Chapter 5.

The display console housed an intensity modulated cathode ray tube and its associated circuitry. The line sweep on the c.r.t. screen was photographed on continuously moving film and appeared the same as the record shown in Figure 14 of Chapter 5, except that only a single echo-dot spacing was required and the range markers were spaced at 250 km intervals. A clock and detector current meter were also photographed at three minute intervals.

The master control unit was substantially the same as for the triple-channel experiment.

## 7.4 Equipment Performance

Throughout the survey the performance of the equipment was continually monitored. Although the experiment started in July 1959, it was not until February 1960 that the whole system was brought into acceptably reliable operation and performance variations were considered to be negligible. Thereafter the experiment ran for a full year until the end of January 1961. During the year the number of hours of observation ran as high as 99.4 percent of the total hours in the month for one month and was never lower than 80 percent. The transmitter power variations were held within four percent and the receiver noise figure was always kept low enough for galactic noise to limit the signal-to-noise ratio. Man-made noise, when it occurred, was the worst hazard and created more gaps in the record than any other cause. The actual steps taken to maintain parameter constancy in the equipment were given by Ellyett and Keay (1962) in a contract report. The relevant extract is reproduced in Appendix 2.

FIGURE 1

The omni-directional transmitting
aerial and elevated reflector screen

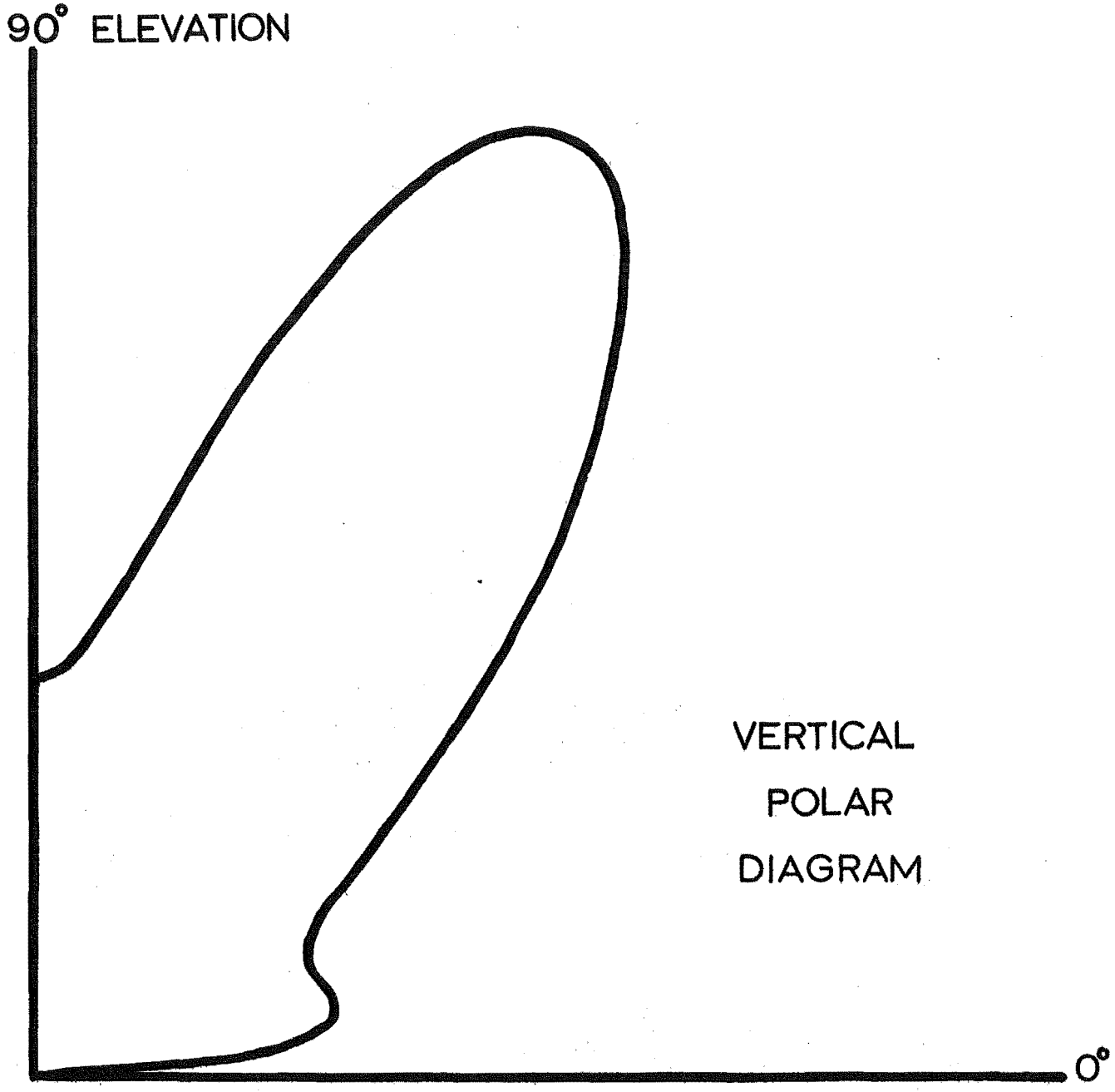


OMNI-DIRECTIONAL AERIAL POWER GAIN

Fig. 2

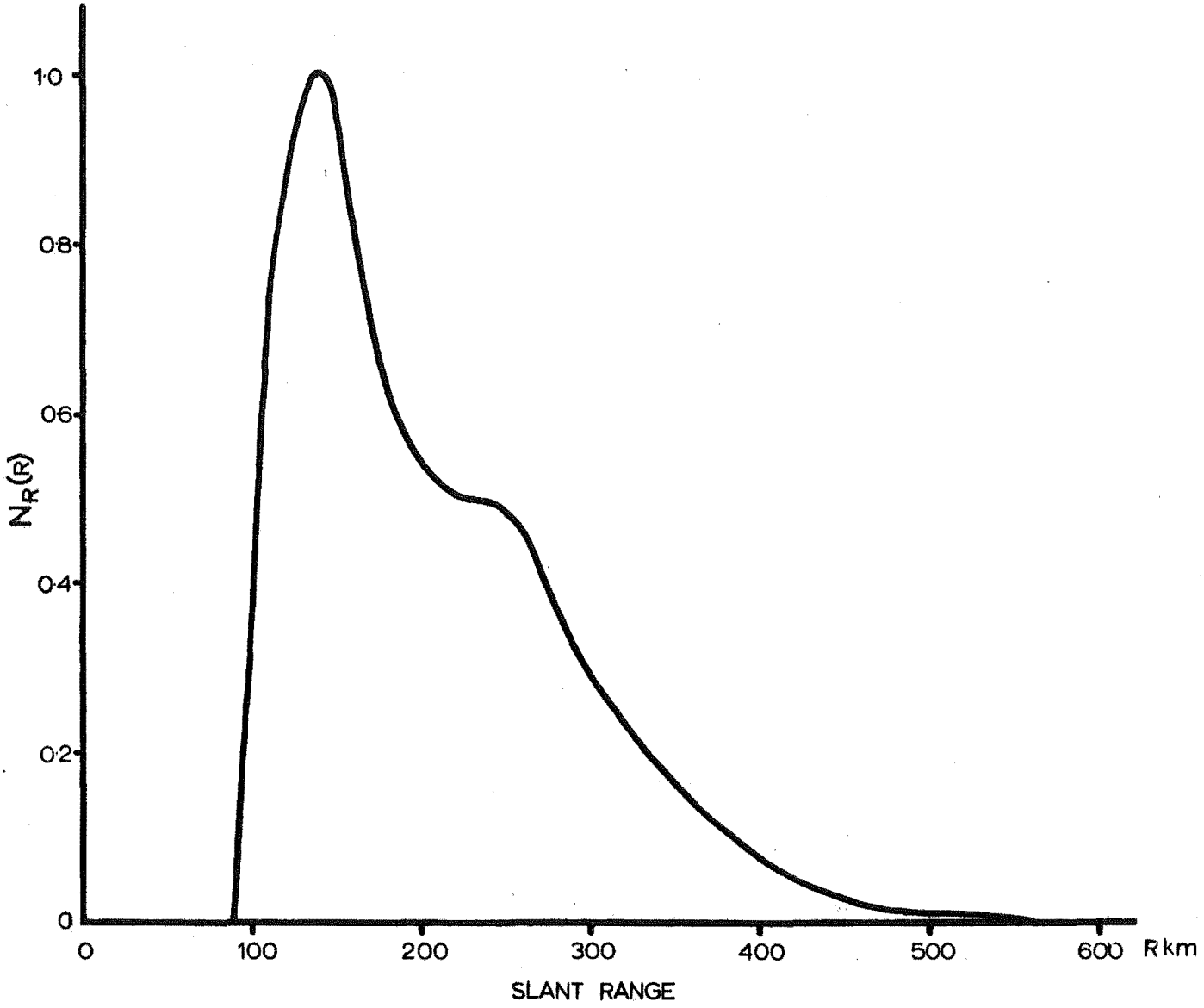


RANGE DISTRIBUTION OF METEOR ECHOES

Fig. 3

## 8. THE SURVEY RESULTS

The hourly values of meteor rate, for each day of the year-long survey, are tabulated in monthly groups in a paper by Ellyett and Keay (1963).

A chart of the meteor activity throughout the whole year is given in Figure 1. This shows the activity at any hour at any time of the year, and brings out the very great rise in activity in late July and again in early December. The activity does not appear or disappear suddenly. The meteor rate over a period of weeks builds up to the peak rate and dies away just as slowly. The significance of these peaks of meteor activity is discussed in Chapter 11.

The peaks, however, only represent a fraction of the total daily activity. This is evident from the histogram in Figure 2 which shows the average number of meteors per day for each month of the survey year. The July and December peaks have increased the total daily activity of those months above that of their neighbours by scarcely ten per cent.

The annual variation depicted by Figure 2 formed the basis of the work described in the next chapter, where it is shown that variations in the space density of meteoric matter around the earth's orbit exert a smaller influence on the observed meteor rates than the angle

between the observing station and the apex of the earth's way. Figure 3 illustrates how this angle is greatest at the vernal equinox and least at the autumnal equinox, being related to the direction of the earth's axial tilt.

Figure 3 also indicates how the diurnal variation in meteor rate arises. Figure 4 shows the diurnal variation averaged over the survey year. This curve would be close to a pure sinewave if the radiants of sporadic meteors were distributed isotropically over the celestial sphere. Such is not the case. The survey showed that the distribution is far from being isotropic and varies from month to month as indicated by the diurnal curves in Figures 5 (a) and (b). These curves were the basis of a study of the radiant distribution of sporadic meteors which is described in Chapter 10.

Diurnal curves were also drawn for each third of a month but in most cases the differences were not great enough to warrant extra analysis. Only in the month of July, when the largest peak of activity occurred, were the differences at all large. This is shown by Figure 6, in which the rate in the early morning is very high in the latter third of the month. However, the three curves coincide quite closely for several hours about the late afternoon minimum. This happened for all other months as well, despite variations in rate during times of shower

activity at night or in the early morning, and provided independent confirmation that the equipment sensitivity remained essentially constant.

Most of the more important results from the survey were given in three published papers. These were first produced as contract reports, which is the format in which they appear in the next three chapters.

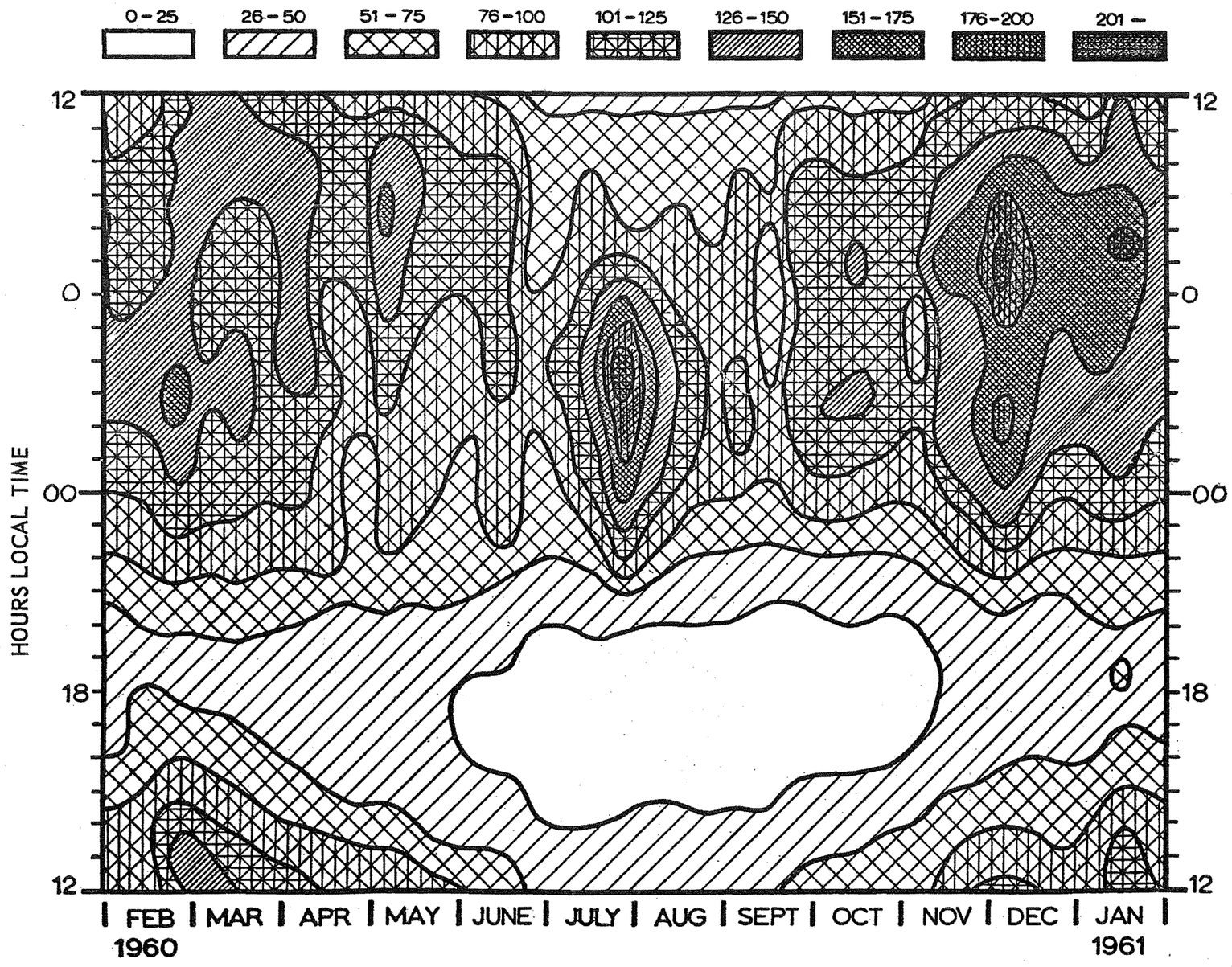


CONTOURS OF CONSTANT METEOR ECHO RATE THROUGHOUT THE YEAR FROM FEBRUARY 1960 TO JANUARY 1961

Fig. 1

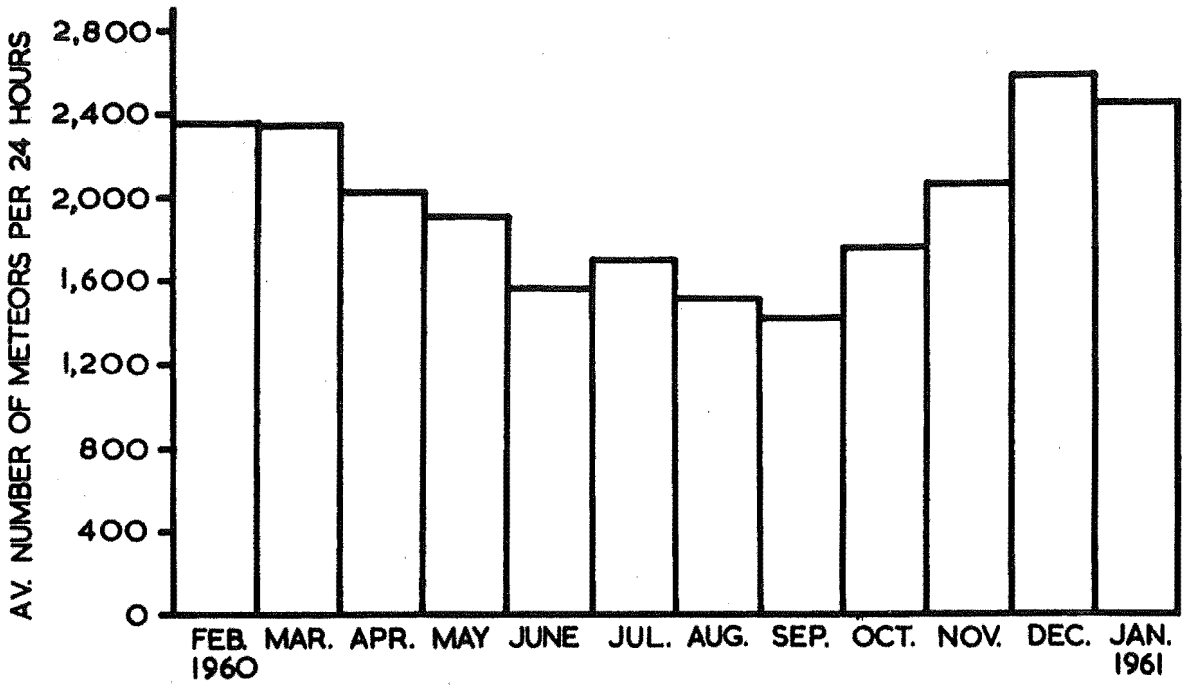


AVERAGE NUMBER OF METEORS PER 24 HOURS.

Fig. 2

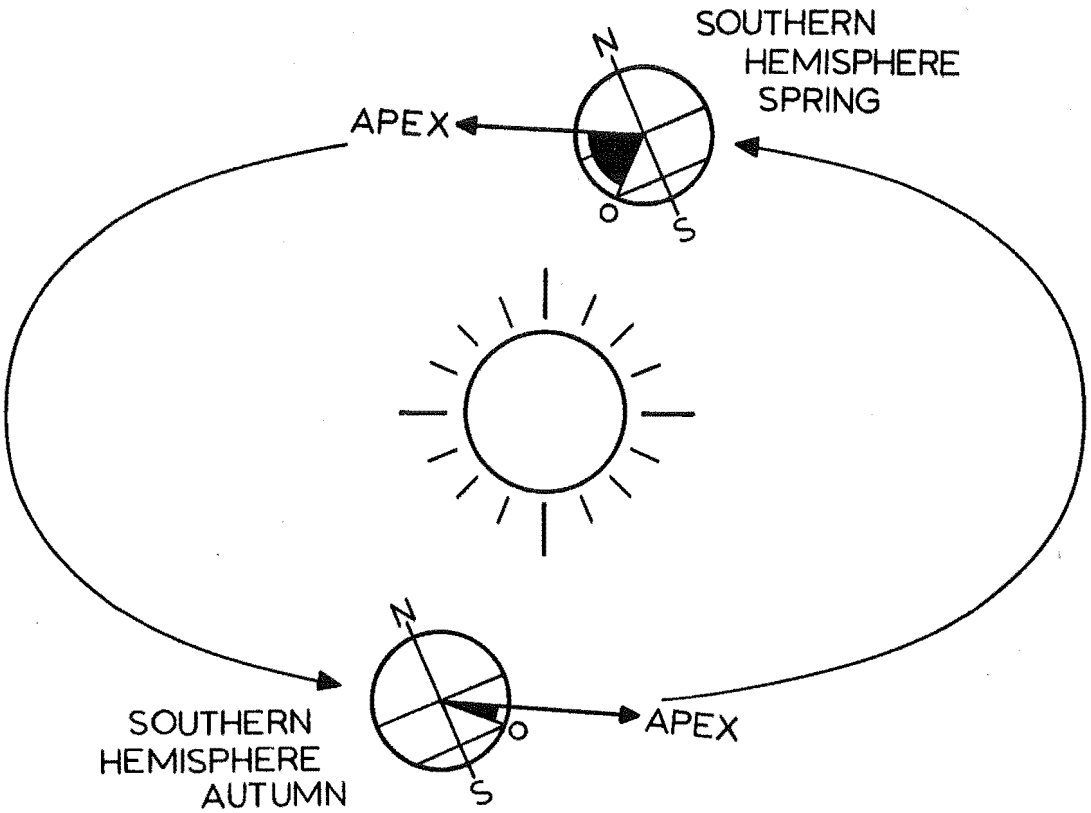


SEASONAL VARIATION IN ANGLE BETWEEN OBSERVING STATION, O, AND THE APEX OF THE EARTH'S WAY.

Fig. 3

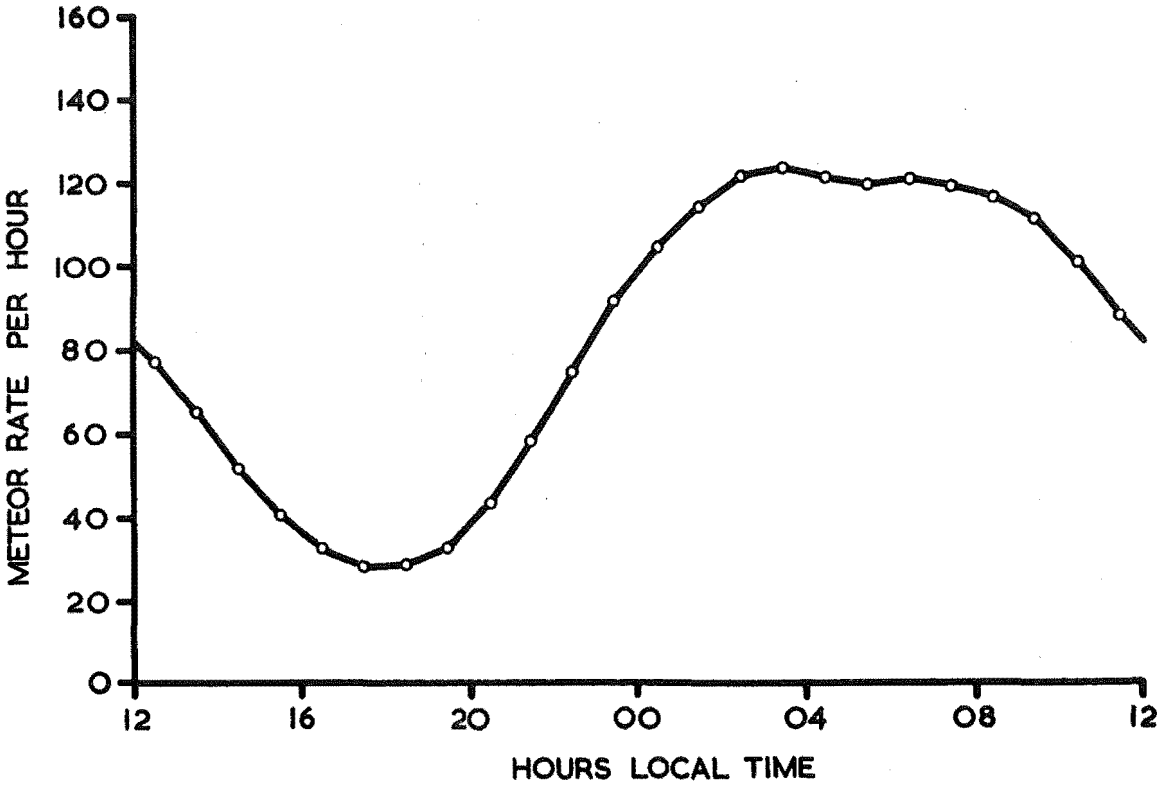


HOURLY METEOR RATES, CENTERED ON THE HALF-HOUR, AVERAGED OVER THE YEAR FEBRUARY 1960 - JANUARY 1961. (Minimum at 1800 H. LT, ≡ 1830 H. NZST, ≡ 0630 H. UT.)

Fig. 4

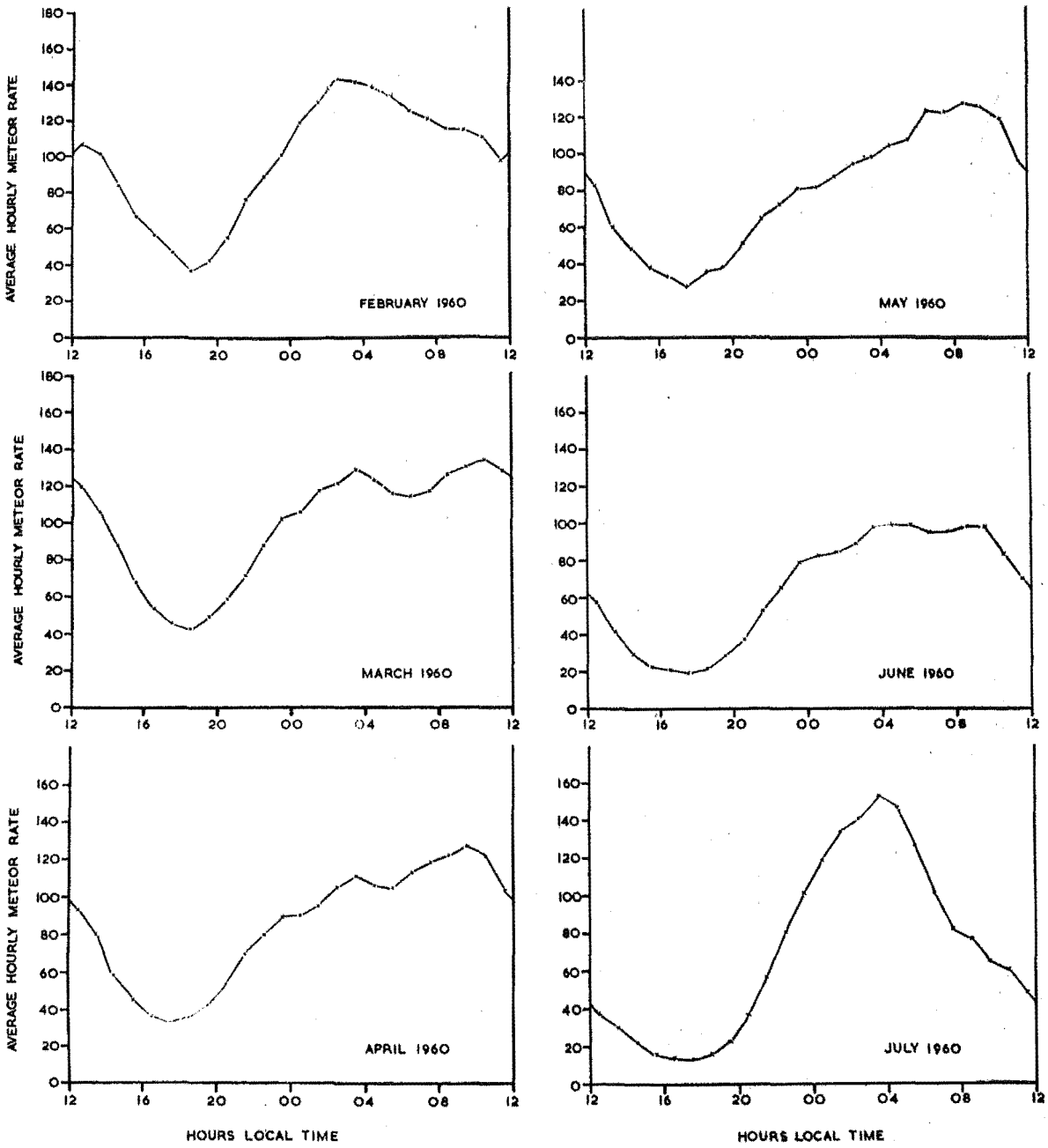


FIG. 5a.

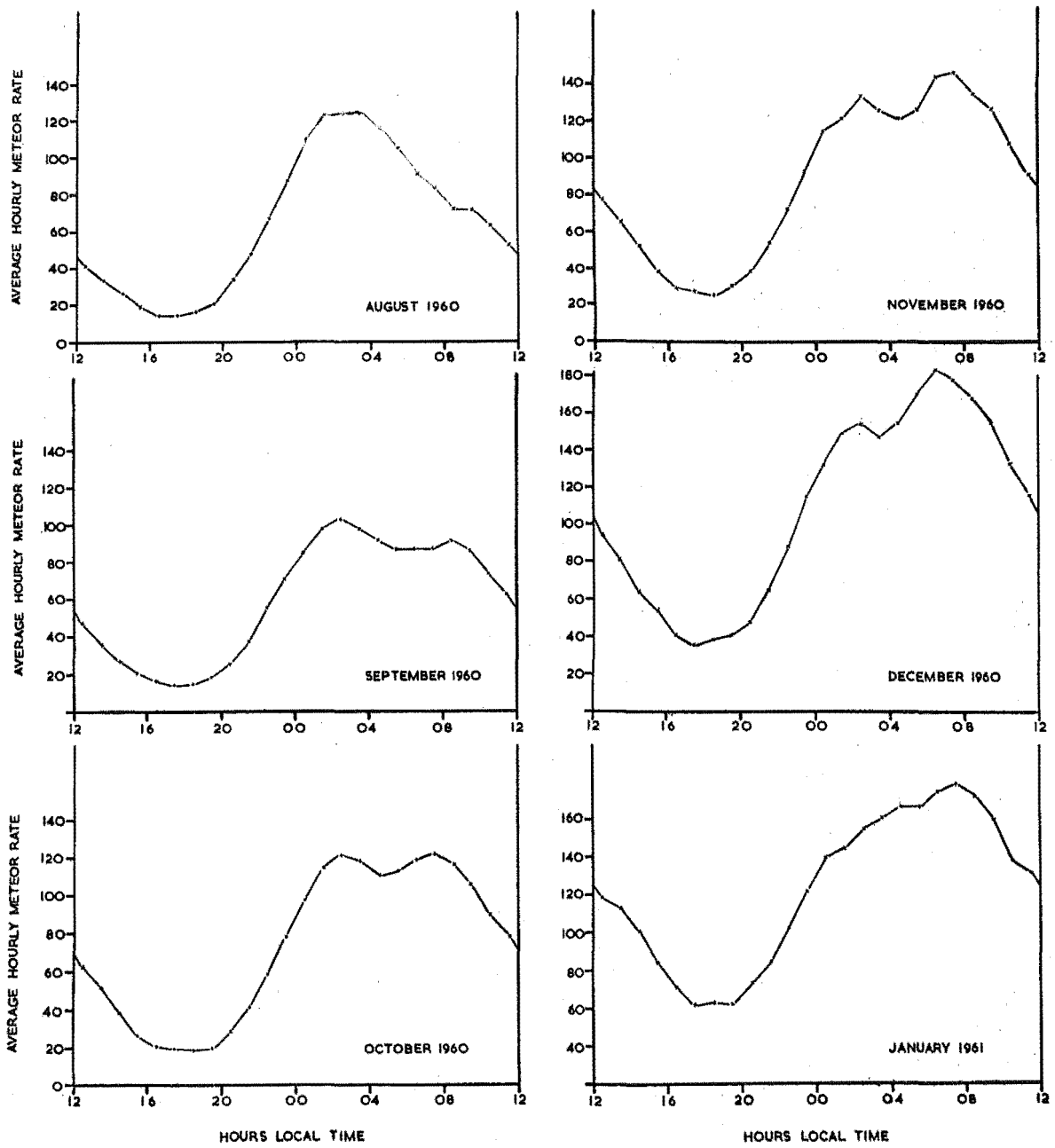
AVERAGE HOURLY METEOR RATE
AUGUST 1960
NOVEMBER 1960
SEPTEMBER 1960
DECEMBER 1960
OCTOBER 1960
JANUARY 1961
HOURS LOCAL TIME
HOURS LOCAL TIME

FIG. 5b.

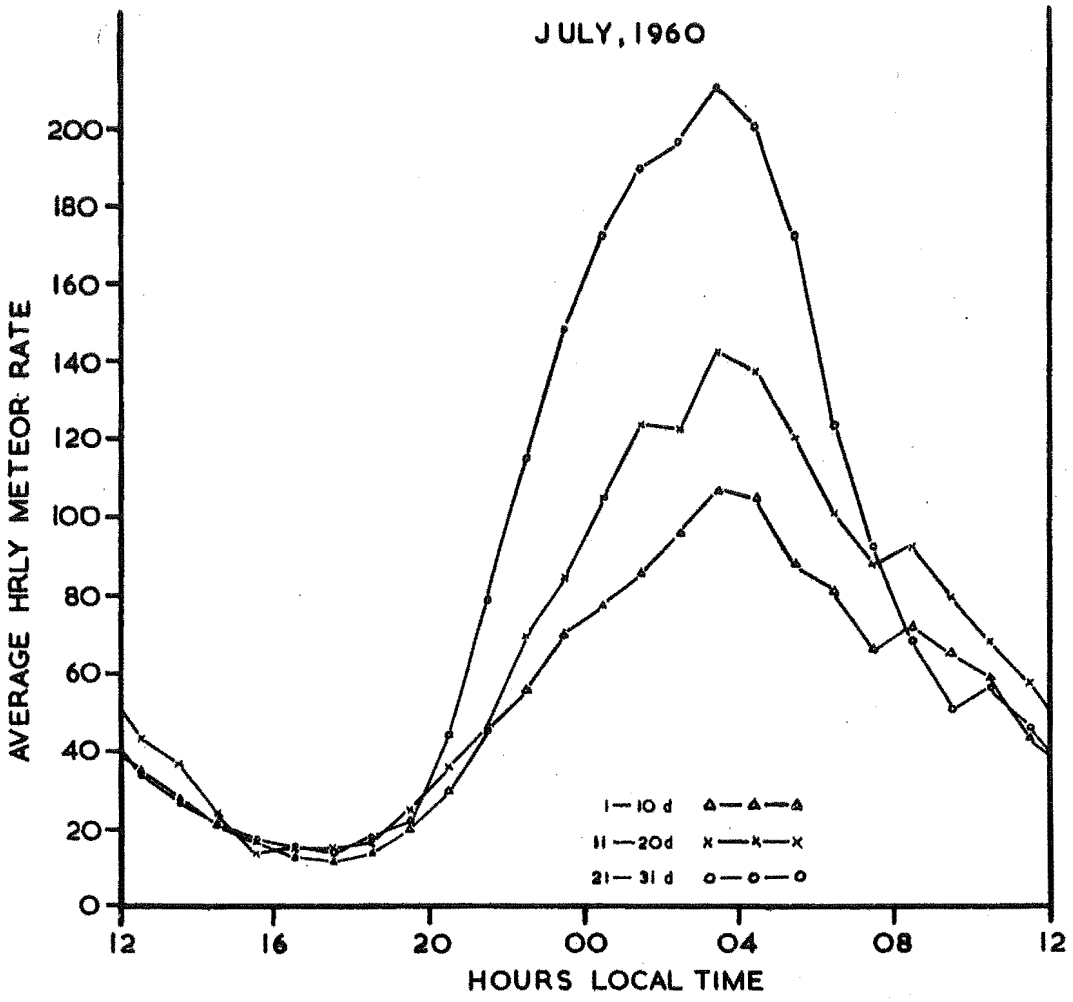
JULY, 1960
AVERAGE HRLY METEOR RATE
200
180
160
140
120
100
80
60
40
20
0
12
16
20
00
04
08
12
HOURS LOCAL TIME
1—10 d
11—20d
21—31 d

Fig. 6

## 9. THE DISTRIBUTION OF METEORS AROUND THE EARTH'S ORBIT

(This Chapter has already been published with the above title as a paper under my name. It appeared in the Monthly Notices of the Royal Astronomical Society, Volume 126, page 165, 1963.)

In this chapter the variation of incident meteor flux with solar longitude is determined and it is confirmed that the spatial density of small-size (sixth magnitude) meteoric matter is greater along the earth's orbit during the latter half of the year. The comparison of results from both hemispheres shows that at mid-latitude observing stations this asymmetrical distribution has a smaller influence than the earth's axial tilt on the seasonal variation in observed meteor rate. Taken together these effects are found to account for most of the differences between the results from both hemispheres.

The relative density of meteoric matter along the earth's orbit was derived by a method adapted from the work of Kaiser (3*). The successive steps in the derivation are outlined schematically in a fold-out flow diagram included as Figure 10 at the end of this chapter. Steps taken to check the validity of the method are also indicated in Figure 10.

---

* The bracketed numbers in this chapter refer to a separate bibliography at the end of the chapter.

1. Introduction - The preliminary results and basic data of a year-long survey of meteoric activity in the southern hemisphere have recently been published (1,2). It is the purpose of this paper to discuss the results more fully, with particular regard to the factors controlling the observed diurnal and seasonal rate variations. The meteor rate data obtained during the survey is particularly good for such an investigation, as the hourly rates, sometimes exceeding 200 per hour, are high enough to ensure that statistical fluctuations in rate are very small. Because of this, and the maintenance of constant equipment sensitivity throughout the whole survey, the true form of the temporal variation is easily recognised.

It has long been realised that the geometrical relationship between the observing station and the apex of the earth's way is the main factor controlling the diurnal variations in meteor rate. However there has been some uncertainty whether the same factor also controls the seasonal variation or whether meteor density variations around the earth's orbit exert a greater degree of control. This question has not until now been properly resolved, mainly for want of meteor rate data of the required accuracy from both hemispheres, although the large number of observations made in the northern hemisphere may be combined to give an accurate curve for the seasonal variation in that hemisphere.

In this paper the equipment sensitivity and consequent magnitude distribution of the detected meteors will first be discussed in order to establish the range of meteoric particle sizes for which the conclusions will be valid. The relationship between radiant elevation and echo rate, for the azimuthally omni-directional aerials used, is next obtained. This allows the theoretical seasonal variation in echo rate to be calculated for any given radiant distribution model. Comparison of the theoretical seasonal variation with that actually observed enables the spatial distribution of meteoric material to be found.

2. Equipment Sensitivity - The minimum detectable line density, $\alpha_p$, of ionization in a meteor trail is related to the system parameters by (3,4)

$$\alpha_p = 6.307 \times 10^{15} \left\{ \frac{1}{\lambda^3} \cdot \frac{R^3}{G_T G_R} \cdot \frac{P_R}{P_T} \right\}^{\frac{1}{2}} \text{ electrons per} \quad (1)$$

metre for decay type echoes, which are those received when $\alpha_p$ is less than $2.4 \times 10^{14}$ electrons per metre.

In equation (1) R is the slant range of the echo and $\lambda$ is the wavelength used (4.31 m. for the present survey); $G_T$ and $G_R$ are the transmitting and receiving aerial gains respectively; $P_R$ is the minimum detectable echo power and $P_T$ is the transmitted peak pulse power. In the case when the

polarisation of the incident wave is transverse to the meteor trail, echo enhancement due to plasma resonance may occur, reducing the value of $a_p$ by a factor of up to two (5). However, with the equipment and aerial characteristics used in the survey, the proportion of decay type echoes exhibiting significant enhancement is small enough for the effect to be ignored. This enhancement does not occur with persistent echoes for which the minimum detectable line density is given by

$$a_p = 9.949 \times 10^{20} \left\{ \frac{1}{\lambda^3} \cdot \frac{R^3}{G_T G_R} \cdot \frac{P_R}{P_T} \right\}^2 \text{ electrons per metre} \quad (2)$$

which holds whenever $a_p$ is greater than $2.4 \times 10^{14}$ electrons per metre.

For the equipment used the minimum detectable echo power, $P_R$, was determined experimentally, using artificial echoes randomly distributed in time, range and amplitude (6). The value of $P_R$ adopted was that of a signal having a 90% probability of detection. For echoes of 0.25 second duration the value of $P_R$ was found to be $1.33 \times 10^{-14}$ watts, which, taking $P_T = 81 \times 10^3$ watts, yields a ratio of received to transmitted power equal to $1.64 \times 10^{-19}$ (188 db). Meteors will still be detectable below the adopted value of $P_R$ since this value - corresponding to 90% detection probability -

is approximately 8 db above noise level; however the duration of weak echoes will certainly be less than 0.25 second corresponding to a higher value of $P_R$ than that adopted. These two effects will tend to cancel each other, making the adopted value of $P_R$ a fairly reasonable one.

For the survey the aerials used were omni-directional in azimuth and the factor $R^3/G_T G_R$ is a function only of the angle of elevation, $\theta$, if the usual assumption is made that the meteoric echoes are returned from a relatively thin layer of the upper atmosphere. Thus we have the geometrical relation

$$R = \{r_e^2 \sin^2\theta + h(2r_e + h)\}^{\frac{1}{2}} - r_e \sin\theta \qquad (3)$$

where $r_e$ is the radius of the earth (taken as 6370 Km) and h is the mean height of the echo layer above the earth. The value of h varies according to the size, speed and angle of incidence of the meteors (7), but for meteors of the mass and velocity range most commonly detected a value of 95 Km is suitable.

At an angle of elevation, $\theta$, of $60^\circ$ the value of $R^3/G_T G_R$ is a minimum, leading to a minimum detectable line density, $\alpha_{p_o}$, equal to $2.80 \times 10^{12}$ electrons per metre for decay type echoes, as shown by the dotted curve in Fig. 1. The maximum error in $\alpha_p$ is less than 20% provided the assumpt-

ions made earlier are valid.

The zenithal radio magnitude of a meteor is usually defined by the relation

$$M_R = 40 - 2.5 \log_{10} \alpha_z = M_V + \Delta M(v) \qquad (4)$$

where $\alpha_z$ is the maximum zenithal line density which the meteor would produce if it entered the atmosphere vertically. For meteors entering the atmosphere at a zenith angle, $\chi$, the zenithal line density is given by

$$\alpha_z = \alpha_m (\cos \chi)^{-1} \qquad (5)$$

where $\alpha_m$ is the maximum line density produced by the meteor. The velocity dependent correction term in equation (4), $\Delta M(v)$, is negligible if the average meteor velocity is 40 Km/sec, (8). This velocity has been adopted, since it is the most commonly encountered meteor velocity, and therefore the absolute visual magnitude, $M_V$, will closely equal the zenithal radio magnitude.

The values of $\alpha_p(\theta)$ shown by the dotted curve in Fig. 1. represent the limiting values of $\alpha_m$. The corresponding values of $\alpha_z$ are shown by the full curve. The ordinate scale on the right hand side of Fig. 1. shows the limiting value of the zenithal radio magnitude as a function of elevation when used with the full curve (the dotted curve will give the app-

arent radio magnitude.)

From Fig. 1. we see that the zenithal radio magnitude of the smallest meteor detected by the equipment was +8.2. These meteors were recorded at an elevation of 53°, corresponding to a range of approximately 120 Km.

During the twelve months of the survey extensive measures were adopted (2) to ensure constancy of all equipment parameters and the elimination of sensitivity variations due to external noise, both man-made and natural.

3. Meteor Echo Distribution - The aggregate range distribution of the meteor echoes was determined by examining selected samples of the film records and reading the range of each echo by means of an interpolation scale based on the range markers. The echoes were counted in range intervals of width, $\Delta R$, equal to 10 Km, and the number of echoes per unit range interval, $n_R(R)$, was obtained as a function of the slant range, R. This enabled the distribution of meteor echoes to be found as a function of elevation, $\theta$ .

In a given time interval the total number of recorded echoes will be

$$N = \int_R n_R(R)\, dR = \int_0^{\frac{\pi}{2}} n_\theta(\theta)\, d\theta \qquad (6)$$

where $\theta$ is the angle of elevation. Accepting the assumption

that the echoes originate from a relatively thin layer at a height of 95 Km, it is valid to use the relation between R and θ given by equation (3) to yield the expression

$$\frac{dR}{d\theta} = - \frac{\text{Cos } \theta}{\frac{1}{r_e} + \frac{\text{Sin } \theta}{R}} \qquad (7)$$

Now $dN = n_R(R)\, dR = n_\theta(\theta)\, d\theta$ for echoes returned from an elemental annular volume of the echo layer, so we may write

$$n_\theta(\theta) = n_R(R)\frac{dR}{d\theta} \qquad (8)$$

The computed elevation distribution of meteor echoes is plotted in Fig. 2, which reveals that a minor lobe at 20 degrees elevation in the vertical radiation pattern of the omni-directional aerial exerts a marked effect on the distribution.

By combining the elevation distribution in Fig. 2 with the equipment sensitivity function in Fig. 1, the magnitude distribution of recorded meteor echoes may be derived. The usual assumption is made that the number of incident meteors, dN, with zenithal radio magnitudes between M and M + dM is given by the incremental law

$$dN = C\, a^M dM \qquad (9)$$

where C is a constant defining the meteor flux and a is the ratio of increase in the number of meteors between magnitudes M and

M + 1. The value of a appears to be closely equal to 2.5 (3,9) over most of the range of meteor magnitudes encountered in the survey.

Integrating equation (9) from $M = -\infty$ to M leads to the relation

$$N(M) = \frac{C}{\ln a} a^{M} \tag{10}$$

where N(M) is the total number of meteors brighter than magnitude M.

For the equipment used, Fig. 1 yields the limiting value of M as a function of elevation angle, $\theta$, and for a small interval $\delta\theta$ we have

$$N(M_\theta) = \frac{C}{\ln a} a^{M_\theta} = n_\theta(\theta) \tag{11}$$

where $n_\theta(\theta)$ is the distribution function shown in Fig. 2.

It follows that the magnitude distribution function $n_M(M)$, or in other words the number of meteors per unit magnitude interval detected between the elevation limits $\theta_1(M)$ and $\theta_2(M)$, is given by

$$n_M(M) = \ln a \int_{\theta_1(M)}^{\theta_2(M)} n_\theta(\theta)\, a^{M-M_o}\, d\theta \tag{12}$$

which may be evaluated numerically. The result is shown in Fig. 3. which reveals that meteors of zenithal radio magnitude +6.2 were those most frequently recorded by the equipment.

In the above derivation no account was taken of the change in detection characteristics of meteors at the transition between decay and persistent-type echoes. This will not, however, alter the value obtained for the magnitude of the most frequently recorded meteor since the number of meteors is relatively small at and beyond the transition point.

4. <u>The influence of radiant elevation on echo rate</u> - When wide aperture omni-directional aerials are used for the detection of meteor echoes the echo rate from a given radiant point at any moment is a function of the radiant elevation and the rate will vary diurnally in a manner depending on the declination of the radiant. The functional relation between radiant elevation and echo rate must be known in order to derive information on radiant distribution from observed echo rates. For the equipment used this equipment response function was obtained by making use of Kaiser's graphical method (3). Normalized meteor sensitivity contours of constant $\rho = \alpha_{p_o} / \alpha_p$ for the dual omni-directional aerial system (comprising identical but separate transmitting and receiving aerials) were drawn on a plane projection of the

echo layer at 95 Km height.

Echo lines, each representing the intersection of the echo layer and the plane through the observing station normal to the radiant direction, were drawn on the above projection for various values of radiant zenith distance. (The geometry of echo production is such that echoes from a radiant at a zenith distance $\chi_o$ are received at elevations up to a maximum of $\theta = \chi_o$). The sensitivity factor may be determined at all points along a given echo line and the total rate $N(\chi_o)$ over all values of range may be obtained by numerical integration from Kaiser's equation

$$N(\chi_o) = F\, f_1(\chi_o, s) \int_1 \rho^{s-1} dl \qquad (13)$$

where F is a function depending on the atmospheric scale height at 95 Km and on the influx of meteors producing maximum line densities greater than $\alpha_{p_o}$. The rate factor $f_1(\chi_o, s)$ has been calculated by Kaiser (3) as a function of $\chi_o$ for various values of s (the meteor mass distribution exponent). Since $s = 1 + 2.5 \log_{10} a$, the chosen value of $a = 2.5$ gives $s = 2$ which considerably simplifies the numerical integration. The resulting equipment response function is shown in Fig. 4.

The valididty of this method and the result it gives has been independently checked by evaluating the integral in

equation (13) along the appropriate intercept of the echo line in order to obtain the echo rate as a function of elevation for radiants at various zenith angles. The resulting set of functions may be summed to give a theoretical curve for the echo elevation distribution $n_\theta(\theta)$ depending on the assumed radiant distribution. A variety of estimates for the latter distribution lead to theoretical curves for $n_\theta(\theta)$ which are very close to that of Fig. 2.

5. Sporadic Meteor Radiant Models - In order to use the foregoing result to compute the spatial variation in the density of meteoric matter around the earth's orbit from the observed annual variation in echo rate it is necessary to adopt a model for the average distribution of sporadic meteor radiants. It has generally been assumed that the distribution is symmetrical about the ecliptic and it is well recognised that the radiants are mainly concentrated in three fairly distinct groupings along the ecliptic: one at the apex of the earth's way and two at points about 60 degrees in ecliptic longitude on the helion and anti-helion sides of the apex (10,11,12). Davies and Gill, in their paper (12), present evidence of a further group of radiants in the direction of the apex, but inclined to the ecliptic plane at angles close to + 60 degrees. This group does not seem as large as the other three and the existence of a similar group at a high southerly inclination has yet to be demonstrated.

To assist calculations the sporadic meteor radiant distribution is usually approximated by a simplified model consisting of three point-radiants of equal strength superimposed on a uniform background. Meeks and James (13) have produced clear evidence that predictions obtained using such a model agree well with the observed diurnal variation of forward scatter meteor rates throughout the year. However the results obtained by Davies and Gill suggest that the apex grouping is weaker than the other two. Also, Weiss and Smith (14) find, from results obtained in Australia, that the apex grouping is the least concentrated. These results are supported by the results from an analysis of the average hourly meteor rate curves obtained during each month of the present survey. The contributions to the echo rate by the helion grouping averaged 2.1 times those from the apex grouping, the ratio varying from 0.8 to 3.7 during the twelve months of the survey. Likewise, the contributions by the anti-helion grouping averaged 2.1 times those from the apex grouping, the ratio varying from 1.1 to 4.0 during the survey. (A detailed discussion of these results is in preparation.)

The standard model adopted here, therefore, consists of a helion source of strength two units at $\lambda = \lambda_\odot - 30^\circ$, an apex source of strength one unit at $\lambda = \lambda_\odot - 90^\circ$ and an anti-helion source of strength two units at $\lambda = \lambda_\odot - 150^\circ$; the three being superimposed on a continuous background of

integrated strength one unit.

It should, perhaps, be remarked that the above source distribution applies only to meteors detected by radio methods, which greatly favour those meteors having geocentric velocities in excess of 15 to 20 Km/sec. When very slow meteors (with velocities near to the earth's escape velocity) enter the earth's atmosphere their angle of entry gives no direct information as to their previous path through space (15). The number of slow meteors detected during the survey is believed to be very small on account of their low ionizing efficiencies.

6. The distribution of meteoric material around the earth's orbit - By comparing the observed meteor rates with those calculated assuming a constant density of meteors along the earth's orbit it is possible to arrive at the true density distribution. The monthly values of the average hourly meteor echo rate between 0400 and 0800 hours L.T., taken from the survey (2) and shown in Fig. 5, were chosen for the comparison since almost all sources of sporadic meteors are then contributing to the observed echo rate. No allowance has been made for the presence of shower meteors because of the difficulties in identifying them. When wide aperture aerial systems are used, as in the present survey, the ratio of shower to sporadic rates is greatly decreased and the need to subtract the shower contribution from the total rate is therefore lessened.

Also, it has been found that faint shower meteors are in any case swamped by the sporadic background (9).

In deriving the theoretical echo rate the sporadic meteor radiant distribution model of the previous section was employed, with the helion, apex and anti-helion sources kept constant in intensity throughout the year. The annual variation in rate thus depends solely on the elevations of the three contributing sources in the manner given by the equipment response function derived in section 4. The resulting theoretical echo rate is shown in Fig. 5. by the dashed curve, which has been scaled to match the mean value of the observed echo rate.

The ratio of the observed/theoretical values, indicating the relative density of meteoric matter around the earth's orbit, is shown in Fig. 6, together with the results obtained in Australia by Weiss (16) and the Northern Hemisphere telescopic meteor observations reported by Kresáková and Kresák (17). The close agreement between these results, derived from observations made at difference periods, confirms that a real assymmetry exists in the spatial distribution of meteoric material. The increased meteor influx from the month of August until the end of the year agrees with similar tendencies noticed by some of the early visual and radar workers. The New Zealand radar results in Figure 6 show that the influx during the second half of the year is some 42 percent

greater than during the first half.

However there is an apparent disagreement between the above results and those obtained at Jodrell Bank by Hawkins (18), who obtains a maximum space density of meteors along the earth's orbit between April and August. Hawkins' result correlates fairly well with the cometary index, which is proportional to the number of comets approaching close to the earth throughout the year. The disagreement may be resolved if it is assumed that cometary material and the larger meteors (which predominated at the low rates recorded in the Jodrell Bank survey discussed by Hawkins) are distributed around the earth's orbit in a different manner from the smaller particles detected by the three surveys represented in Fig. 6*.

7. The seasonal variation in meteor echo rate - The seasonal variation in the daily influx of meteors has been extensively

---

Referee's comment: An alternative explanation for Hawkins' results may be that his data were contaminated by meteors from the summer daytime streams, especially as his meteors were rather brighter than those of the present survey, and were observed with an equipment designed to favour shower as against sporadic meteors. Even after subtracting obvious shower meteors, those observed in side-lobes may have made a significant contribution in Hawkins' observations.

investigated in the Northern Hemisphere by a variety of methods. Results obtained from radar back scatter, (18,19,20), forward scatter (21) telescopic (17) and visual (22) observations are shown in Fig. 7, which emphasizes the close agreement between the various methods of observation. When the average of these results is taken (as scaled in Fig. 7.) and compared with the Southern Hemisphere seasonal variation as revealed by the present survey it is at once apparent that the form of the curves is almost identical and that they are completely out of phase (Fig. 8), thus proving that the tilt of the earth's axis is one major factor controlling the seasonal variation in meteor rate.

The latitudes at which the Northern Hemisphere observations were made range from about 35°N to 52°N, which compares with the latitude of 43½°S at Christchurch, New Zealand, where the present survey was conducted. The two curves in Fig. 8. should therefore be equal in the extent of their amplitude variation if the seasonal variation due to the tilt of the earth's axis is the sole controlling factor. This is not so; and the difference may be attributed to the increased meteor density encountered by the earth during the latter half of the year. As a result the amplitude of the seasonal variation in the Northern Hemisphere is enhanced and in the Southern it is diminished. This also accounts for the time displacement of

five months, rather than six months, between the two curves.

The combined effect of the earth's axial tilt and the asymmetrical meteor distribution along the earth's orbit also influences the form of the diurnal meteor rate curves throughout the year. The extreme values of the daily minimum rate in the Southern Hemisphere (Fig. 9) are found to occur about one month earlier than they would if the tilt of the earth's axis was the only controlling factor.

8. Conclusions - The value of meteor rate data obtained at constant sensitivity over a period of one year has been demonstrated. It has, as a result, proved possible to isolate the major factors responsible for the temporal variations in observed echo rate. Using the above results as a datum and employing the same radiant model it will now be possible to investigate the year-by-year variations, if any, in the distribution of meteoric material along the earth's orbit.

## References


(1) Ellyett, C. and Keay, C.S.L., J. Geophys. Res., 66, 2590, 1961.

(2) Ellyett, C. and Keay, C.S.L., Mon. Not. R. Astr. Soc. (In press)

(3) Kaiser, T.R., Mon. Not. R. Astr. Soc., 121, 284, 1960.

(4) Kaiser, T.R., Mon. Not. R. Astr. Soc., 123, 265, 1961.

(5) Kaiser, T.R. and Closs, R.L., Phil. Mag., 43, 1, 1952.

(6) Ellyett, C. and Fraser, G.J., Aust. J. Phys., 8, 273, 1955.

(7) Greenhow, J.S. and Hall, J.E., Mon. Not. R. Astr. Soc., 121, 174, 1960.

(8) Hawkins, G.S., Astrophys. J., 124, 311, 1956.

(9) Kaiser, T.R., Annales de Geophysique, 17, 50, 1961.

(10) Hawkins, G.S., Astron. J., 61, 386, 1956.

(11) Davies, J.G., "Radio Observation of Meteors" in Adv. in Electronics and Electron Physics (Academic Press, New York), 9, 95, 1957.

(12) Davies, J.G. and Gill, J.C., Mon. Not. R. Astr. Soc., 121, 437, 1960.

(13) Meeks, M.L. and James, J.C., J. Atmos. Terr. Phys., 16, 228, 1959.

(14) Weiss, A.A. and Smith, J.W., Mon. Not. R. Astr. Soc., 121, 5, 1960.

(15) Dole, S.H., J. Planet. Space Sci., 9, 541, 1962.

(16) Weiss, A.A., Aust. J. Phys., 10, 77, 1957.

(17) Kresáková, M. and Kresák, L., Contrib. Astron. Obs. Skalnaté Pleso, 1, 40, 1955.

(18) Hawkins, G.S., Mon. Not. R. Astr. Soc., 116, 92, 1956.

(19) Lovell, A.C.B., "Geophysical Aspects of Meteors" in Handbuch der Physik (Springer-Verlag. Berlin), 48, 427, 1957.

(20) Evans, G.C., Jodrell Bank Ann., 1, 280, 1960.

(21) Vogan, E.L. and Campbell, L.L., Can. J. Phys., 35, 1176, 1957.

(22) Murakami, T., Publ. Astro. Soc. Japan 7, 49, 1955.

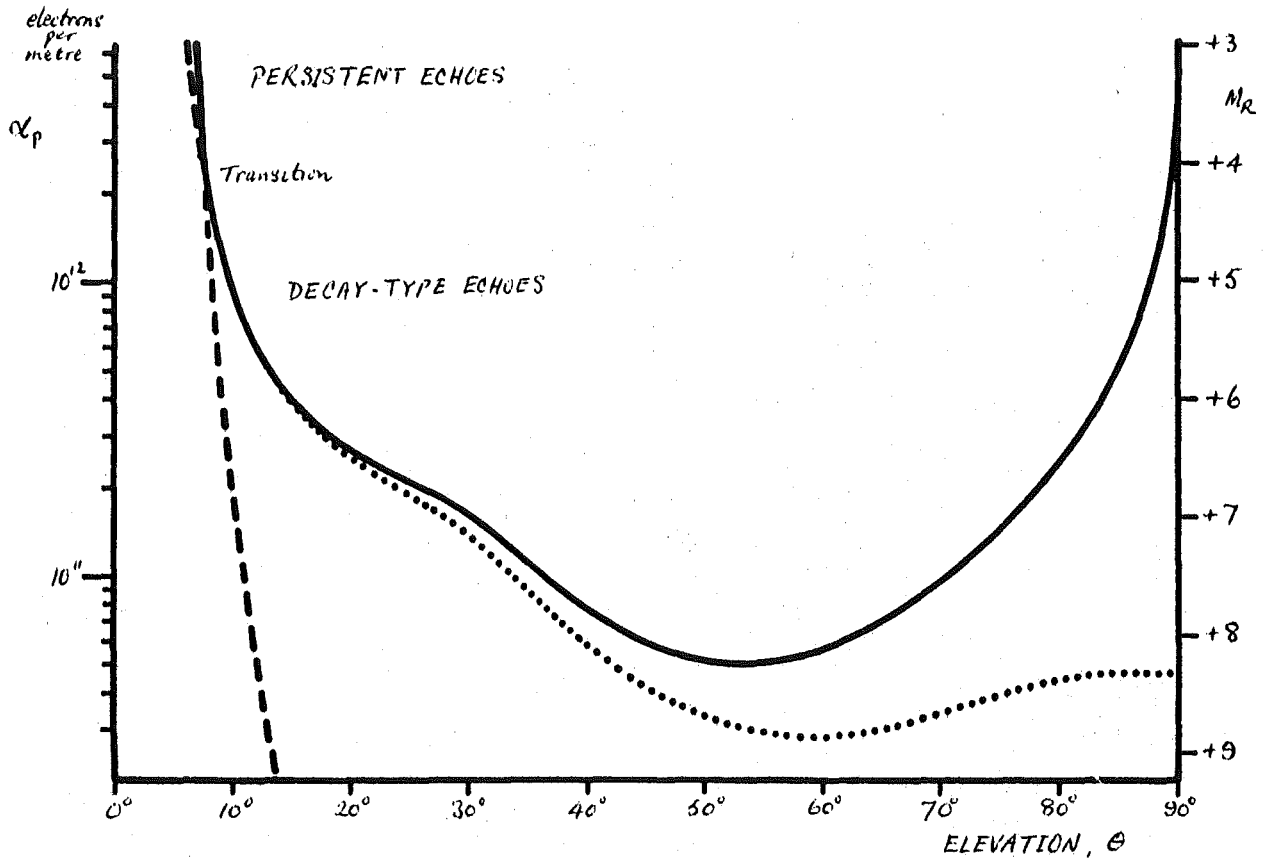


Fig. 1: The limiting sensitivity of the meteor detection equipment.

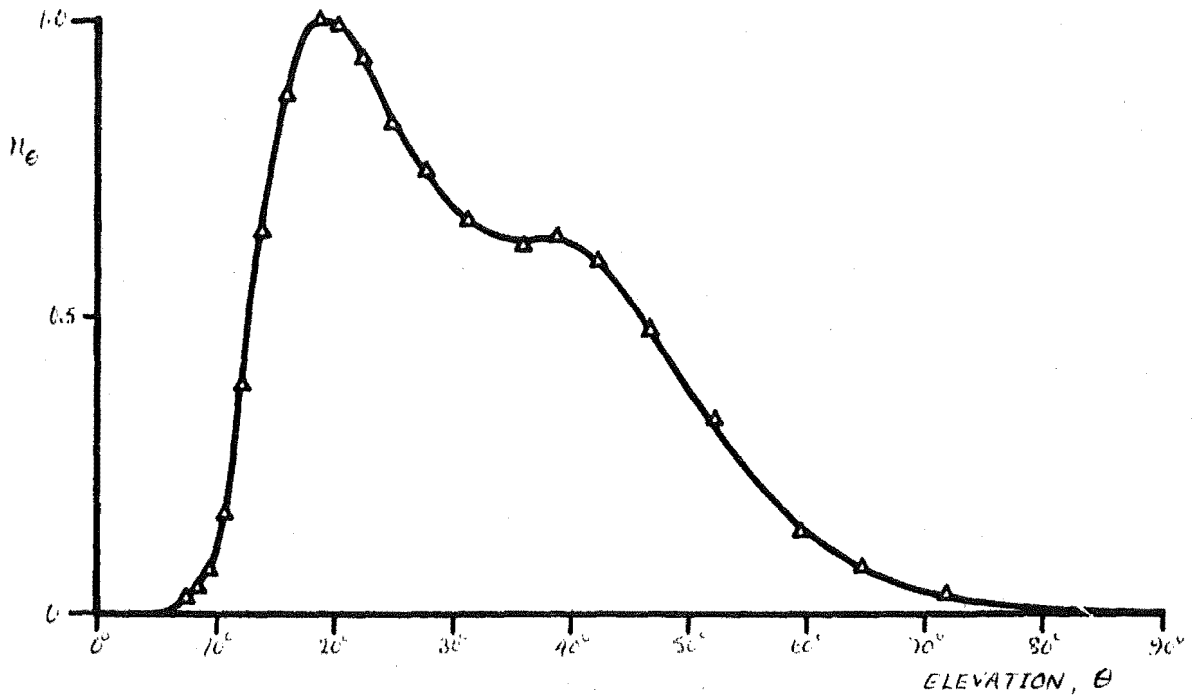


Fig. 2: The elevation distribution of detected meteors

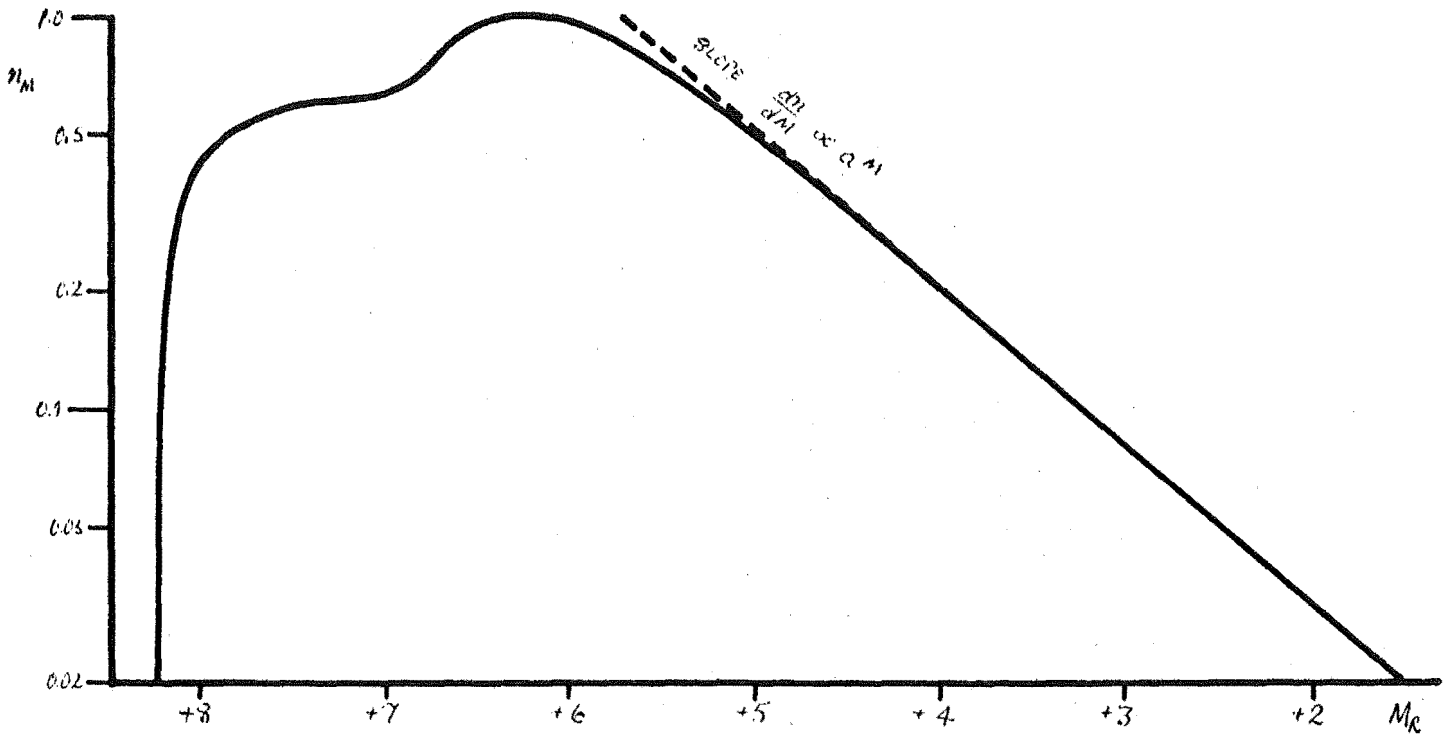


Fig. 3: The magnitude distribution of detected meteors

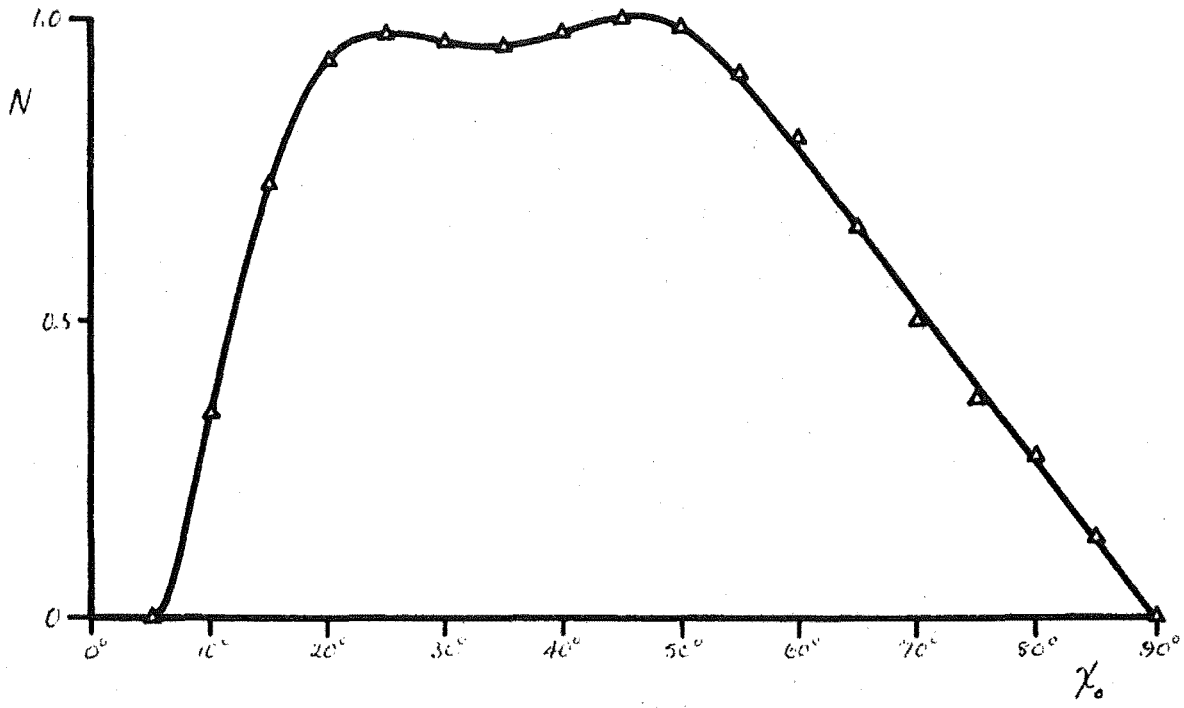


Fig. 4: The calculated response function of the equipment as a function of radiant elevation.

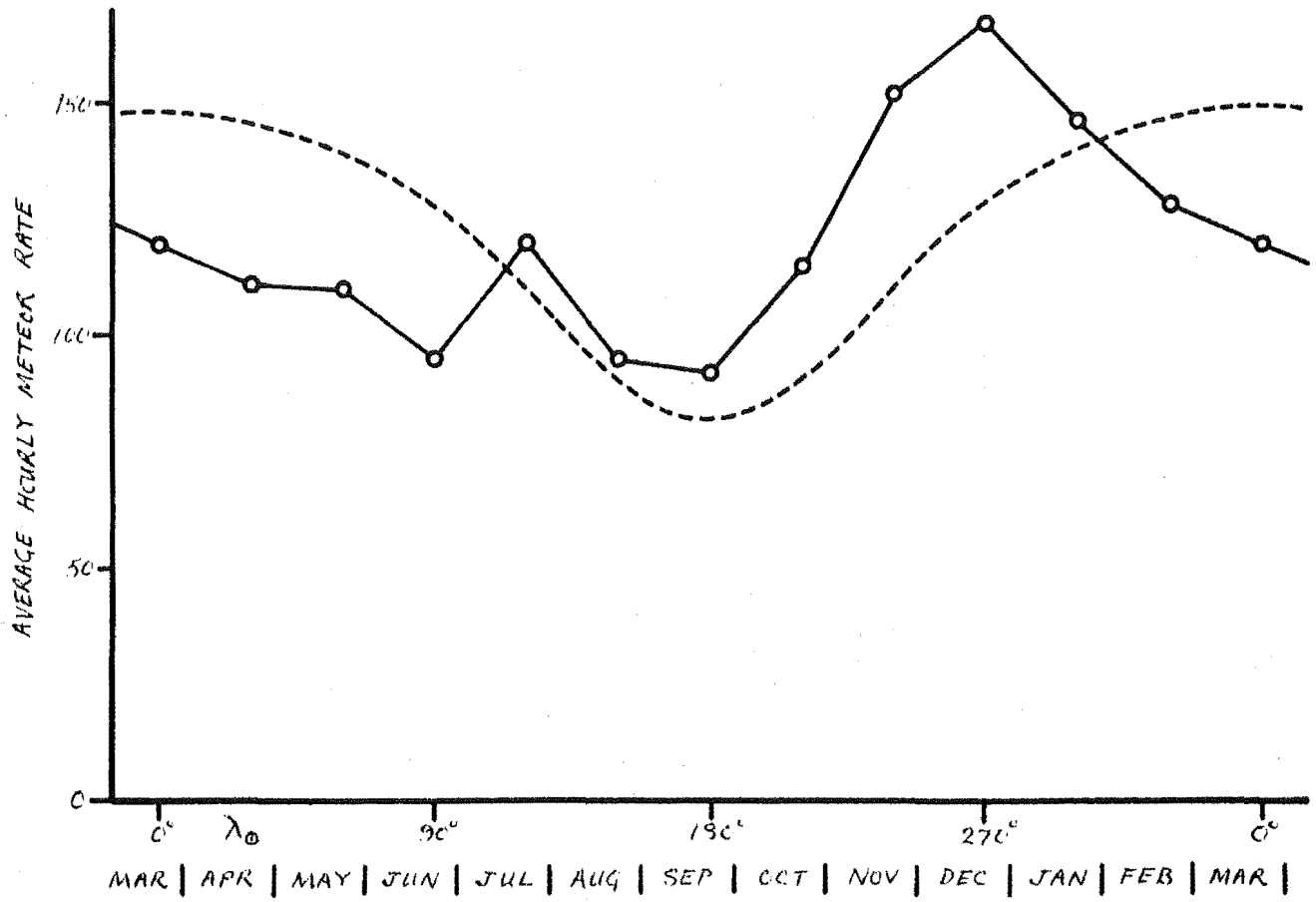


Fig. 5: Average hourly meteor rates at the time of culmination of the apex compared with the theoretical variation computed using the radiant source model adopted (section 5).

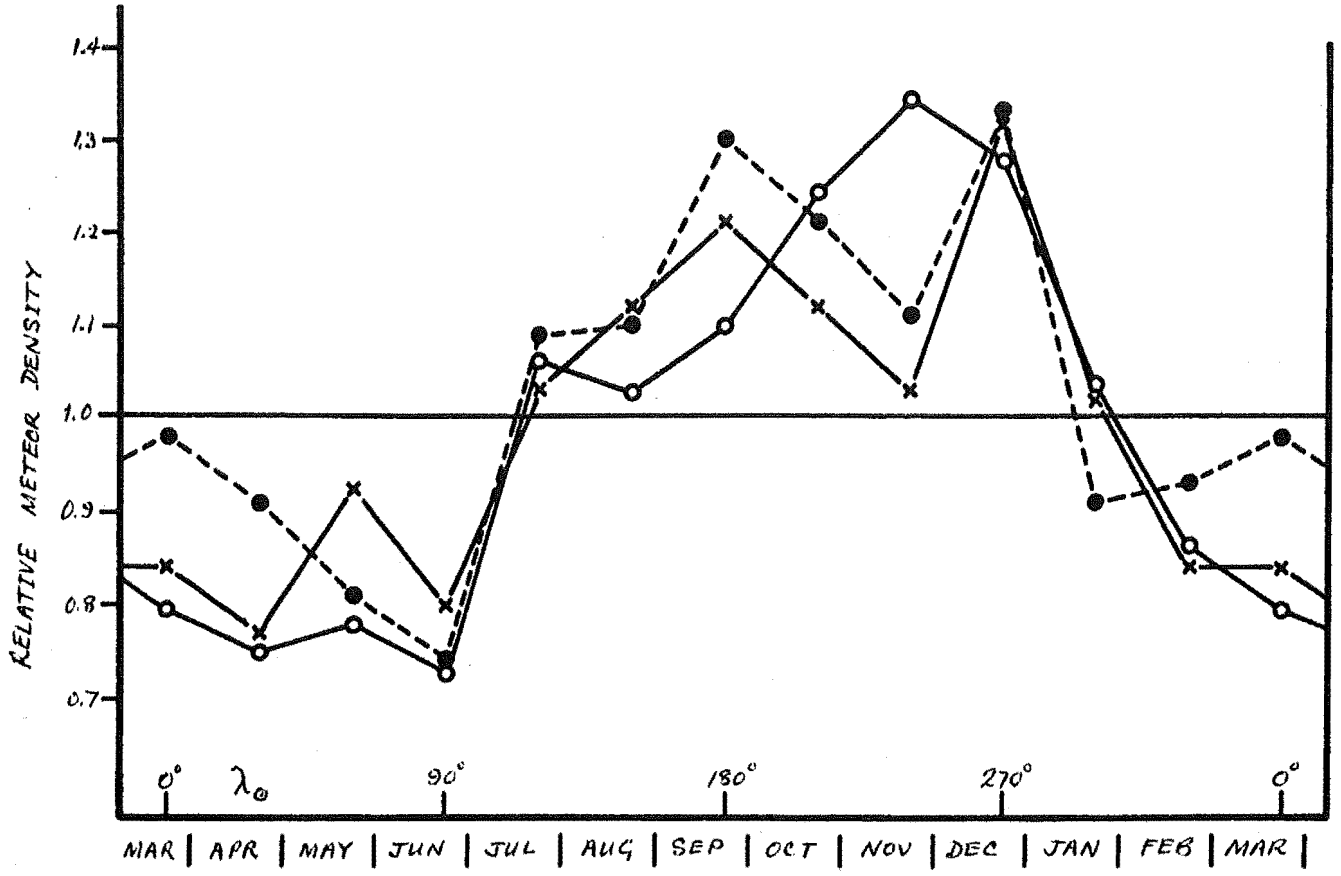


●--●--● Northern Hemisphere telescopic, Skalnaté Pleso, 49°N (Kresáková and Kresák, 1955)

○—○—○ Southern Hemisphere radar, Christchurch, 43½°S

×—×—× Southern Hemisphere radar, Adelaide, 35°S (Weiss, 1957)

Fig. 6: The variation of the space density of meteors with solar longitude.

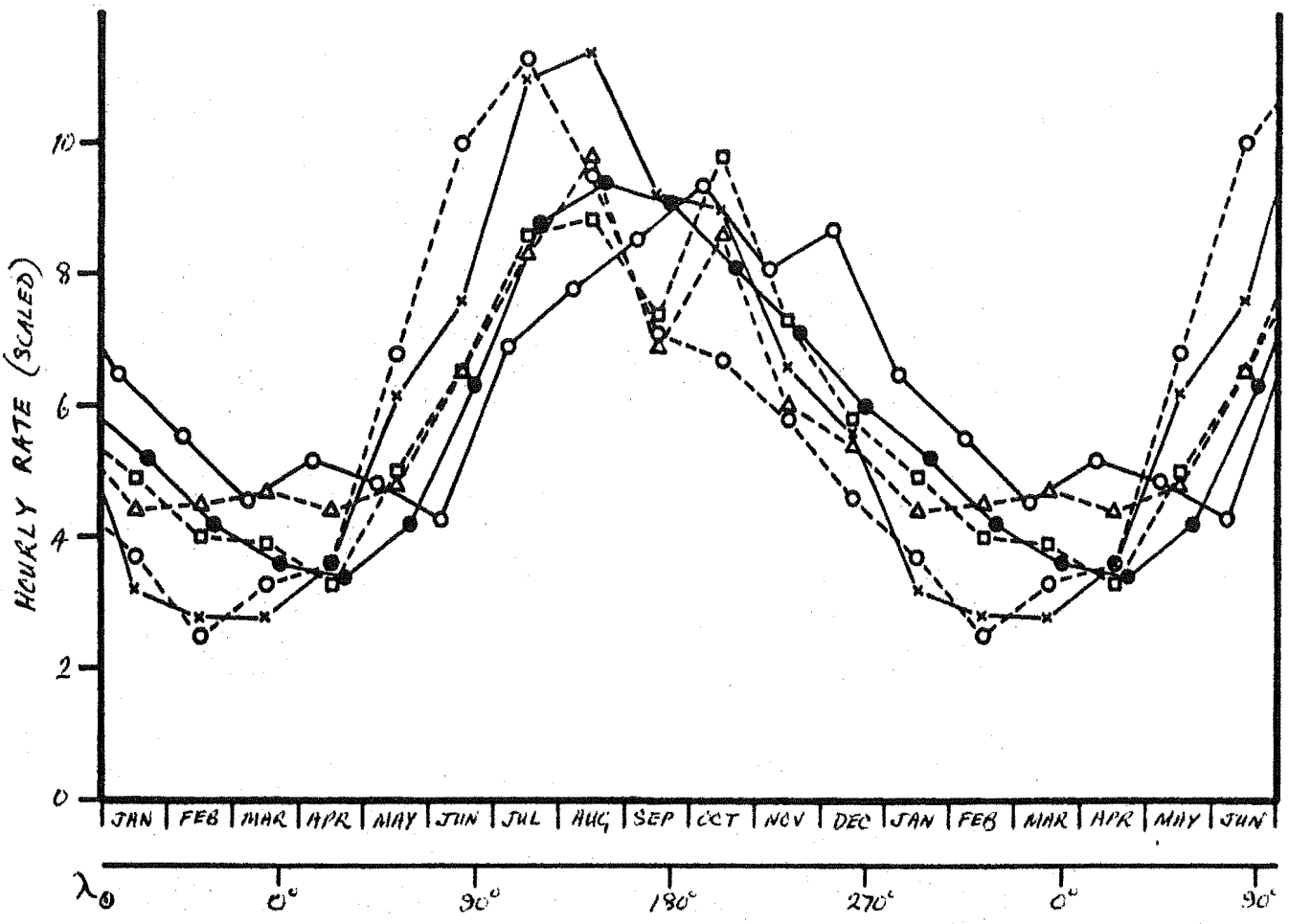


△---△---△ Radar (Evans) Divide ordinate by 1.5

○---○---○ Radar (Hawkins)

□---□---□ Radar (Lovell) Divide ordinate by 1.5

×——×——× Forward scatter (Vogan and Campbell) Multiply ordinate by 5

○——○——○ Telescopic (Kresáková and Kresák) Divide ordinate by 2

●——●——● Visual (Murakami)

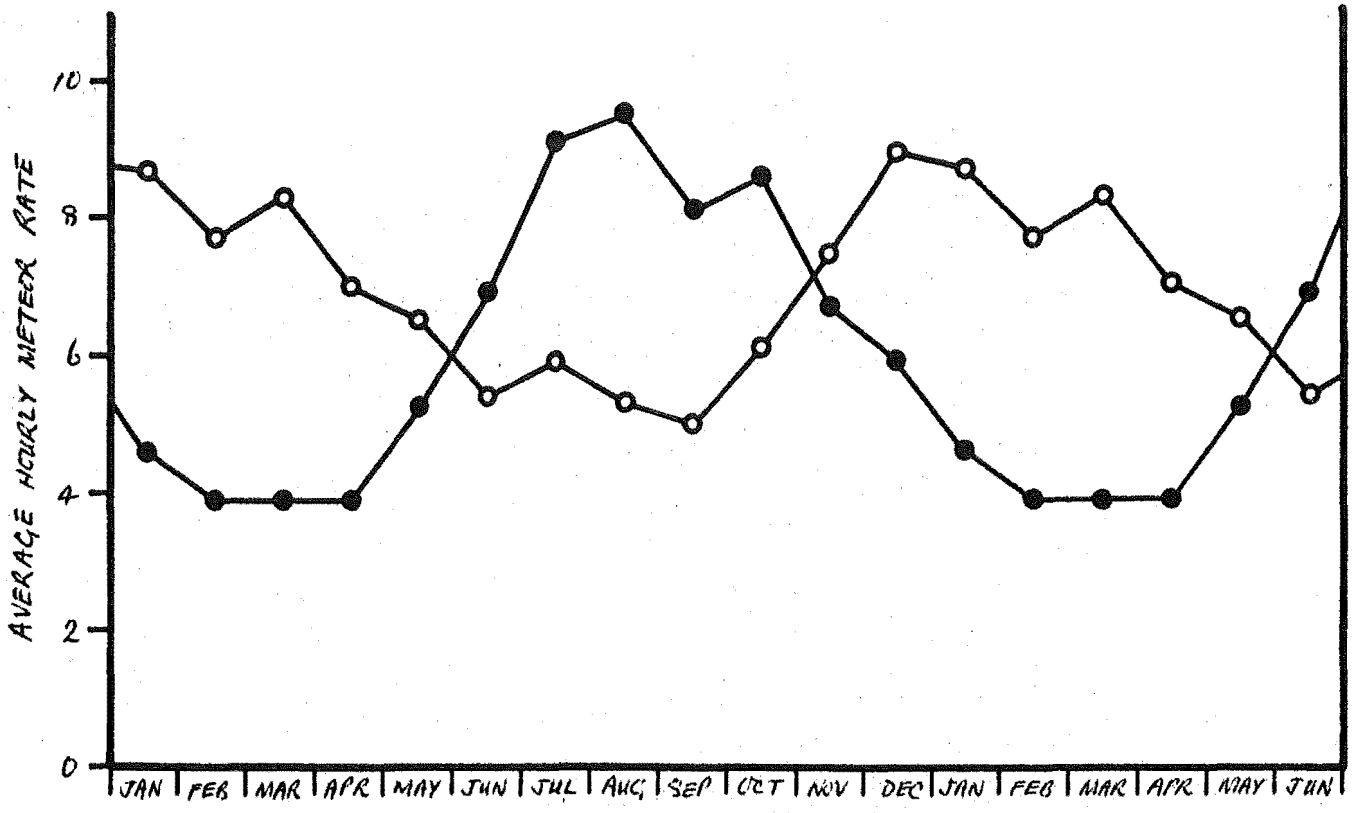


Northern Hemisphere (Average from Fig. 7)

Southern Hemisphere (Radar, multiply ordinate by 12)

Fig. 8: The seasonal variation of meteor rates in both hemispheres compared.

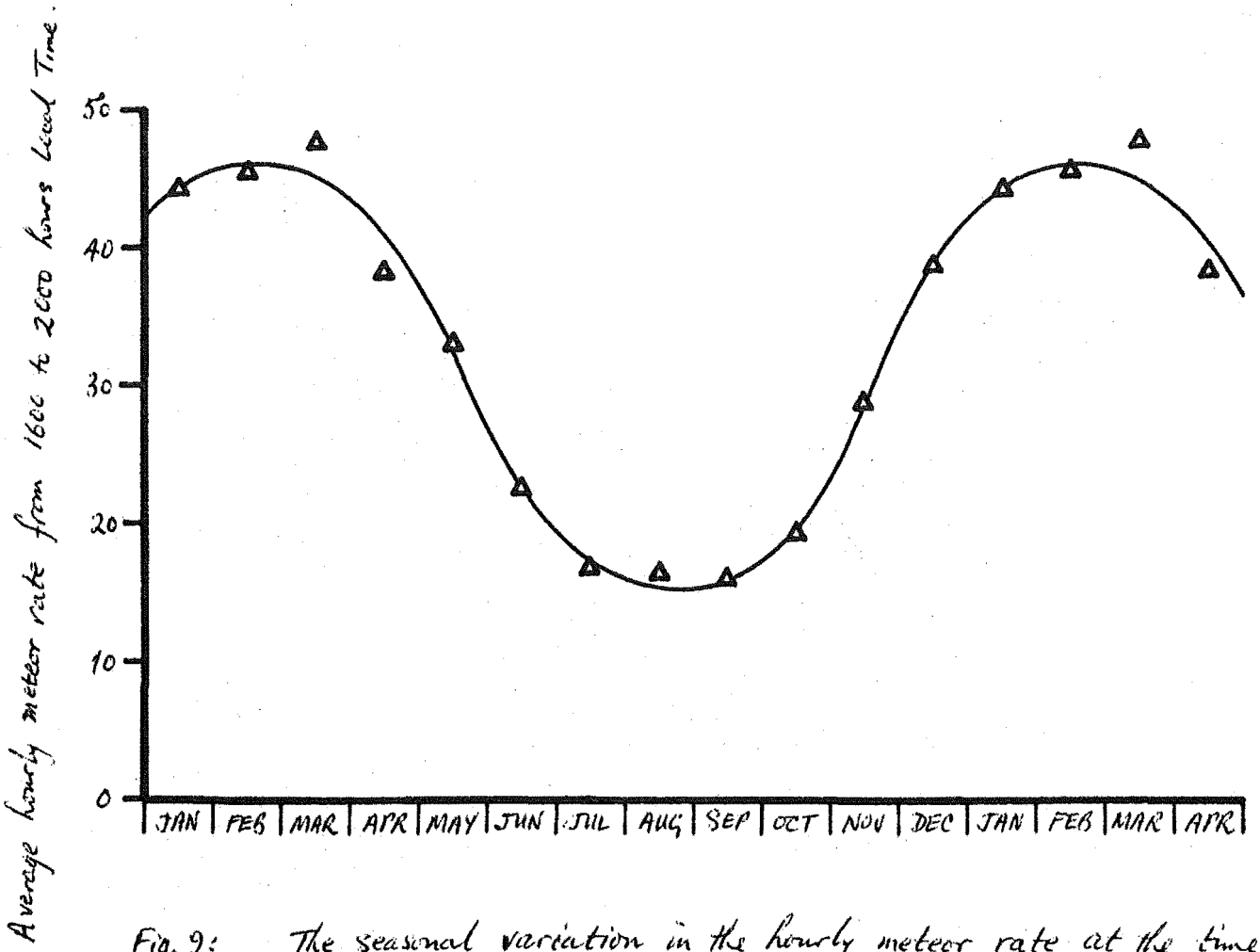


Fig. 9: The seasonal variation in the hourly meteor rate at the time of culmination of the antapex, 6 PM Local Time, when the diurnal rate is at its minimum.

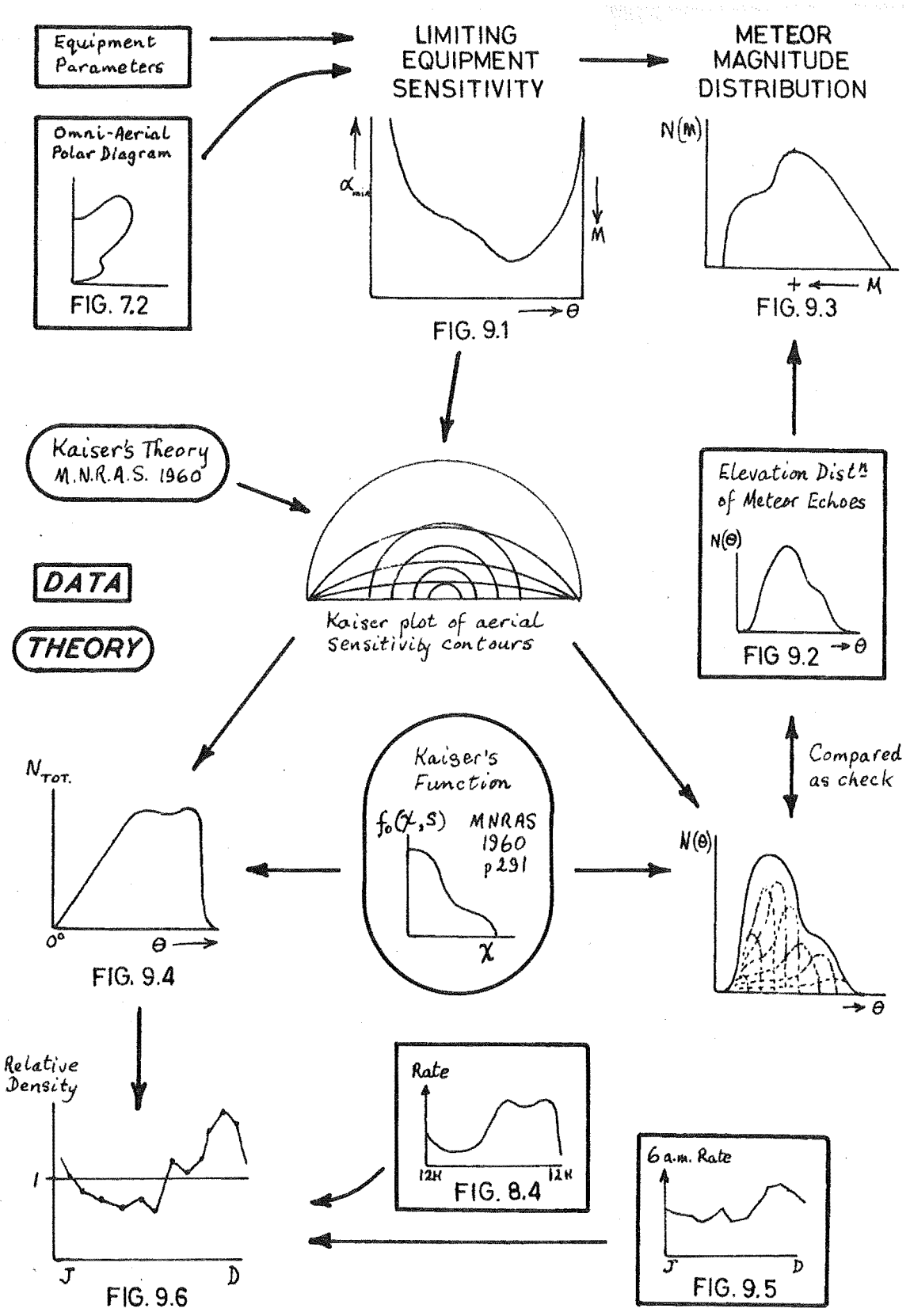


FIG. 10 Flow diagram showing the derivation of the Relative Density of Meteors.

## 10. THE ANNUAL VARIATION IN THE RADIANT DISTRIBUTION OF SPORADIC METEORS

(This chapter has already been published with the above title as a paper under my name. It appeared in the Journal of Atmospheric and Terrestrial Physics, Volume 25, page 507, 1963.)

In this chapter the monthly curves of the diurnal variation in meteor rate obtained during the rate survey are analysed to confirm the northern hemisphere result that the strengths of the helion, apex and antihelion sources of sporadic meteor activity are in the ratio 2:1:2 when averaged over a whole year. During the year the helion and antihelion source strengths vary from 0.8 to 4.0 times that of the apex.

## INTRODUCTION

In the course of a year-long survey of meteoric activity during 1960-61 data of high quality was obtained with much intrinsic information concerning the distribution of meteors in the region of space traced out by the earth's orbit. The results of the survey have been fully reported by ELLYETT and KEAY (1961, 1963). Using these results KEAY (1963) has confirmed that the density of meteors around the earth's orbit is greater in the second half of the year. This fact, combined with the seasonal effects of the axial tilt of the earth, satisfactorily explains the main features of the observed annual and diurnal variations in meteoric activity.

In this paper the survey results mentioned above have been further analysed to show that although the three recognised ecliptic concentrations of sporadic meteor radiants are always present their relative strengths vary considerably throughout the year.

## SPORADIC METEOR RADIANT DISTRIBUTION MODEL

In recent years it has been definitely established that the radiants of sporadic meteors tend to be clustered into three major groupings along the ecliptic. On the basis of observations made between 1930 and 1949 by visual observers organised by the British Astronomical Association, PRENTICE

and HAWKINS (1953 and 1957) have shown how the distribution of sporadic meteor radiants in ecliptic latitude is sharply concentrated on the ecliptic itself, while the distribution in ecliptic longitude shows two prominent peaks, one at the apex of the earth's way and one near the anti-helion point. Daylight naturally prevented the visual observation of any peak within about 60 degrees of the sun's position.

A detailed analysis by HAWKINS (1956 a,b) of radar observations of sporadic meteors obtained between 1949 and 1951 confirmed the visual result and disclosed a third radiant grouping located near the helion point. Subsequent triple-station radar measurements by DAVIES and GILL (1960) of the orbits of sporadic meteors, and radar observations by WEISS and SMITH (1960) using equipment similar to that used by HAWKINS, have substantiated the previous findings. All of these workers are in agreement that three major groupings of radiants exist but there is some disagreement as to the relative strengths of the groupings. It is generally agreed that the apex grouping is much less compact than the other two, a result to be expected since the apparent concentration of radiants near the apex is a consequence of the streaming effect brought about by the earth's orbital motion.

In the light of these results it is clear that a radiant distribution model consisting of three discrete independent sources superimposed on a uniform background

would represent a simple approximation to the observed meteor radiant distribution. Such an approximation has been used quite effectively by MEEKS and JAMES (1959) in their predictions of the monthly variations in mean echo rate observed in forward scatter communication links. When used with the results of the Christchurch survey, in which very low resolution aerial systems were employed, a discrete-source approximation yields even better concord between the computed and observed echo rates.

In the published results there is agreement that the helion and anti-helion sources are located between 60 and 70 degrees in ecliptic longitude on their respective sides of the apex of the earth's way. The obliquity of the ecliptic ($23.45^{\circ}$) is such that 65 degrees in ecliptic longitude is equivalent to 65 degrees in right ascension to within $\pm$ 3 percent, depending on season. It would therefore be legitimate for the purpose of this paper to treat these coordinates as equivalent and assume the helion and anti-helion sources to be located at a fixed hour-angle on either side of the apex position. In order to simplify calculations this difference in hour angle was taken to be exactly four hours in each case; or, in other words, the local mean time of meridian transit of the anti-helion source was taken to be 0200 hours, the apex source 0600 hours and the helion source 1000 hours.

## SYNTHESIZED DIURNAL RATE CURVES

The aerial system employed during the survey was omni-directional in azimuth and its vertical radiation pattern was known. This enabled the equipment response to be determined as a simple function of the elevation of a radiant (KEAY, 1963). The diurnal variation in meteor rate can therefore be calculated for any given radiant distribution.

The triple-source radiant distribution model defined in the previous section leads to diurnal rate curves (averaged on a monthly basis) which are very close to those actually observed, provided the relative strengths of the three sources are adjusted for best fit. The contributions from the sources are added to the background level defined by the minimum value of the observed diurnal rate curve. The minimum always occurs close to 1800 hours L.T. at the time of transit of the antapex when all three model sources are below the horizon and therefore not contributing to the echo rate. Typical results are shown in Fig. 1., in which the rates calculated from the model distribution are drawn as histograms and the measured hourly rates (centred on the half-hour) are shown as connected dots. The calculated rates for May and September show close agreement with the measured rates. This was also the case for the months of February, April, June and October.

The histogram for July is the extreme example of the inadequacy of the simple triple-source radiant model to cope with a situation where meteors are incident from a complex of radiants not coincident with any of the three source positions defined for the model. Smaller discrepancies of a similar nature were obtained with the diurnal rates calculated for the months of March and August.

A different situation is exemplified by the histogram for December. Here it is the positions as well as the strengths of the model sources which need adjustment in order to obtain best fit to the measured rate values. The anti-helion source evidently culminates somewhat earlier during December while the apex maximum appears to be delayed by the presence of meteoric activity which the simple model cannot encompass. The curves for November and January show a similar, but smaller degree of source misalignment.

During the year two very pronounced peaks of meteoric activity occur, one at the end of July and the other in December (ELLYETT and KEAY, 1963), and it was for these two months that the synthesized rate curves (histograms) were the worst approximations to the observed diurnal curves. Even so the values obtained for the source strengths at these times would never be more than 30 percent in error except for a possible underestimate of 40 percent for the

anti-helion source in July and August (see Fig. 2) if the intense meteor showers then present are included in the anti-helion source contribution.

## ANNUAL VARIATION OF SOURCE STRENGTHS

The source strengths which yield best fit between the synthesized rates and those actually observed vary greatly during the year. The mean source strengths for each calendar month are plotted in arbitrary units in Fig. 2 and the amounts by which the source strengths can be varied while still maintaining a reasonably good fit are indicated by the upper and lower limits.

The variation in strength of the apex source follows the same pattern as the already established annual variation in the number of sporadic meteors encountered by the earth (KEAY, 1963), but, having a maximum to minimum strength ratio of four to one, it is twice as accentuated. This is readily explained when it is remembered that measurements of the annual variation of sporadic meteor influx includes the helion and anti-helion contributions as well as those associated with the apex.

The variation in strength of the anti-helion source follows a fairly similar pattern, in marked contrast to that of the helion source which stays remarkably constant in strength throughout the year. As a result the anti-helion

source is predominant during the latter months of the year while the helion source predominates from March until June.

This helps to explain the observed variations in the time of the daily maximum in the sporadic meteor rate throughout the year. The Jodrell Bank radar results quoted by LOVELL (1957) exhibited a daily maximum which occurred between 0330 and 0800 hours L.T., as shown by the middle plot in Fig. 3. The Christchurch results, on the other hand, usually exhibited two distinct peaks; one before, and the other after, 0600 hours L.T. Fig. 3 reveals that each set of results follows the same trend. From March to June when the helion source predominates and the anti-helion source is at its weakest the peaks occur later in the morning, and towards the end of the year when the anti-helion source is very strong the peaks are displaced earlier.

## RATIOS OF SOURCE STRENGTHS

From Fig. 2 it is clear that the relative contributions from each of the three sources varies considerably throughout the year. The ratios of the source strengths referred to the strength of the apex source are shown on a logarithmic scale in Fig. 4 from which it may be seen that both the helion/apex and anti-helion/apex ratios average close to 2 over a full year. This is in excellent agreement with the northern hemisphere results obtained by DAVIES and

GILL (1960). However the month-by-month agreement with the results of DAVIES and GILL is not at all good, possibly because of the fact that their equipment was operated for only 24 hours in each month.

In both northern and southern hemisphere results the anti-helion source varies more than the other two throughout the year although the maximum values occur six months apart in the two sets of results. This disagreement must be due to an observational effect not being properly allowed for in one or possibly both sets of results. Since a fairly low proportion of the meteors observed by DAVIES and GILL were identified as shower meteors it seems surprising that they recorded their highest rates during May, June and July when, according to data from both hemispheres (KEAY, 1963), the relative number of meteors encountered by the earth is low. Nor may their result be explained as an effect due to the axial tilt of the earth which leads to maximum rates during September in the northern hemisphere.

## FURTHER WORK

The foregoing remarks show that while the main features of the radiant distribution of sporadic meteors are clear there remains some disagreement concerning the annual variation in the distribution. Since this is of considerable astronomical interest it would be worthwhile to clarify the

situation by examining other suitable meteor data such as that accumulated during the operation of communication links utilising meteor forward scatter propagation. Had MEEKS and JAMES attempted to obtain best fit between their calculated rates and those measured over the various communication paths considered, they would have obtained the annual variation in each of the three model sources. Alternatively it is possible that other sufficiently consistent meteor data exists which could be analysed to yield the annual source variations.

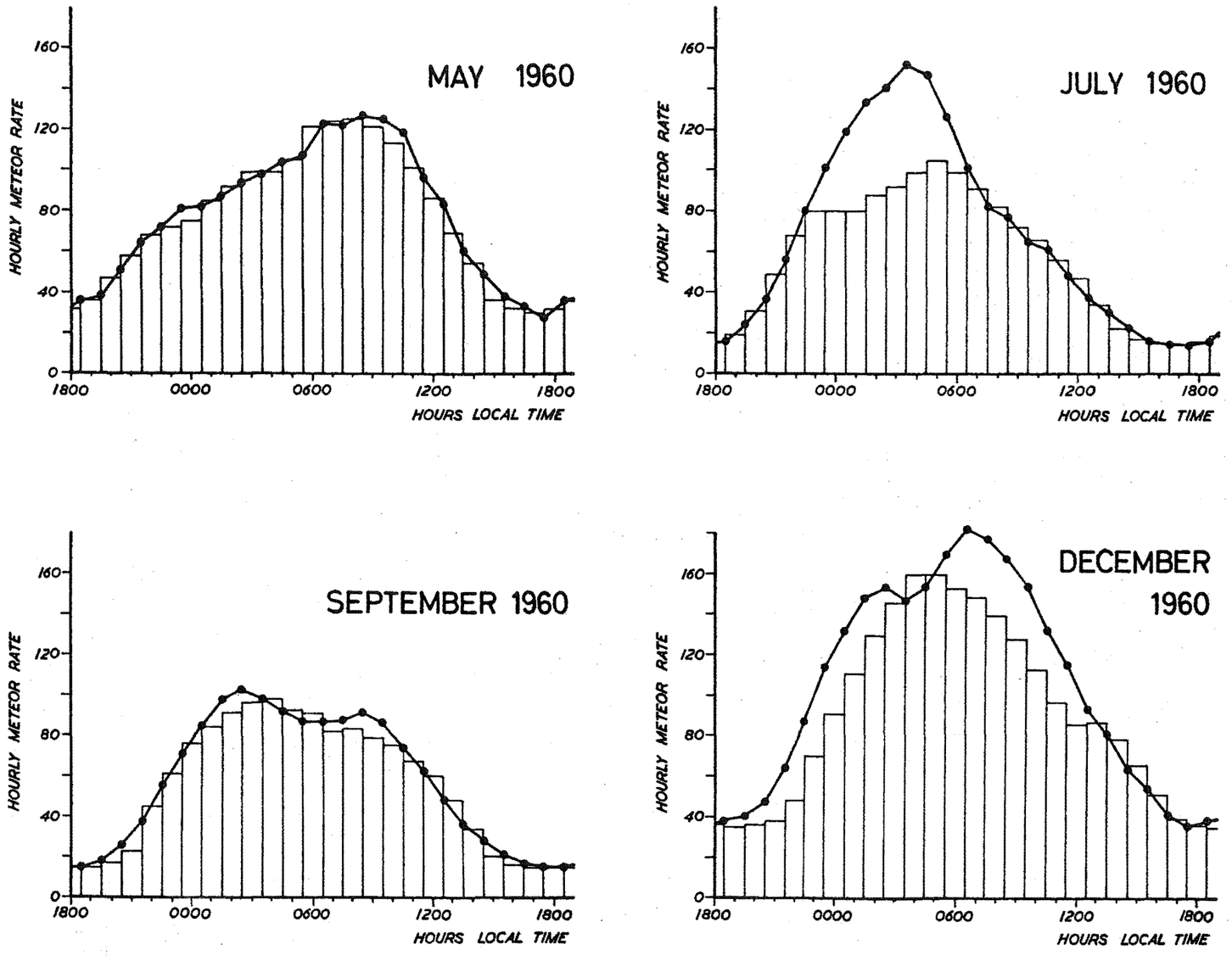


Fig. 1 For each of four selected months the observed diurnal variation in meteor rate is shown by a series of connected dots. The accompanying histograms represent synthesized rates obtained by adjusting for best fit the strengths of each of the three sources in a simple model representing the actual distribution of sporadic meteor radiants.

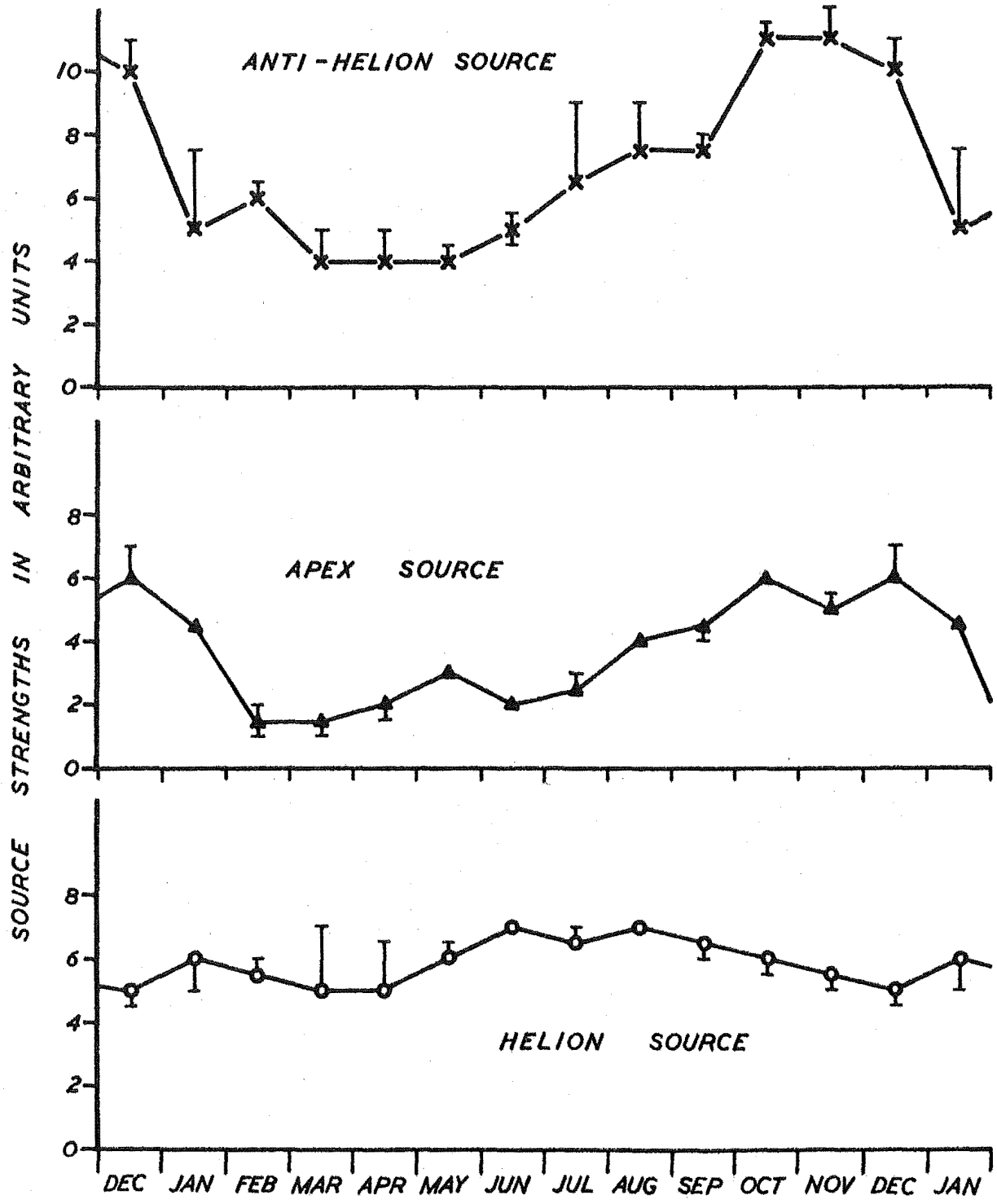


Fig. 2 The calculated annual variation in strength of each of the three major groupings of sporadic meteor radiants along the ecliptic.

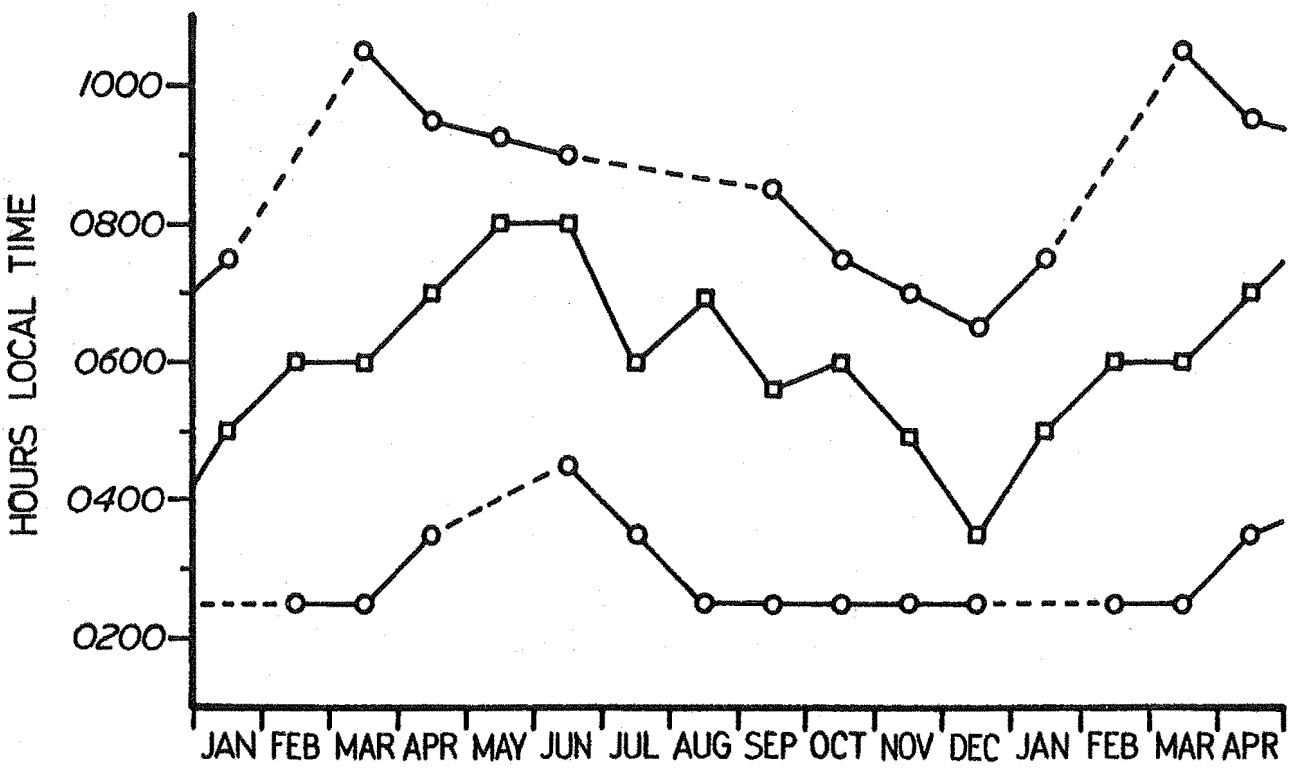


Fig. 3 The observed variations in the time of the daily maximum in the sporadic meteor rate throughout the year. The single maximum observed with the Jodrell Bank equipment is shown by the squares, while the circles show the two maxima usually observed with the Christchurch equipment.

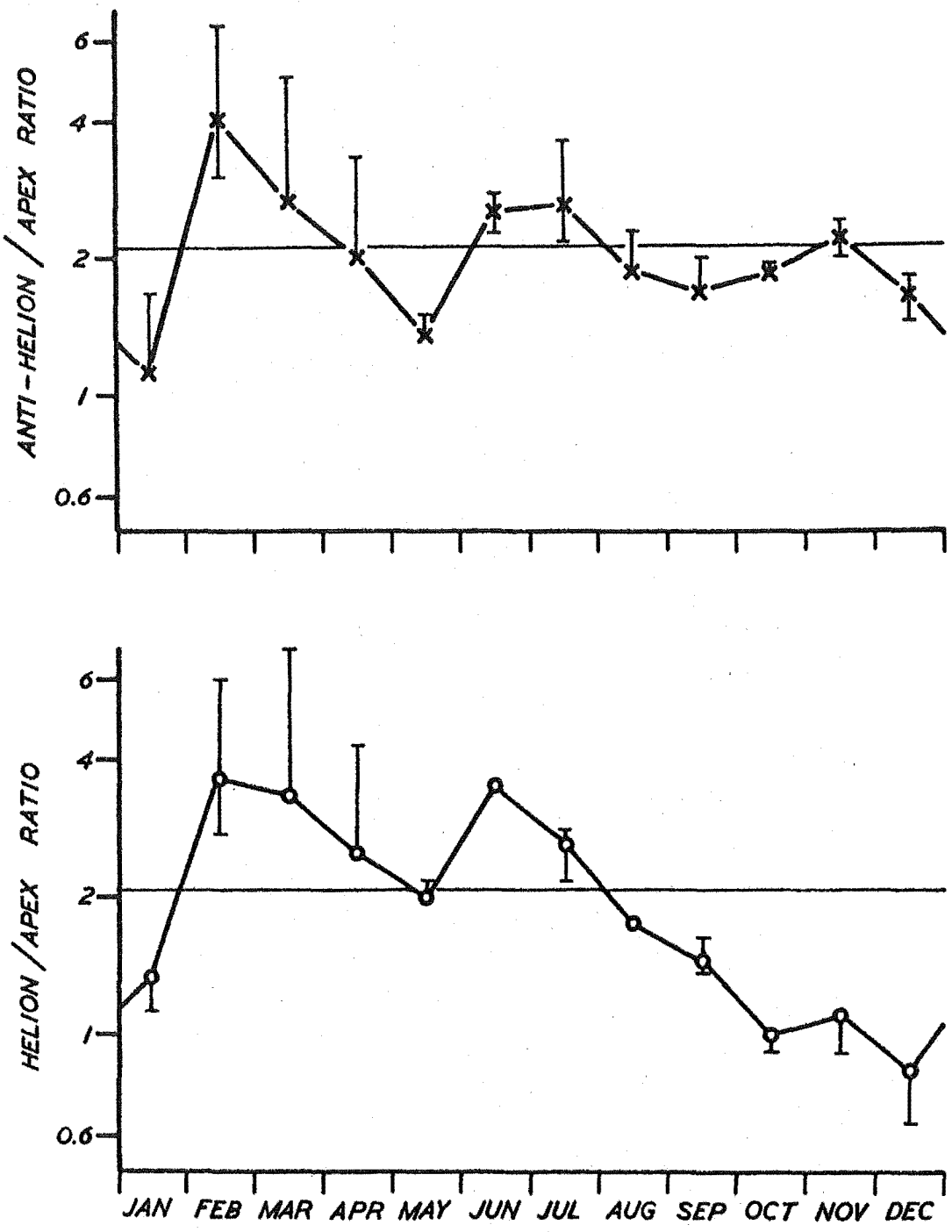


Fig. 4 The annual variation in the ratios of the source strengths.

## 11. SIGNIFICANCE OF THE PEAK METEOR RATES

(This chapter has been published with the title "Some Salient Features of the Occurrence of Meteors". It appeared under my name in the Astronomical Journal, Volume 69, page 98, February 1964.)

In this chapter the results of the meteor rate survey are compared with meteor data obtained by visual and photographic methods in other countries. A considerable measure of detailed agreement is revealed. It is quite apparent that there exist two or more distinct, large-scale associations of meteoroids encountered by the earth during the year. The implications of the existence of these associations are discussed, including estimates of their ages.

1. INTRODUCTION:

From a station near Christchurch, New Zealand, (lat. $43\frac{1}{2}^{o}$S) a year-long survey of meteor activity has been undertaken using monopulse radar techniques at a frequency of 69.5 Mc (Ellyett and Keay, 1963). Low gain aerials, omni-directional in azimuth, were employed with the intention of detecting meteors from all radiants above the horizon and not favouring only those culminating near the zenith, which is a danger when narrow beam aerials are employed (Keay and Ellyett, 1961). The survey data embraces over 700,000 meteors, their rate of detection being measured by taking counts over three-minute intervals.

During the period covered by the survey, from February 1960 to January 1961 inclusive, the equipment sensitivity and other parameters were held as constant as possible in order that meaningful information would be obtained on the diurnal and seasonal variations in meteor activity. As a result it has been confirmed that the earth's axial tilt exerts a dominant influence on the seasonal variation in meteor rate, but that there is definitely a greater influx of small-size (sixth magnitude) meteoric matter during the latter half of the year (Keay, 1963a). Also, the annual variation in the

diurnal rate curve has yielded some information on the distribution of radiants, and hence orbits, of the bulk of these small meteoric particles (Keay, 1963b).

It is the purpose of this paper to compare these and further results of the Christchurch survey with other available meteor data.

## 2. COMPARISON OF RADAR AND VISUAL OBSERVATIONS:

Observations made by hundreds of visual observers during the years from 1901 to 1958 inclusive have been used by Olivier (1960) to compile tables of the average hourly rates of visual meteors for each night of the year. These observations were not confined to the northern hemisphere (an appreciable fraction originating from southern hemisphere observers) which suggests that the rates should give a good indication of the true variation in visual meteor activity throughout the year.

From Olivier's tables a contour map has been drawn (Fig. 1 a) showing the average hourly meteor rate as a function of hour of day and time of year. When constructing the map, point values were found by taking, for each hour of the day, mean values of the average rate at intervals of a third of a month. Contours were

then drawn at intervals representing rate increments of 5 meteors per hour. Because of daylight conditions, no rates could be obtained for the region outside the dotted boundaries.

Radar hourly meteor rates obtained by Ellyett and Keay are shown in Figure 1 b, which covers the same diurnal period as Figure 1 a except that two hours have been added in order to include the December peak of morning activity.

The similarity between the two maps is indeed striking, to say the least. Not only are the two great peaks of meteor activity in July-August and in December common to both, but some of the seemingly minor details have their counterparts. This is all the more surprising when it is remembered that Figure 1 a represents meteor activity averaged over a period of nearly sixty years, whereas Figure 1 b was obtained from one year of radar observations. It would seem to indicate that there is little change in the overall pattern of meteor activity from year to year.

There is, however, quite a noticeable tendency for the peak radar rates to occur a few weeks earlier than the corresponding peaks of visual activity, thus confirming an effect first reported by Lindblad (1952)

who found evidence indicating that faint radio meteors of the δ-Aquarid stream are observed at an earlier date than the bright photographic meteors. According to Watson (1956) visual observers record the greatest number of meteors at the third and fourth magnitudes. On the other hand, the meteors most commonly detected by radar during the Christchurch survey were of zenithal radio magnitude +6.2, while the smallest detectable meteors were two magnitudes fainter (Keay, 1963a). If an average meteor velocity of 40 Km/sec is taken, the zenithal radio magnitude of a meteor is close to its absolute visual magnitude, so we may say that the meteor population represented by Figure 1 b is about 3 magnitudes fainter than that of Figure 1 a .

The displacement of the peaks in Figure 1 is thus accounted for, since there exist several dispersive effects (summarized by Lovell, 1954) which act differentially on meteoroids of various sizes. The most powerful of these is the well-known Poynting-Robertson effect which causes the smallest meteoric particles to spiral most rapidly into the sun. Also, Whipple (1955) and Kresák (1960) have shown that ablative sputtering by the solar wind gradually reduces the size of all meteoroids and acts in a similar manner to the Poynting-

Robertson effect. Such effects force bright and faint meteors to separate and travel in different orbits, as found by Davies and Gill (1960) who have shown that a difference of three magnitudes can make a very great difference in the distribution of the reciprocal semi-major axes of meteor orbits: the brighter meteors being in noticeably larger orbits.

There is also a small diurnal displacement in the peaks between Figure 1 a and 1 b . It is most obvious for the main December peak which occurs between 4 and 5 hours local time for visual meteors and at 7 hours local time for radar meteors. The difference is probably attributable to the fact that this is really a daytime peak which visual observers cannot fully observe because of the onset of daylight. This also appears to be true of a smaller peak in the month of May. Apart from these two peaks, the diurnal displacement is insignificant.

## 3. COMPARISON OF RADAR AND PHOTOGRAPHIC OBSERVATIONS:

Despite the large number of photographic meteor observations which have been made in recent years, especially by the Harvard group, there exists insufficient data with which to construct a map of activity

similar to Figure 1. However, the photographic data is of such high accuracy that any comparison with the radar survey results should be revealing.

The distribution of longitude of perihelion for meteors is of considerable cosmological importance. Being related to the time of encounter with the earth at one of the nodal crossings, this distribution can be deduced from the radar data, provided that we consider only those meteors which move in direct orbits of low inclination to the ecliptic. Fortunately these are by far the majority, as evidenced by the work of Hawkins (1956) and Davies and Gill (1960), who have also shown that such meteors tend to originate from two pronounced radiant groupings situated close to the ecliptic about 65 degrees in longitude either side of the apex of the earth's way. These are often referred to as the helion and anti-helion sources. The seasonal variation in strength of these two sources has been derived from the radar survey data (Keay 1963b) and is shown in Figure 2. From March to June the helion source is the stronger, while the anti-helion source predominates from September to December, implying a distinctly anisotropic distribution of orbit perihelia around the sun.

In the absence of any readily available data relating numbers of observed meteors and the difference in ecliptic longitude between their perihelia and point of interception by the earth, this relationship had to be inferred from other observational data, namely: the number distribution of radio meteors as a function of observed velocity (McKinley, 1961) and the distribution of radio meteor radiants as a function of ecliptic longitude measured from the apex (Davies and Gill, 1960). The calculated relationship is shown in Figure 3a and Figure 3b together with the corresponding histograms, which give the probability $P(\Delta\lambda)$ that a meteor encountering the earth at an ecliptic longitude $\lambda$ will have its longitude of perihelion $\pi$ within 15 degrees of $\lambda + \Delta\lambda$. If $N_H(\lambda)$ and $N_{AH}(\lambda)$ are the numbers of meteors originating from the helion and anti-helion sources respectively when the earth is at ecliptic longitude $\lambda$, the number of meteors whose perihelia are at longitude $\pi$ will be given by

$$N_\pi(\pi) = \sum_{\lambda+\Delta\lambda=\pi} [N_H(\lambda)P_H(\Delta\lambda) + N_{AH}(\lambda)P_{AH}(\Delta\lambda)]$$

The result is shown in Figure 4, together with the distribution of longitude of perihelion for photographic meteors with $q' < 5$ a.u. and $q' < 3$ a.u. as found

by McCrosky and Posen (1961). (The curve for $q' < 5$ a.u. was obtained by adding the curves for $q' < 3$ a.u. and $3 \leq q' < 5$ a.u. given by McCrosky and Posen. Their curve for accurately reduced meteors with orbits for which $q' < 5$ a.u. was not used since it refers to a total of only 106 meteors.) It has been found that the majority of radio meteors have aphelia of less than 5 a.u., hence these samples of photographic meteors should correspond tolerably well with the radio meteors, bearing in mind that radio observations are more sensitive to meteors of higher velocity, i.e. those in rather elliptic orbits.

Several points arise from Figure 4. Firstly, the radar survey data, when combined as it is with other orbital parameters known only on a statistical basis, cannot reveal the finer detail of the distribution of perihelion longitudes. However, the very large sample of meteors involved ensures that the broad hump in the distribution is real. The photographic data, on the other hand, represent a relatively small sample of highly accurate individual determinations, leading to a much more detailed form of the longitude distribution.

As they stand, the correlation between the Christchurch survey distribution and each of McCrosky

and Posen's distributions in Figure 4 is positive (correlation coefficient equalled +0.35 in each case) but not strongly so. The agreement may be considerably improved if the Christchurch survey curve is displaced about two months to the right. This increases the correlation coefficient to +0.57 and +0.61 respectively between McCrosky and Posen's distributions for $q' < 5$ a.u. and $q' < 3$ a.u., and the Christchurch results. Such a displacement implies that the small radio meteors (sixth magnitude) are distributed ahead of the photographic meteors whose modal magnitudes are close to 1. This is in agreement with the findings of the previous section where visual and radio observations were compared, the greater shift in this case arising from the increased magnitude difference between the radio and photographic meteor samples. The cause of the dispersion between the photographic and radar meteors is probably the same as that mentioned in Section 1, but in this case the dispersion involves an apparent shift in the line of apsides of the meteor orbits.

Finally, the distribution of perihelia of radio and photographic meteors exhibits a minimum near 0 degrees and a maximum near 180 degrees longitude, which is quite the opposite to the observed distribution of

perihelion longitude for asteroids. It must be remembered, however, that this observed distribution applies to all known asteroids, the vast majority of which have perihelia well outside the earth's orbit. A connection between them and the meteors crossing the earth's orbit would be somewhat surprising. On the other hand, the possibility of some connection between meteors and those few asteroids which have their perihelia within the earth's orbit is not at all prejudiced.

## 4. POSSIBLE RELATION BETWEEN METEORITES AND RADIO METEORS:

In a recent paper Kresák (1963) has presented a detailed analysis of all known meteorite falls, and in particular has considered the selection factors involved in their observation and recovery. By far the greater number of falls have been recorded in the northern hemisphere, so Kresak divided the total number of falls by thirds into three latitude groups: high northern; mid-northern; and equatorial, embracing low northern and southern latitude falls. The falls in this latter group occurred at latitudes of less than + 32.2 degrees, with the group average at +9.6 degrees indicating the paucity of recorded falls in the southern hemisphere.

The equatorial group shows the smallest seasonal effect and probably gives the best representation of any real associations that might be present among meteorite orbits. A contour map of times of fall of meteors in this group is shown in Figure 5a; while Figure 5b shows the Christchurch radar survey results as in Figure 1b, but redrawn with less closely spaced hourly rate contours. Some degree of likeness is evident: both show two major seasonal peaks of activity with each peak occurring within three weeks of its counterpart. Chance alone may have brought about this correlation but it appears more likely that some kind of relationship exists. There is also a hint of some connection between the smaller peaks but the number of meteorites in the sample is too small to make this significant.

Although there is a seasonal similarity between the two contour maps the diurnal times of occurrence are altogether different - an expected result since meteorites tend to fall near the time of culmination of the antapex whereas meteor rates are lowest at this time of day.

## 5. CONCLUSIONS:

It is clear that the earth encounters two great peaks of meteoric activity during the course of a year; and possibly several minor ones as well. This indicates that the so-called sporadic (i.e. non-shower) meteoroids are distributed in a much less random manner than it has been customary to believe. The very fact that such large yet discrete associations of small meteoroids exist at the present time demands that they were formed rather late in the history of the solar system, otherwise they would long since have been scattered by the various ever-present dispersive forces.

Wyatt and Whipple (1950) have calculated the length of time required for the Poynting-Robertson effect to separate fifth magnitude meteoroids from those of magnitude -2, for various showers, so that the earth will pass from one limit to the other in a period of 5 days. These figures indicate that for sporadic meteors in typical orbits it will take a time of the order of $10^6$ years (1Myr.) to separate those of magnitude +3 and +6 by an amount sufficient to require the earth to take one day in passing between them. Thus we may obtain a crude estimate of the age of the meteoroid associations from

the relative displacement of the peaks of activity in Figure 1, as detailed in Table 1:

TABLE 1 PEAKS OF METEOR ACTIVITY

| RADAR | VISUAL | DIFFERENCE |
|---|---|---|
| July 27 | August 15 | 19 d. |
| October 13 | October 22 | 9 d. |
| December 7 | December 14 | 7 d. |

The time differences lead to an approximate age of 20 Myr. for the July/August association, which embraces the δ-Aquarid, Pisces Australid, Capricornid showers and possibly a Cetid shower (Ellyett et al., 1961). The October and December associations, though more diffuse, appear to be even younger, having approximate ages of the order of 10 Myr.

Such brief lifetimes, astronomically speaking, are entirely in accordance with Wyatt and Whipple's conclusion that meteoroids of density 4 $gm/cm^3$ and radius 0.05 cm, corresponding to about 5th magnitude meteors, moving in the orbit of Halley's comet, would be drawn into the sun in about 10 Myr. A time-scale of this order is supported by the change in slope near magnitude +5 in the sporadic meteor magnitude distributions obtained by Kaiser (1963) and others.

Meteoroid lifetimes of the order of tens of millions of years are also rather reminiscent of the cosmic ray exposure agres found for chrondritic aerolites (chrondrites). According to Anders (1962) there is a striking degree of clustering in the $H^3$-$He^3$ ages of chrondrites, with a large proportion (6 out of 13 measured samples) aged 22 $\pm$2 Myr. This particular cluster is attributed to the break-up of a larger body about 22 Myr. ago. Against this, Mason (1960) argues on mineralogical grounds that chrondrites may never have formed part of a disrupted planet or other large body.

Whatever their previous history, chrondrites form the largest proportion (over 80% according to Mason) of all meteorite falls and it seems more than a mere coincidence that many of their ages should be close to the age of the large meteoroid association encountered in July-August every year. This revives the old question concerning cometary versus asteroidal origin of the smaller, meteor-producing, meteoroids.

While many meteor streams have been identified with comets, there are almost as many which are not related to any known comet. It is worth noting that none of the streams related to comets include any which are closely connected with the July-August association of

meteoroids. Also, it is well-known that the occurrence of meteorites is not coincident with shower activity although there seems to be some relationship with the meteoroid associations, as demonstrated by Figure 5.

On the other hand, Jacchia and Whipple (1961) have decided from a study of photographic meteor orbits that less than 1% of such meteors show any sign of a typically asteroidal origin. Likewise Whipple and Hawkins (1959) have pointed out that an asteroidal source of meteorites is not supported by the known orbits of asteroids, few of which have perihelia within the earth's orbit.

Nevertheless these few atypical asteroids, whose perihelia do lie between the earth and the sun, and whose irregular light-curves suggest that they are fragments from a once larger body, may very well provide a clue to the origin of the meteoroid associations.

Appendix (Unpublished)

The known distribution of radio meteor velocities and the distribution of meteor radiants in ecliptic longitude were taken as starting points for calculating the number of observed meteors as a function of the difference in ecliptic longitude between perihelion and point of encounter with the earth.

McKinley (1961) has published radio velocity measurements originating from three different meteor observing programs, one being that conducted by Davies and Gill. These results were averaged and the component representing meteoroids moving in direct orbits was extracted, as shown in Figure 6. This component has an upper velocity limit of approximately 48 Km/sec if a minimum perihelion distance of 12 solar radii is assumed (see below).

Davies and Gill (1960) have obtained the distribution of radiants in ecliptic longitude for meteors travelling in orbits of low inclination. The two prominent peaks at approximately 65 degrees on either side of the apex of the earth's way, referred to earlier as the helion and antihelion groupings, are reproduced in Figure 7. The meteor distributions shown in Figures 6 and 7 were obtained by radio techniques and should therefore apply fairly closely to the present radar results.

Since the problem is restricted to the helion and antihelion radiant groupings which are centred close to the

ecliptic throughout the year, it is a legitimate approximation to consider the relationships between orbit parameters in the plane of the ecliptic only, as shown in Figure 8. Under these conditions the difference in ecliptic longitude between the orbit perihelion and the point of interception, $\Delta\lambda$, for any given meteoroid is a simple single-valued function of the observed meteor velocity, $V_{G_o}$, and the geocentric elongation from the apex of the apparent radiant of the meteor, $\epsilon_G$, measured along the ecliptic. The geocentric meteor velocity in the absence of gravitational acceleration is given by $V_G^2 = V_{G_o}^2 - V_{esc.}^2$ where $V_{esc.}$ is the velocity of excape from the earth. A simple two-dimensional treatment shows that the difference in longitude between perihelion and the point of encounter (node) is given by

$$\text{Cos}\,\Delta\lambda = \frac{\eta - 2}{\sqrt{3 - 2\eta + \left[(1-\eta)\,\text{Sec}\,\epsilon_G\right]^2}}$$

where

$$\eta = \frac{V_G\,\text{Cos}\,\epsilon_G}{V_E}$$

$V_E$ being the earth's orbital velocity. The $\Delta\lambda$ distribution is therefore bivariate and representable by a two dimensional array of values where the rows are of constant $V_{G_o}$ and the columns of constant $\epsilon_G$. Two arrays are needed: one for positive values of $\epsilon_G$ (helion radiants) and the other for negative values (antihelion radiants).

Let $n_{ij}$ be the number of meteors in the cell in the i th column and the j th row, the values of i and j being defined by

$$\epsilon_G = (40 + 5i) \text{ degrees, for } 1 \leq i \leq 9$$

$$V_{G_o} = (10 + 5j) \text{ Km/sec, for } 1 \leq j \leq 7$$

The resulting 9 x 7 array embraced values of $V_{G_o}$ in 5 Km/sec intervals from 15 Km/sec to 45 Km/sec which is near to the maximum velocity observable for meteors moving in direct orbits. The values of $\epsilon_G$ ranged in 5 degree intervals from $+45^\circ$ to $+85^\circ$ for meteors in the helion radiant groupings and from $-45^\circ$ to $-85^\circ$ for meteors in the antihelion radiant grouping.

Summing the number of meteors one column at a time

$$n_{j.} = \sum_{j=1}^{7} n_{ij}$$

and the 9 values of $n_{i.}$ represent the number distribution of meteors as a function of their geocentric elongation. This is known for both helion and antihelion groupings, which means that the marginal column totals are known for both arrays.

Similarly the 7 values of $n_{.j}$ represent the known distribution of meteors as a function of their observed velocity. These marginal row totals are the same for each array by virtue of the reversibility of the encounter geometry of Figure 8.

If the total of meteors in the sample is N

then $$N = \sum_{i=1}^{9} n_{i\cdot} = \sum_{i=1}^{9} \sum_{j=1}^{7} n_{ij}$$

but the order of summation is immaterial, so also

$$N = \sum_{j=1}^{7} n_{\cdot j}$$

and the problem becomes one of distributing the N meteors among the cells of the array to satisfy the known values of the marginal totals. The number of possible solutions is greatly restricted due to the following conditions which must be obeyed:

1. Certain cells are forbidden because they represent meteoroids moving in either hyperbolic orbits or in orbits passing too close to the sun. In view of the findings of Jacchia and Whipple (1961), who have made precise determinations of the orbits of photographic meteors, a value of 0.05 a.u. (12 solar radii) was taken to be the minimum allowable perihelion radius for a meteoroid to survive many approaches to the sun. There seems to be no reason why this photographic result should not equally apply to the radar meteors, which are, for the most part, smaller and more susceptible to solar influences when near to the sun.

2. The distribution of the $n_{ij}$ values in any row or column should be unimodal and as smoothly varying as possible. Furthermore cells corresponding to the higher values of orbital eccentricity were favoured in order to comply with the known preference for high eccentricity among sporadic radio meteors, as found by Davies and Gill (1960). This preference is also shown by photographic meteors according to McCrosky and Posen (1961).

The solution obtained for each array should therefore be a reasonably good representation of the actual bivariate distribution of meteors. The final step was to take the values of $\Delta\lambda$ corresponding to each permissible combination of i and j and plot curves of $n_{ij}$ (at fixed i) as a function of $\Delta\lambda$, making due allowance for the finite second differences in the $\Delta\lambda$ values. These curves were then summed to give the meteor distribution as a function of $\Delta\lambda$, as shown in Figures 3a and 3b. In each Figure a histogram was drawn for 30 degree intervals of $\Delta\lambda$ such that the ordinate values represent the probability $P(\Delta\lambda)$ of a meteoroid, encountering the earth at an ecliptic longitude $\lambda$, having its perihelion within 15 degrees of $\lambda + \Delta\lambda$.

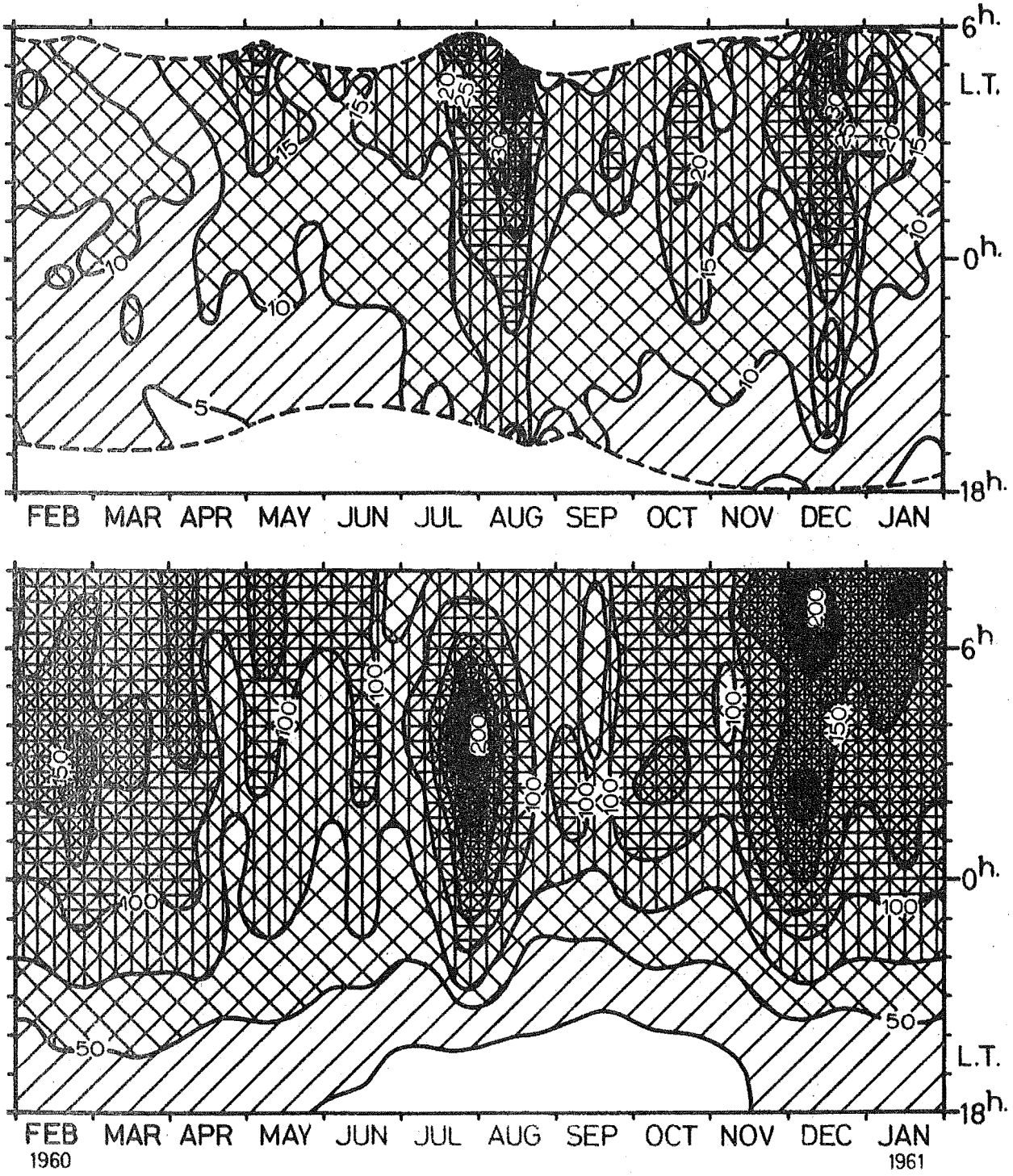


ıre 1a (upper): Observed visual meteor rates (Olivier, 1960)

1b (lower): Incidence of radio meteors (Ellyett & Keay, 1963)

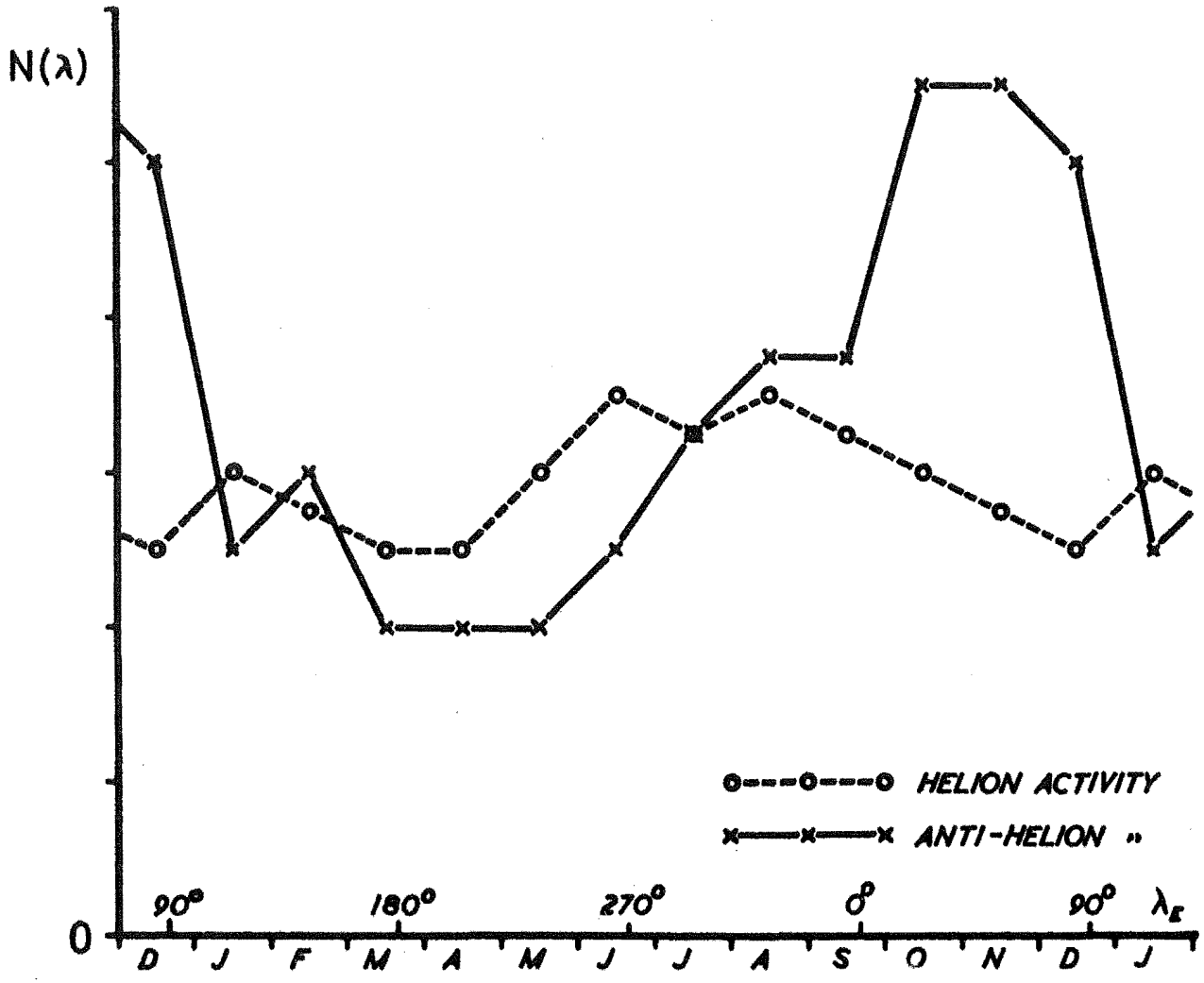


FIGURE 2. The variation throughout the year in the activity of meteors whose radiants belong to the helion and anti-helion groupings.

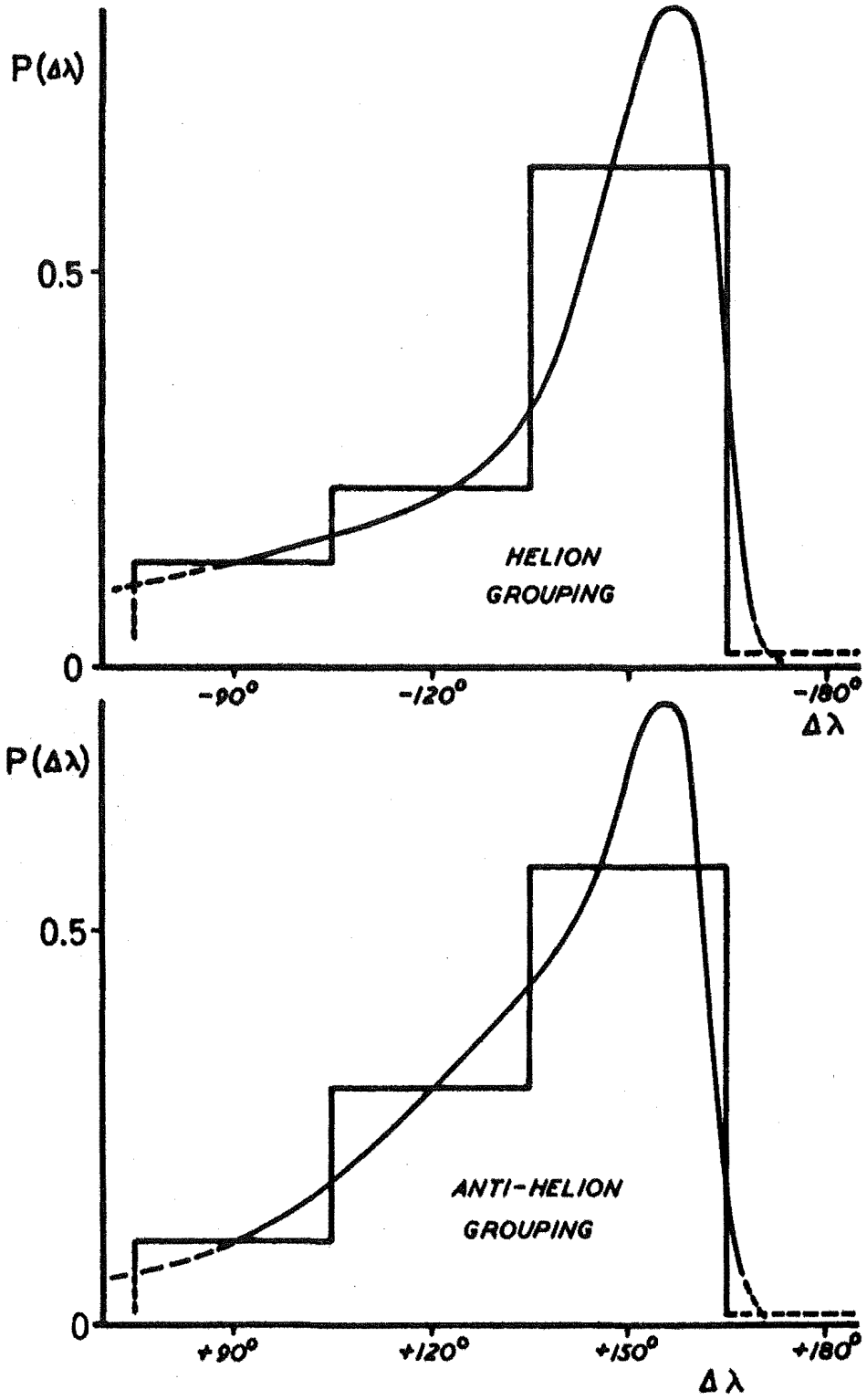


FIGURE 3. Calculated probability that a meteoroid encountering the earth at any given ecliptic longitude $\lambda$ will have its perihelion within 15 degrees of $\lambda + \Delta\lambda$ .

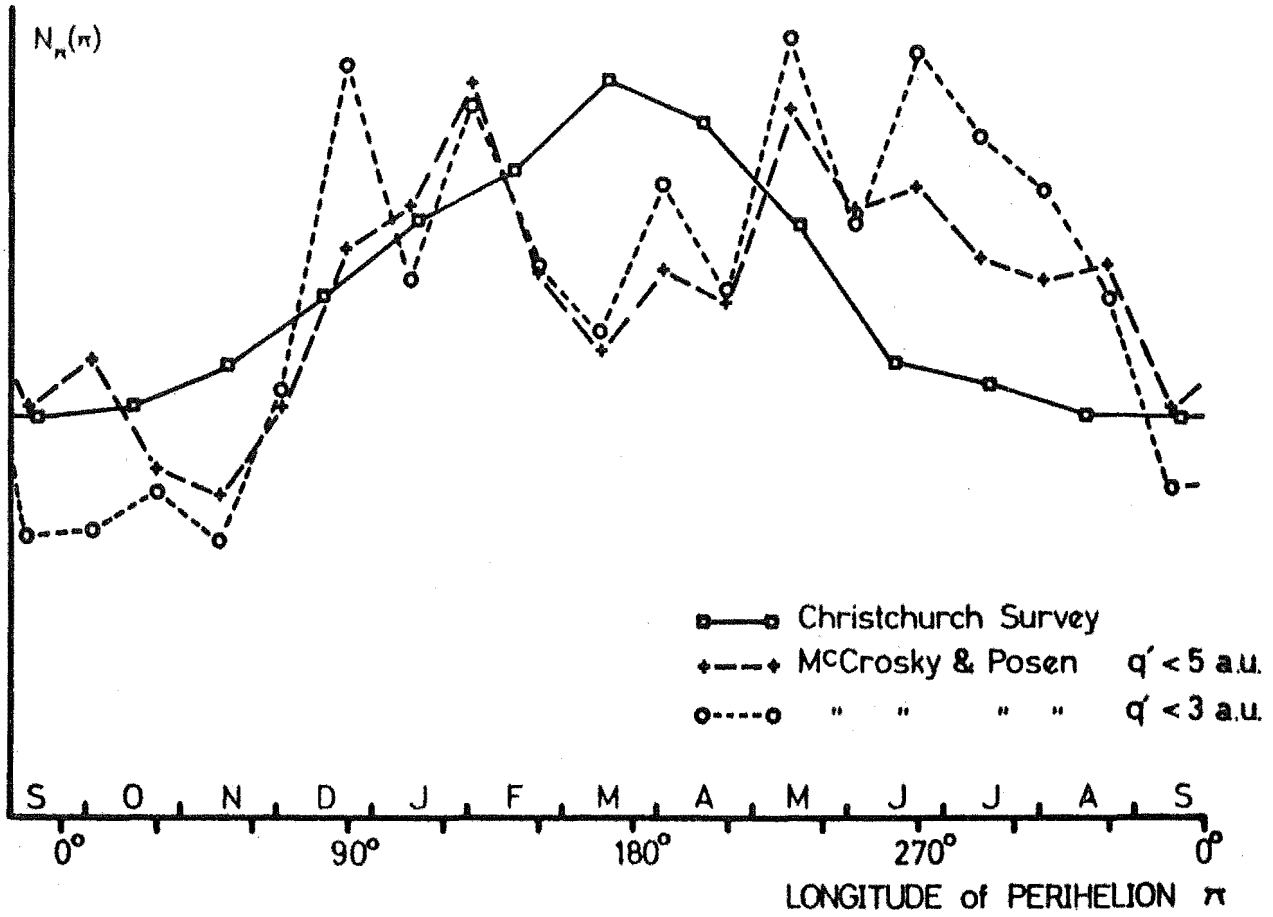


FIGURE 4. The distribution of the longitudes of perihelion for radar and photographic meteors.

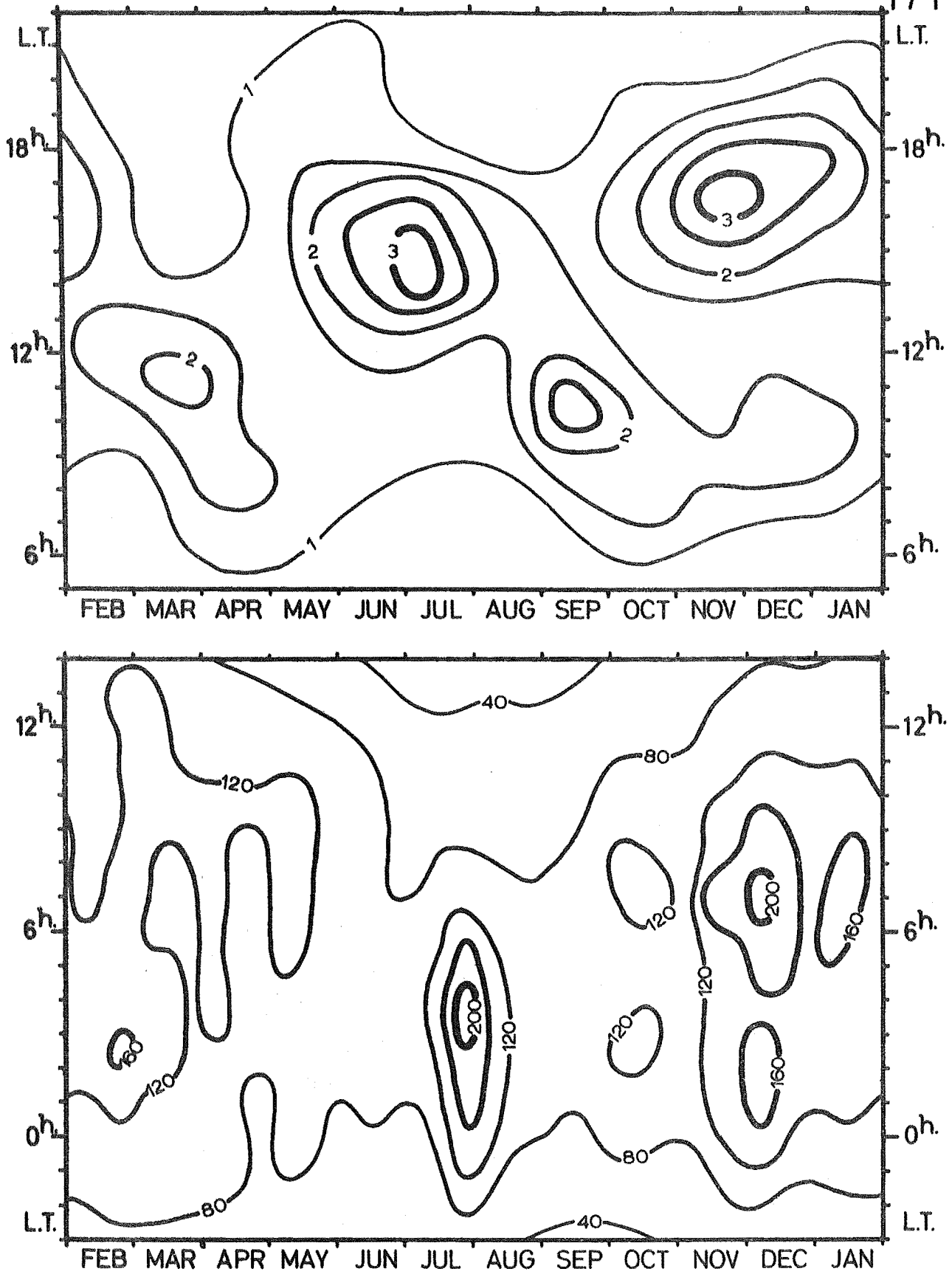


Figure 5a (upper): The occurrence of meteorite falls (after Kresák, 1963)
5b (lower): The incidence of radio meteors

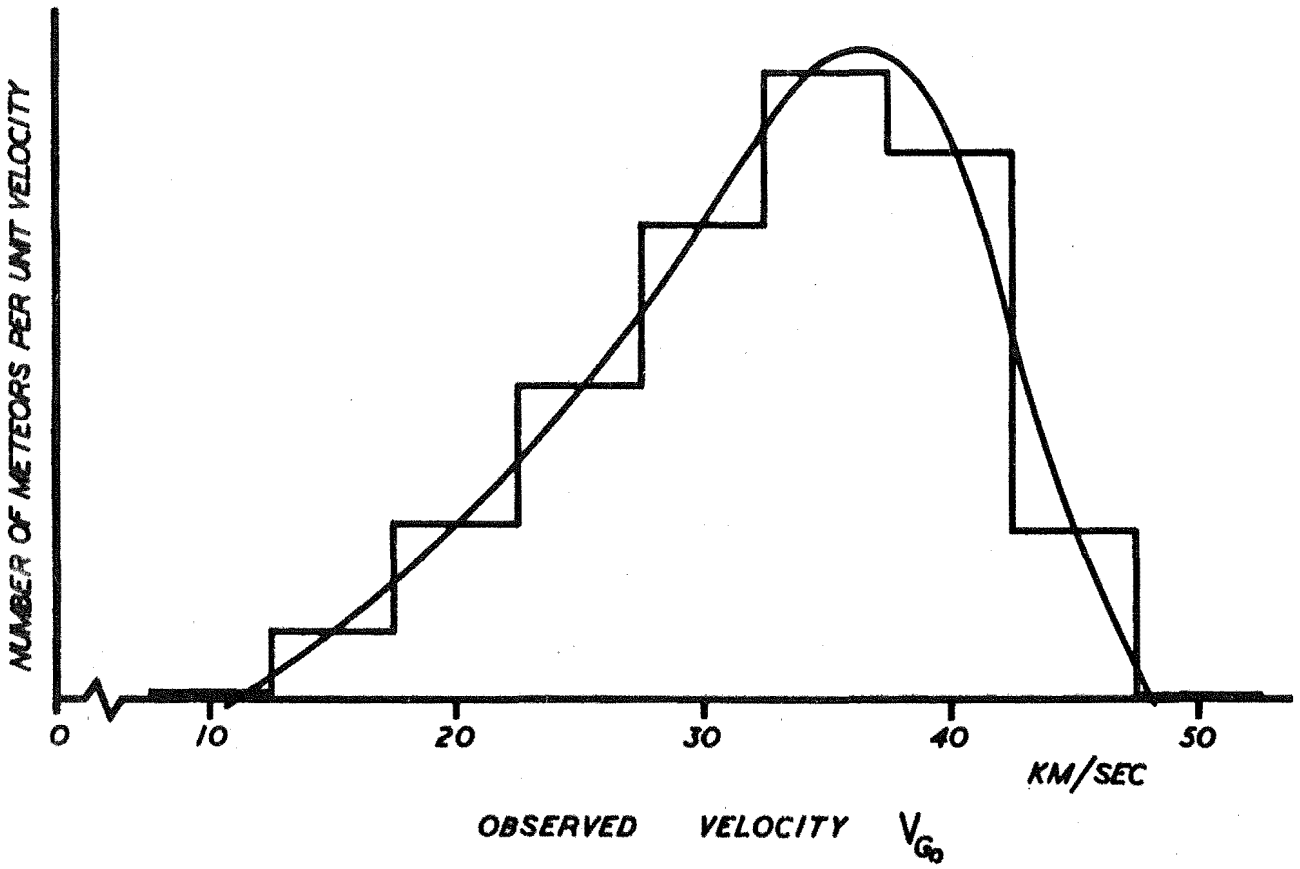


FIGURE 6. The velocity distribution of radio meteors moving in direct orbits.

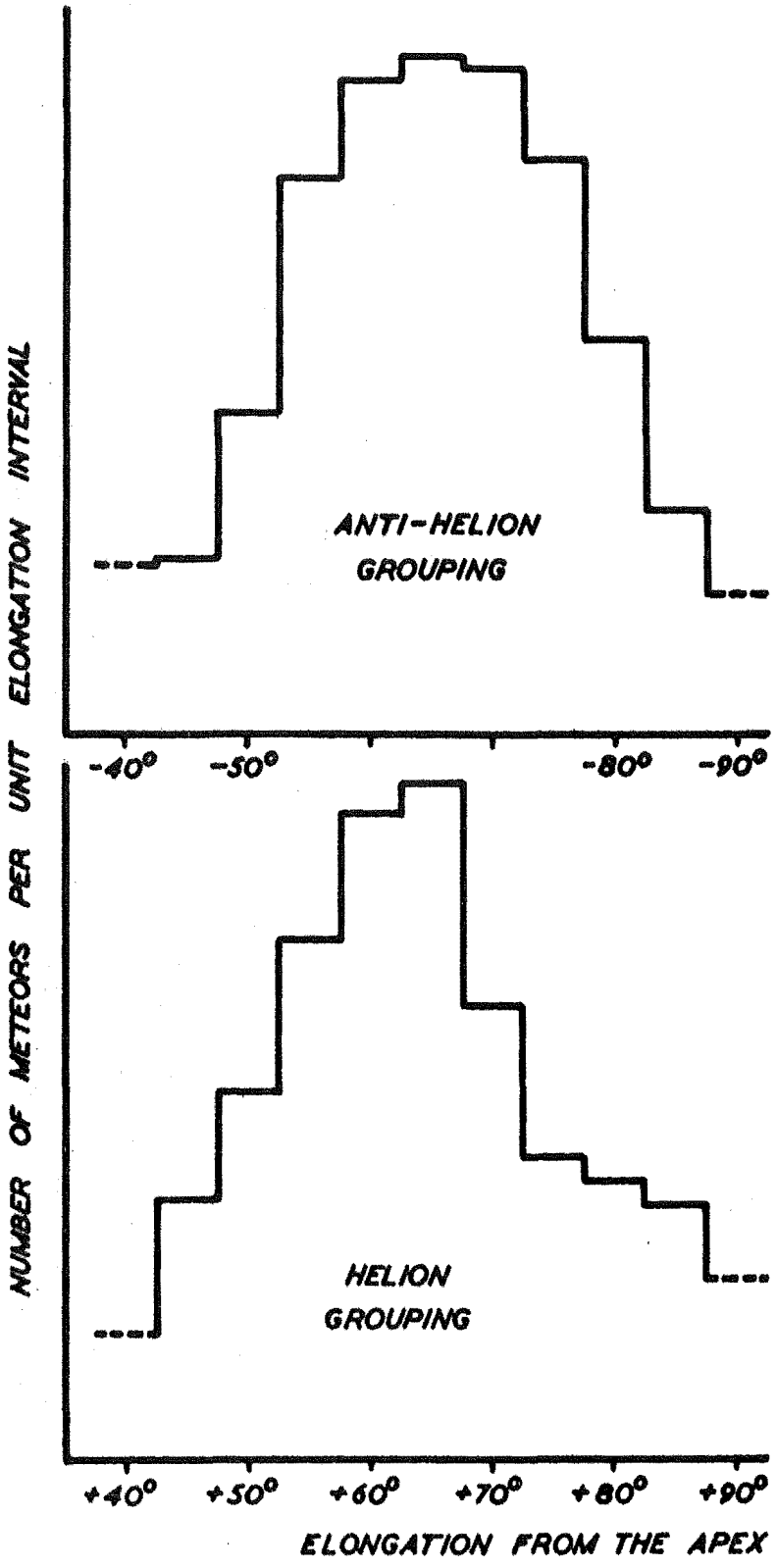


FIGURE 7. The distribution of meteor radiants in ecliptic longitude for each of the two ecliptic groupings.

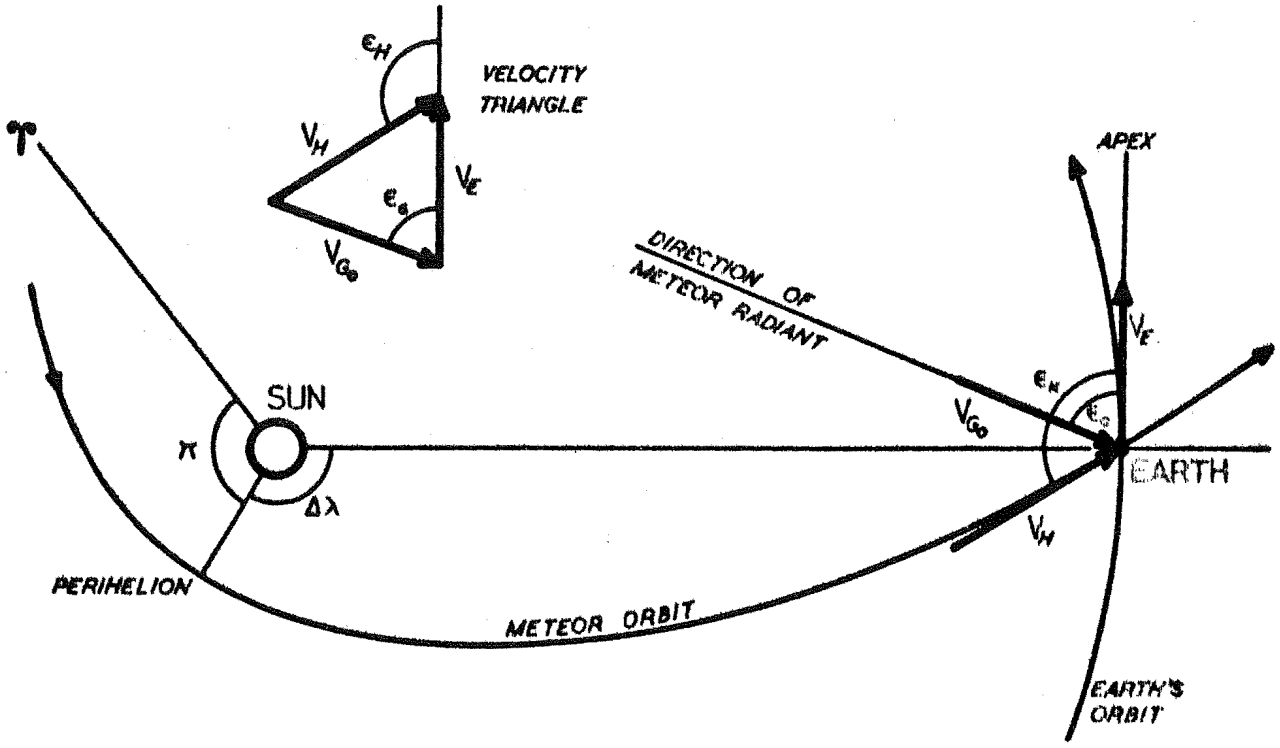


FIGURE 8. Encounter conditions when a meteoroid moving outwards in a direct orbit in the plane of the ecliptic is intercepted by the earth. In this example the apparent radiant of the meteor belongs to the helion grouping.

## 12. SOME PRELIMINARY RESULTS FROM A RESURVEY OF METEOR RATES

In February 1963 a resurvey of meteor rates was begun and is still continuing. Preliminary results are now available up to December 1963. The time-lag is due to the manual processes of film-reading and totalling and checking of the half-hourly rates. The subsequent processing is much faster than it was with the first survey because the half-hourly totals, together with detector current readings, are punched on I.B.M. cards. Computer programs have been developed to check their consistency and produce the monthly sheets of hourly totals very quickly in a similar format to the rate tables from the first survey.

A few tentative comparisons may be made between the two surveys. Figure 1 shows the diurnal variation in meteor rate for three selected months. Although the curves for these months differ considerably from one another, it is obvious that the shape of the curve for a given month (when scaled by an appropriate amount) does not vary from year to year. Thus the radiant distribution of sporadic meteors, as derived in Chapter 10, remains constant from year to year.

The most puzzling feature of the two surveys is that for many of the months of the second survey the observed meteor rates were almost double what they were at the corresponding time of the first survey. This is apparent

in Figure 1. It is even more apparent in Figure 2, which shows the average hourly rate at the time of passage of the antapex when the influence of showers is least. The sudden drop between September and October in the otherwise smooth curve for the second survey may arise from the fact that man-made interference was particularly bad during October and much of November. But this does not explain why the 1963 survey has produced higher rates throughout. The whole problem is under investigation but it is interesting to note that the five-year Canadian survey (Millman, 1963) obtained average monthly rates which differed from year to year by factors of up to two. They did not, however, record a difference as consistent as that shown in Figure 2. In order to help resolve this difficulty the present survey is being extended beyond the original time limit of one year.

Finally, the second survey results reveal the same prominent peaks of meteor activity as were present in the original survey, although no contour map of activity similar to that of Figure 1, Chapter 8, has yet been prepared.

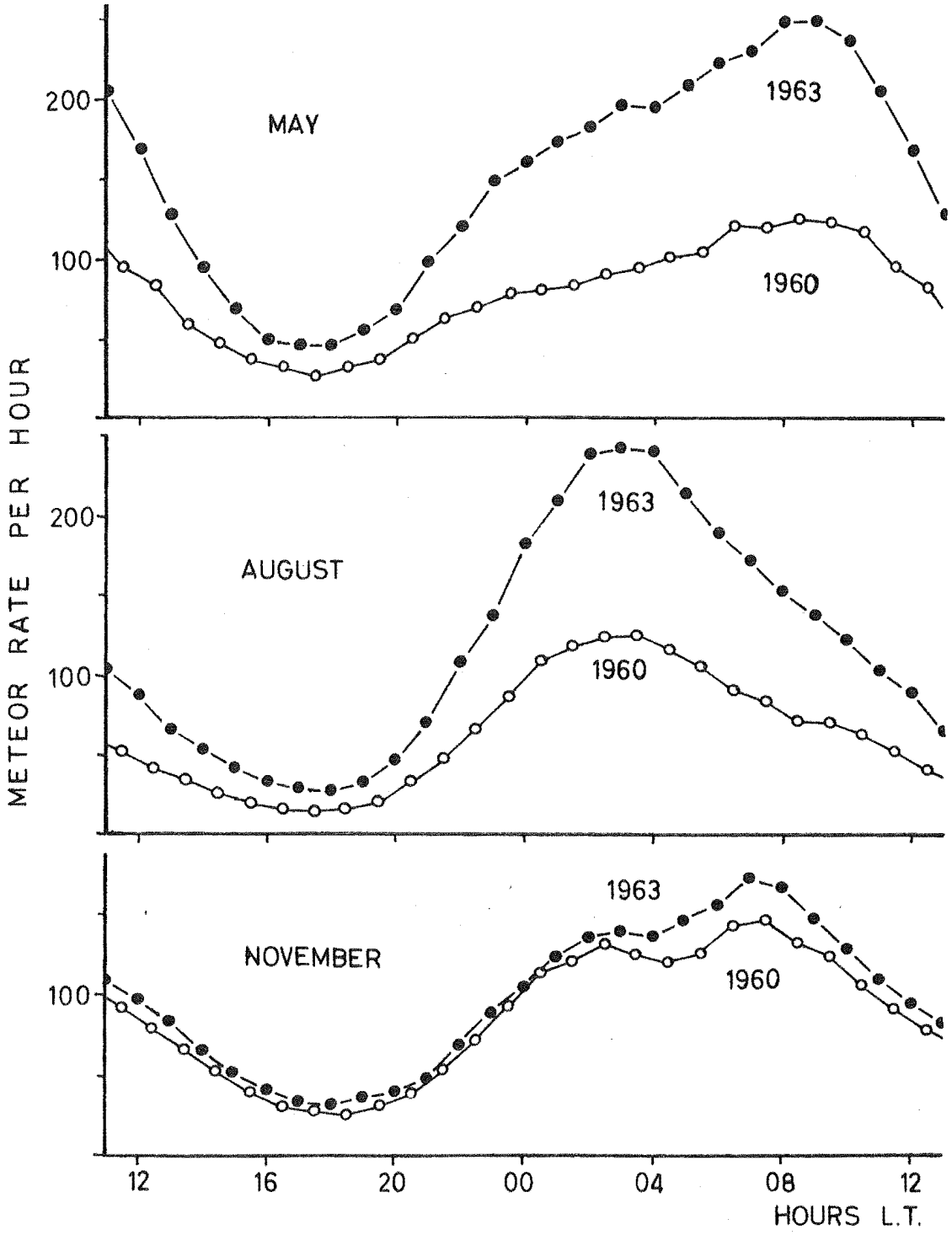


FIG. 1. AVERAGE METEOR RATE FOR CORRESPONDING MONTHS OF THE TWO SURVEYS.

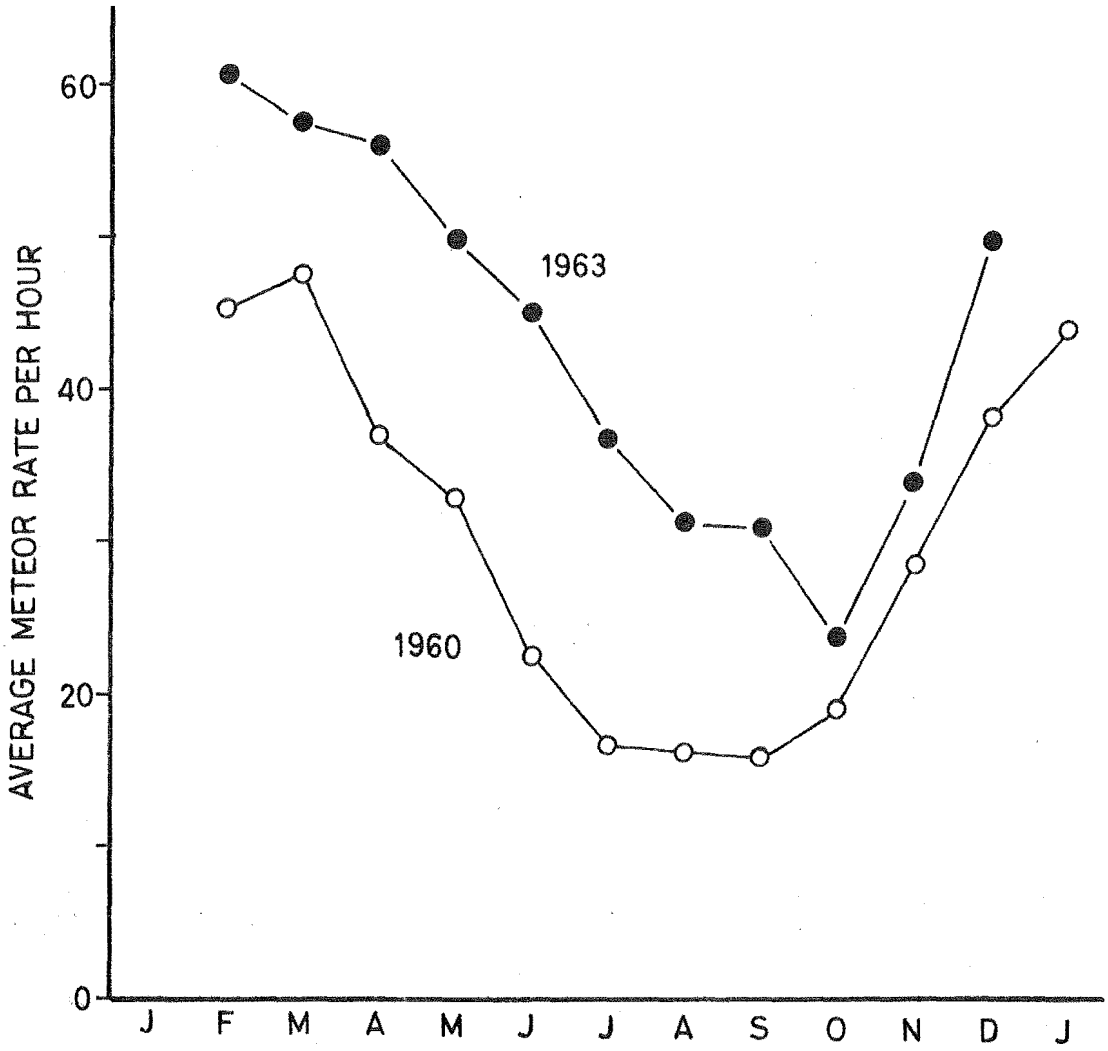


FIG. 2. AVERAGE METEOR RATE AT THE TIME OF TRANSIT OF THE ANTAPEX.

BIBLIOGRAPHY:

Almond, M., Bullough, K. and Hawkins, G.S.,; Jodrell Bank Annals, 1, 13, 1952.

Anders, E.; Rev. Mod. Phys., 34, 287, 1962.

Aspinall, A., Clegg, J.A. and Hawkins, G.S.; Phil. Mag., 42, 504, 1951.

Bennett, R.G.T.; M.Sc. Thesis, University of New Zealand, 1953.

Bennett, R.G.T.; Ph.D. Thesis, University of New Zealand, 1958.

Bowden, K.R.R. and Davies, J.G.; J. Atmos. Terr. Phys., 11, 62, 1957.

Bowen, E.G.; Aust. J. Phys., 6, 490, 1953.

Bowen, E.G.; J. Meteorology, 13, 142, 1956.

Bullough, K.; Jodrell Bank Annals, 1, 68, 1954.

Chapman, S. and Bartels, J.; "Geomagnetism", Oxford Univ. Press, 2, 582, 1951.

Clegg, J.A.; Phil. Mag., 34, 577, 1948a.

Clegg, J.A.; J. Brit. Astr. Assoc., 58, 271, 1948b.

Davidson, T.W.; Jodrell Bank Annals, 1, 116, 1956.

Davies, J.G.; "Radio Observation of Meteors" in Adv. in Electronics and Electron Physics (Academic Press, New York), 9, 95, 1957.

Davies, J.G. and Gill, J.C.; Mon. Not. R. Astr. Soc., 121, 437, 1960.

Dole, S.H.; J. Planet. Space Sci., 9, 541, 1962.

Elford, W.G. and Robertson, D.S.; J. Atmos. Terr. Phys., 4, 271, 1953.

Ellyett, C.D. and Fraser, G.J.; Aust. J. Phys., 8, 273, 1955.

Ellyett, C.D. and Keay, C.S.L.; Aust. J. Phys., 9, 471, 1956.

Ellyett, C.D. and Keay, C.S.L.; J. Geophys. Res., 66, 2590, 1961.

Ellyett, C.D. and Keay, C.S.L.; Final Report, AFCRL Contract AF64(500)-6, 1962.

Ellyett, C.D. and Keay, C.S.L.; Mon. Not. R. Astr. Soc., 125, 325, 1963.

Ellyett, C.D., Keay, C.S.L. and McLauchlan, E.C.; Final Report Research Grant NsG-219-62, National Aeronautics and Space Administration, 1963.

Ellyett, C.D., Keay, C.S.L., Roth, K.W. and Bennett, R.G.T.; Mon. Not. R. Astr. Soc., 123, 37, 1961.

Ellyett, C.D. and Roth, K.W.; Aust. J. Phys., 8, 390, 1955.

Ellyett, C.D. and Roth, K.W.; to be published, 1964.

Evans, G.C.; Jodrell Bank Annals, 1, 280, 1960.

Fraser, B.J.; M.Sc. Thesis, University of Canterbury, 1961.

Fraser, G.J.; M.Sc. Thesis, University of New Zealand, 1954.

Forsyth, P.A., Vogan, E.L., Hansen, D.R. and Hines, C.O.; Proc. I.R.E., 45, 1710, 1957.

Gallagher, P.B. and Eshleman, V.R.; J. Geophys. Res., 65, 1846, 1960.

Gray, R.E.; M.Sc. Thesis, University of Canterbury, 1961.

Greenhow, J.S. and Hall, J.E.; Mon. Not. R. Astr. Soc., 121, 174, 1960.

Hawkins, G.S.; Mon. Not. R. Astr. Soc., 116, 92, 1956a.

Hawkins, G.S.; Astron. J., 61, 386, 1956b.

Hawkins, G.S.; Astrophys. J., 124, 311, 1956c.

Hawkins, G.S.; Smithsonian Contrib. Astrophys., 7, 53, 1963.

Hawkins, G.S. and Almond, M.; Mon. Not. Roy. Astr. Soc., 112, 219, 1952a.

Hawkins, G.S. and Almond, M.; Jodrell Bank Annals, 1, 1, 1952b.

Hawkins, G.S. and Prentice, J.P.M.; Astron. J., 62, 234, 1957.

Hoffmeister, C.; "Meteorstrome" (Weimar), Ch.9, 1948.

Jacchia, L.G. and Whipple, F.L.; Smithsonian Contr. Astrophys., 4, 97, 1961.

Kaiser, T.R.; Phil. Mag. Supp., 2, 515, 1953.

Kaiser, T.R.; "Meteors", Suppl. J. Atmos. Terr. Phys., 2, 119, 1955.

Kaiser, T.R.; Mon. Not. R. Astr. Soc., 121, 284, 1960.

Kaiser, T.R.; Annales de Geophysique, 17, 50, 1961a.

Kaiser, T.R.; Mon. Not. R. Astr. Soc., 123, 265, 1961b.

Kaiser, T.R.; Sp. Sci. Rev., 1, 554, 1963.

Kaiser, T.R. and Closs, R.L.; Phil. Mag., 43, 1, 1952.

Keay, C.S.L.; M.Sc. Thesis, University of New Zealand, 1956.

Keay, C.S.L.; Aust. J. Phys., 10, 471, 1957.

Keay, C.S.L.; Mon. Not. R. Astr. Soc., 126, 165, 1963a.

Keay, C.S.L.; J. Atmos. Terr. Phys., 25, 507, 1963b.

Keay, C.S.L.; Astron. J., 69, 98, 1964.

Keay, C.S.L. and Ellyett, C.D.; J. Geophys. Res., 66, 2337, 1961.

Keay, C.S.L. and Gray, R.E.; Tech. Memorandum, TM X-940, National Aeronautics and Space Administration, Washington D.C., 1964a.

Keay, C.S.L. and Gray, R.E.; Electronics Engng., 36, 322, 1964b.

Kresak, L.; Bull. Astron. Inst. Czech., 11, 1, 1960.

Kresak, L.; Bull. Astron. Inst. Czech., 14, 52, 1963.

Kresak, L.; Bull. Astron. Inst. Czech., 15, 53, 1964.

Kresakova, M. and Kresak, L.; Contrib. Astron. Obs. Skalnate Pleso, 1, 40, 1955.

Lindblad, B.; Trans. Chalmers Univ. Tech., Gothenburg, Sweden, 129, 3, 1952.

Lovell, A.C.B.; "Meteor Astronomy", Oxford, 1954.

Lovell, A.C.B.; "Geophysical Aspects of Meteors" in Handbuch der Physik (Springer-Verlag, Berlin), 48, 427, 1957.

Mason, B.; J. Geophys. Res., 65, 2965, 1960.

McCrosky, R.E. and Posen, A.; Smithsonian Contr. Astrophys., 4, 15, 1961.

McKinley, D.W.R.; "Meteor Science and Engineering", McGraw-Hill, New York, 1961.

McLauchlan, E.C.; Aust. J. Phys., 13, 750, 1960.

Meeks, M.L. and James, J.C.; J. Atmos. Terr. Phys., 16, 228, 1959.

Millman, P.M.; Report, R. and E.E. Division, N.R.C. Canada, 1963.

Murakami, T.; Publ. Astro. Soc. Japan, 7, 49, 1955.

Neale, M.J.; Bulletin, R. and E.E. Division, N.R.C. Canada, 8, 11, 1958.

Olivier, C.P.; Smithsonian Contr. Astrophys., 4, 1, 1960.

Prentice, J.P.M.; J. Brit. Astr. Assoc., 63, 175, 1953.

Vogan, E.L. and Campbell, L.L.; Can. J. Phys., 35, 1176, 1957.

Watson, F.G.; "Between the Planets", Rev. Ed., Harvard Univ. Press, 1956.

Weiss, A.A.; Aust. J. Phys., 10, 397, 1957.

Weiss, A.A.; J. Atmos. Terr. Phys., 14, 19, 1959.

Weiss, A.A.; Aust. J. Phys., 13, 522, 1960.

Weiss, A.A. and Smith, J.W.; Mon. Not. R. Astr. Soc., 121, 5, 1960.

Whipple, F.L.; Astrophys. J., 121, 750, 1955.

Whipple, F.L. and Hawkins, G.S.; "Meteors" in Handbuch der Physik (Springer-Verlag, Berlin), 52, 519, 1959.

Wyatt, S.P. and Whipple, F.L.; Astrophys. J., 111, 134, 1950.

APPENDIX 1

## CHARACTERISTICS OF AERIALS USED IN THIS WORK

| AERIAL: | Rotatable Array | Multiple Yagi Array (2 of) | Fan Beam Array | Omni-directional (2 of) |
|---|---|---|---|---|
| Configuration: | Twelve $\lambda/2$ dipoles | Eight 7 element Yagis | Three folded dipoles | Crossed folded dipoles |
| Azimuth of beam centre: | Any | (i) 67.5°E (ii) 112.5°E | 90°E | - |
| Horizontal beam width between half-power points: | 22.5° | 4.4° | 90° | - |
| Elevation at which maximum power is radiated: | 12° | 9.5° | 14° | 60° |
| Vertical beam width between half-power points: | 14° | 11.5° | 16.5° | 38° |
| Gain over isotropic*: | 125 | 1000 | 32 | 4.4 |

*These values may be taken as plus or minus 10%.

APPENDIX 2

(Extract from "The Annual and Diurnal Variation of Meteor Rates in the Southern Hemisphere", by C. D. Ellyett and C. S. L. Keay, Final Report, AFCRL Contract AF64(500)-6, Chapter 3, May 1962.)

## MAINTENANCE OF PARAMETER CONSTANCY

### (a) Transmitter

i) Absolute power. A dummy load, consisting of eight 60 W strip lamps in parallel, was connected to the transmission line as close as possible to the aerial, and carefully matched. A standing wave ratio of 1.18:1 was obtained on the open feeder lines, which was the normal ratio with the aerial in use. By standard comparison techniques against a mains-operated lamp, together with an accurate measurement of the pulse width, a peak pulse power of 81 KW was obtained.

ii) Relative power monitoring. A peak-reading relative field strength meter and dipole aerial some 60 yards from the transmitting aerial fed to an Esterline-Angus recorder giving an automatic hourly measurement of radiated power. The deviation from the monthly mean ranged between 2 and 4%.

(b) Receiver and Display

Complete and systematic checking of all the apparatus has been in operation throughout the entire experiment. Advantage was taken of the time off to reload the camera at three and four day intervals to carry out checks on receiver noise figure and sensitivity, transmitter-receiver tuning, and brilliance setting of the display tube.

A voltage standing wave ratio measurement of the transmitter aerial feeder system, together with a bridge measurement of the receiver aerial feeder termination, was taken at frequent intervals. No major variations were detected. Receiver gain control settings were standardized at each film change, using the standard noise generator as a reference signal. A fortuitous permanent echo some miles distant provided a convenient, ready check of the frequency stability of the system.

In addition, a noise generator automatically replaced the aerial for some seconds once per hour. The noise diode anode current and the receiver detector current meters were photographed simultaneously onto the meteor film to give an hourly record of the receiver sensitivity.

Finally, at three minute intervals (except on the hour) the receiver-detector current meter was photographed to provide a measure of the aerial noise. It had

been thought that it would be necessary to use these readings - chiefly of slowly varying galactic noise - to reduce all rates to a standard noise level, but the introduction of the video compression unit maintained constancy of background level and rendered this unnecessary.